AD-A107 513 DAVID W TAYLOR NAVAL SHIP RESEARCH AND DEVELOPMENT CE--ETC F/G 10/2
ACTIVE SUPERCONDUCTIVE GENERATOR DEVELOPMENT 400-HORSEPOWER GEN--ETC(U)
OCT 81 H O STEVENS, M J CANNELL

UNCLASSIFIED DINSRDC/PAS-81/14 NL

1 OF 2
AD
A107513

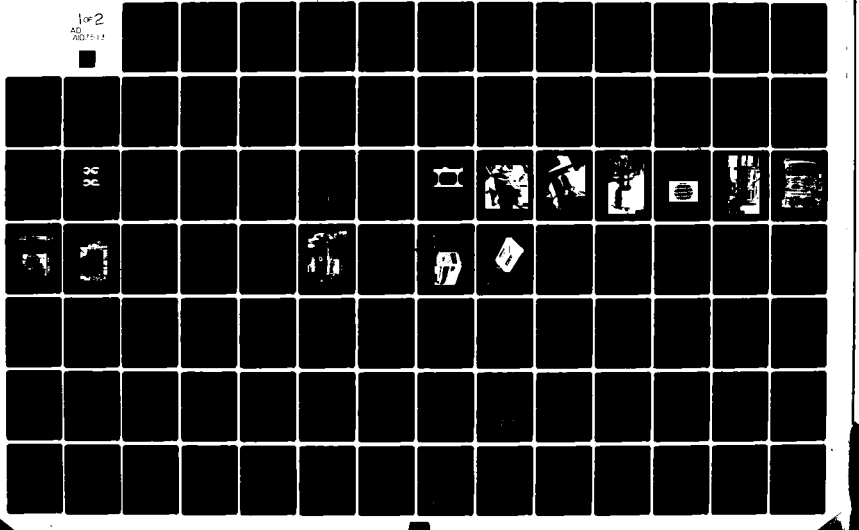

DAVID W. TAYLOR NAVAL SHIP RESEARCH AND DEVELOPMENT CENTER

Bethesda, Maryland 20084

ACYCLIC SUPERCONDUCTIVE GENERATOR DEVELOPMENT 400-HORSEPOWER GENERATOR DESIGN

by

H. O. Stevens and M. J. Cannell

APPROVED FOR PUBLIC RELEASE; DISTRIBUTION UNLIMITED.

PROPULSION AND AUXILIARY SYSTEMS DEPARTMENT
RESEARCH AND DEVELOPMENT REPORT

October 1981

DTNSRDC / PAS-81/14

MAJOR DTNSRDC ORGANIZATIONAL COMPONENTS

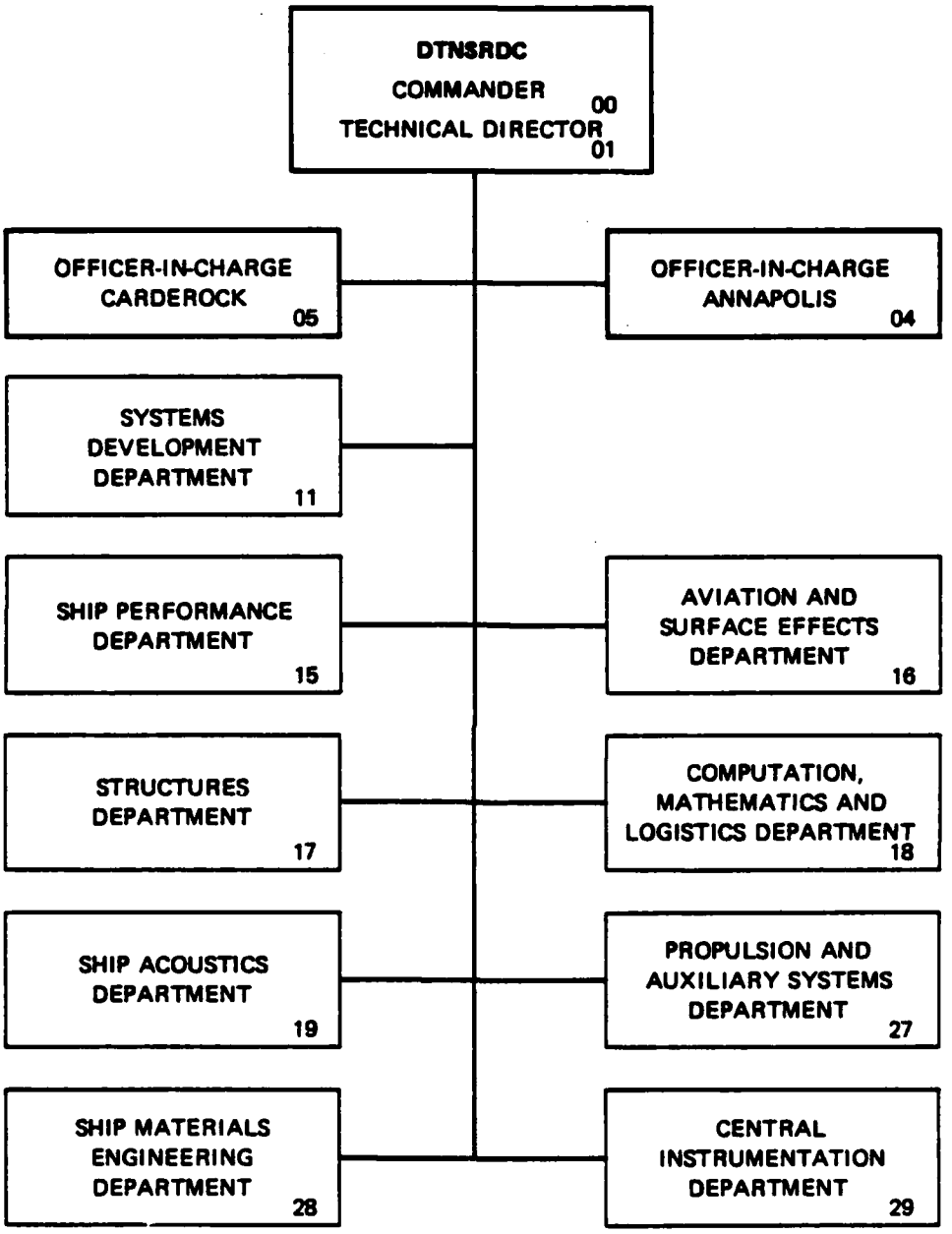

UNCLASSIFIED

SECURITY CLASSIFICATION OF THIS PAGE *(When Data Entered)*

REPORT DOCUMENTATION PAGE		READ INSTRUCTIONS BEFORE COMPLETING FORM
1. REPORT NUMBER PAS-81/14	2. GOVT ACCESSION NO. AD-A107 513	3. RECIPIENT'S CATALOG NUMBER
4. TITLE *(and Subtitle)* ACYCLIC SUPERCONDUCTIVE GENERATOR DEVELOPMENT 400-HORSEPOWER GENERATOR DESIGN		5. TYPE OF REPORT & PERIOD COVERED Research and Development 6. PERFORMING ORG. REPORT NUMBER
7. AUTHOR(s) Howard O. Stevens and Michael J. Cannell		8. CONTRACT OR GRANT NUMBER(s)
9. PERFORMING ORGANIZATION NAME AND ADDRESS David Taylor Naval Ship R&D Center Annapolis, Maryland 21402		10. PROGRAM ELEMENT, PROJECT, TASK AREA & WORK UNIT NUMBERS (See Reverse Side)
11. CONTROLLING OFFICE NAME AND ADDRESS Naval Sea Systems Command (SEA 05R11) Washington, DC 20362		12. REPORT DATE October 1981 13. NUMBER OF PAGES 111
14. MONITORING AGENCY NAME & ADDRESS*(if different from Controlling Office)*		15. SECURITY CLASS. *(of this report)* UNCLASSIFIED 15a. DECLASSIFICATION/DOWNGRADING SCHEDULE

16. DISTRIBUTION STATEMENT *(of this Report)*

APPROVED FOR PUBLIC RELEASE; DISTRIBUTION UNLIMITED.

17. DISTRIBUTION STATEMENT *(of the abstract entered in Block 20, if different from Report)*

18. SUPPLEMENTARY NOTES

19. KEY WORDS *(Continue on reverse side if necessary and identify by block number)*

Superconducting Generators
Superconductivity
Liquid Metals
Acyclic Machines
Motors and Generators
Electric Propulsion

20. ABSTRACT *(Continue on reverse side if necessary and identify by block number)*

A superconductive acyclic generator has been designed and constructed using the unique current-carrying capabilities of superconducting wire in the field winding to produce a very high flux density in the rotor region. This, along with the use of liquid-metal current collectors in lieu of conventional brushes has yielded a very high power density machine designed to operate at gas turbine speeds. The nominal 300-kilowatt generator is 0.66 meter long and 0.46 meter in diameter (26 x 18 inches) and is designed to operate at 19,500 revolutions per minute. Extrapolation of the design analyses indicates no barriers to operation up to 750 kilowatts. Efficiencies of 98% are estimated over the practical operating range.

DD FORM 1 JAN 73 1473 EDITION OF 1 NOV 65 IS OBSOLETE
S/N 0102-LF-014-6601

UNCLASSIFIED

SECURITY CLASSIFICATION OF THIS PAGE *(When Data Entered)*

(Block 10)
Program Element 63508N
Project S0380SL
Task 16761
Work Units 1-2722-100, 1-2791-100,
and 1-2706-100

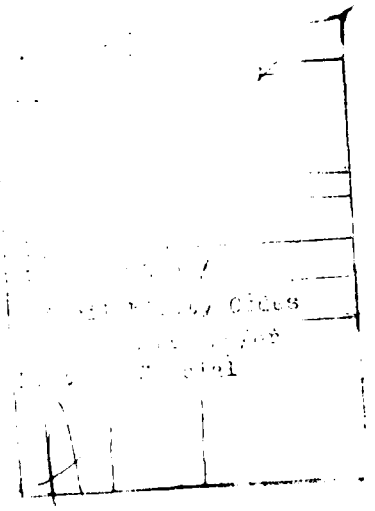

TABLE OF CONTENTS

LIST OF FIGURES

LIST OF TABLES

LIST OF ABBREVIATIONS

ac	Alternating current
amps	Amperes
atm	Atmospheres
°C	Degrees Celsius
cm	Centimeter
cm^2	Square centimeters
cm^3/min	Cubic centimeters per minute
dc	Direct current
°F	Degrees Fahrenheit
ft-lb	Foot-pounds
ft^3/hr	Cubic feet per hour
ft^3/min	Cubic feet per minute
ft/s	Feet per second
G	Gauss
H	Henry
hp	Horsepower
Hz	Hertz
ID	Inside diameter
IED	Independent Exploratory Development
J	Joule
K	Kelvin
kg	Kilogram
kG	Kilogauss
kg/s	Kilogram per second
kJ	Kilojoule
kVa	Kilovolt ampere
kW	Kilowatt
ℓ/hr	Liters per hour
lb/hr	Pounds per hour
m	Meter
m^2	Square meter
m^3	Cubic meter
max	Maximum

MHD	Magnetohydrodynamic
mm	Millimeter
NaK	Potassium
N/m^2	Newtons per square meter
OD	Outside diameter
ppm	Parts per million
psi	Pounds per square inch
psig	Pounds per square inch gage
rpm	Revolutions per minute
s	Second
S/C	Superconducting
SES	Surface effect ship
T	Tesla
temp	Temperature
TRIM	Triangular Irregular Mesh
typ	Typical
Vdc	Volts direct current
W	Watt
Wb	Webers

ABSTRACT

A superconductive acyclic generator has been designed and constructed using the unique current-carrying capabilities of superconducting wire in the field winding to produce a very high flux density in the rotor region. This, along with the use of liquid-metal current collectors in lieu of conventional brushes has yielded a very high power density machine designed to operate at gas turbine speeds. The nominal 300-kilowatt generator is 0.66 meter long and 0.46 meter in diameter (26 x 18 inches) and is designed to operate at 19,500 revolutions per minute. Extrapolation of the design analyses indicates no barriers to operation up to 750 kilowatts. Efficiencies of 98% are estimated over the practical operating range.

ADMINISTRATIVE INFORMATION

The superconductive generator design effort described herein was initiated under the Independent Research and Independent Exploratory Development Program at this Center, and subsequently supported by the Naval Sea Systems Command (SEA 05R11). The work was acomplished in the Electrical Propulsion and Machinery System Branch of the Propulsion and Auxiliaries Department at Annapolis under Program Element 63508N, Project S0380SL, Task 16761, and Work Units 1-2722-100, 1-2791-100, and 1-2706-100.

INTRODUCTION

This report is a description of the design process and results obtained for a high-speed acyclic generator utilizing superconductive field windings. The design rating for this generator is 300 kVa* at 19,500 rpm. General design considerations are included as well as detailed treatment of critical design areas.

BACKGROUND

The development of intrinsically stable superconducting wire during the past decade has given rise to the evolution of many concepts for both ac and dc rotating electrical machines utilizing superconducting field windings. All such machine concepts exhibit a significant size and weight reduction compared to conventional electrical machinery. Size and weight advantage depends on the concept considered; but

*Definitions of abbreviations used are given on page vii.

reductions of the order of a factor of five are realizable for machines in the range of 1000 hp or more. This size and weight reduction is principally a consequence of the extremely high current density capability of the superconducting wire and the resultant high magnetic flux generation. In addition, the size and weight of such machines has been further reduced by innovative design related to current collection, liquid cooling, and other improvements in the nonsuperconducting portions of the machines.

The development work described herein was begun under the Independent Exploratory Development (IED) Program at this Center during Fiscal Year 1971 as a separate program effort. During this period, several design concepts were developed for superconductive acyclic generators in the 50- to 400-hp range. This effort was subsequently combined with a concurrent superconducting motor program at the Center, with the aim of developing complementary motor and generator designs representative of the type needed for naval propulsion systems. This work continued under the IED Program and later with direct funding from NAVSEA. This latest change in scope has necessitated significant change in the generator design approach to satisfy the requirements of shipboard equipment, and allow compatibility with realistic superconducting motor designs and system requirements as described elsewhere in this report. The objectives of this program have thus changed from demonstration of single concept feasibility to development of a model system, demonstrating to the maximum practical extent the feasibility of producing hardware qualified in all respects for full-scale shipboard installation.

APPLICATIONS

The application of superconducting electric machinery of primary interest to the Navy is in the area of electric ship propulsion. Electric drives have been recognized in the past as providing superior arrangement flexibility and control. The former being of special significance in some new ship concepts.[1]* However, the size and weight of conventional electric machinery has precluded its widespread application in naval ship propulsion systems. The size and weight reduction made possible with the use of superconductivity allows the design of electric drive systems competitive in size and weight with mechanical drive systems, yet retaining the advantages of electric drive. Detailed treatment of such applications is given elsewhere.[2-4]

The machine designs possible with superconducting field windings fall into two categories; ac synchronous machines and dc acyclic machines with several variations possible within these categories. The dc acyclic machines appear to be more suited to ship propulsion applications due to a greater degree of control flexibility, e.g., full torque at all speeds, and lower refrigeration requirements, compared to ac synchronous-type machines. The effort at this Center has therefore been concentrated in the area of dc superconducting machinery developments.

*A complete list of references appears on page 109.

SUMMARY

The second section of this report gives an overview of dc superconducting generator design considerations, and the design requirements to be met by the subject generator.

The third section is a detailed technical description of the generator design, and results of analyses conducted relative to this particular design. The theoretical performance of the generator under various operating conditions is presented in the fourth section.

SUPERCONDUCTIVE DIRECT CURRENT GENERATOR DESIGN CONCEPTS

DESIGN OPTIONS

The basis of operation for any dc acyclic machine is Faraday's Law of induction:

$$V = \frac{d\phi}{dt} \tag{1}$$

where V is the voltage induced in the circuit and ϕ is the magnetic flux enclosed by the circuit. If a portion of the circuit is constrained to remain stationary while the rest is allowed to move perpendicular to the flux lines, it is possible to arrange the geometry such that $d\phi/dt$ is nonzero when integrated over the circuit (as indicated in Figure 1), and generator action ensues. Conversley, if a current is passed through the circuit, a force is exerted on the conductor according to the relationship:

$$\vec{dF} = \vec{J} \times \vec{B}\, dv \tag{2}$$

where $\vec{J}$ is the current density, $\vec{B}$ is the local magnetic field, and dv is a volume element of the conductor-carrying current. The integral of dF around the circuit yields the resultant net forces on both the moving and stationary parts.

An acyclic generator must consist of the following five basic parts.

1. Field magnet to generate the flux, ϕ.
2. A moving conductor (rotor) to produce voltage.
3. A static current path (stator) to carry current from the rotor to the load and back, and to absorb reaction torque.
4. Current collectors to carry current between rotor and stator.

5. As an optional feature necessary for many applications, a magnetic shield to confine and/or localize the high magnetic fields associated with a superconducting field winding.

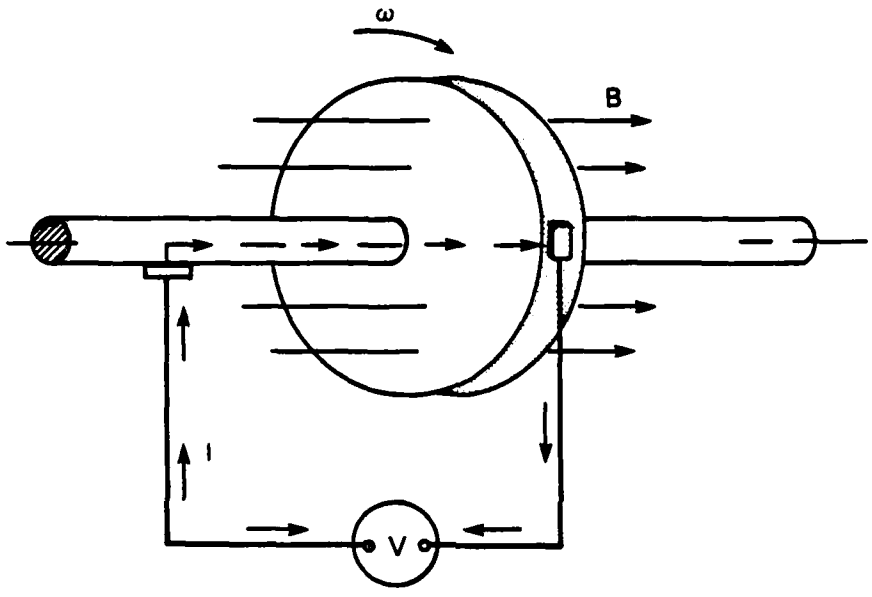

Figure 1 — Acyclic Generator Circuit

There may be several choices for each of these elements available to the designer, and all combinations of these choices consistent with feasibility may be considered candidate designs. The requirements of the application will ultimately dictate the final generator design.

Field Magnet

The field magnet may be a simple solenoidal dipole or a combination of simple dipoles of opposite polarity to form a higher order flux distribution. In addition, the magnet may be located internal or external to the rotor/stator structure.

Rotor

The rotor geometry for an acyclic machine may take the form of one or more disks with current collection at the inner and outer radii, or a set of one or more concentric conducting drums with current

collectors at each end. There are almost infinite number of variations between these two extremes which are topologically equivalent as far as voltage production is concerned. The rotor may be formed to any shape, as long as the current collection regions remain fixed, with no effect on voltage production.

Stator

The stationary portion of the electrical circuit in an acyclic machine must be complementary to the rotor geometry, since, in addition to providing external connections, the stator serves to interconnect the rotor segments in series and/or parallel to provide the desired output voltage.

Current Collectors

Direct current acyclic machines share a common difficulty regardless of design details. All tend to be high current, low voltage devices as compared to conventional electrical machinery. Current collectors must therefore be capable of operating at very high current densities with an extremely low voltage drop to produce a viable machine design. Conventional carbon or metal-graphite solid brushes are thus ruled out in any practical machine design. Existing technology provides two alternatives; liquid metal to provide electrical contact between rotor and stator, advanced-design solid brushes consisting of metal-plated carbon fibers bundled together to form a "brush,"[5] the latter being only marginal in satisfying the required performance and then only at some sacrifice in machine size. One might conceive of exceptions to the above, but no practical alternatives appear to exist.

Shielding

The magnetic shield may or may not be a functional portion of the machine. Internal magnet designs[6,7] depend on the ferromagnetic shield to shape the flux utilization. The generator design described in this report uses a ferromagnetic shield which has only minimal effect on generator performance. The British have chosen to use an active shielding technique which may be detrimental to machine performance, since it tends to reduce the flux available for power generation. The active shield consists of a secondary set of field coils used to cancel the external magnetic signature of the primary field coils. The third alternative of no shield may be attractive in some applications where stray magnetic field is of no consequence, since a significant size and weight reduction is possible in some generator configurations by eliminating the shield.

Illustrations of many of these options may be found in a previous report.[7]

DESIGN CONSIDERATIONS

Upon further examination, it is evident that many of the options listed in the preceding section are incompatible. Some combinations, although possible, have intrinsic shortcomings which make the resulting machines unattractive.

Field Magnet

Locating the field magnet inside the rotor structure is attractive from the standpoint of efficient flux utilization; however, in high-speed generators, this arrangement tends to increase the rotor diameter and may lead to unacceptably high rotor tip speeds.

A quadrupole magnet configuration composed of two identical solenoids axially aligned with opposing fields results in half as many current collectors as a dipole magnet configuration, since the inner collectors are replaced by a direct connection as indicated in Figure 2. This consideration may be important in high speed machines where the current collectors are the chief source of inefficiency and complexity.

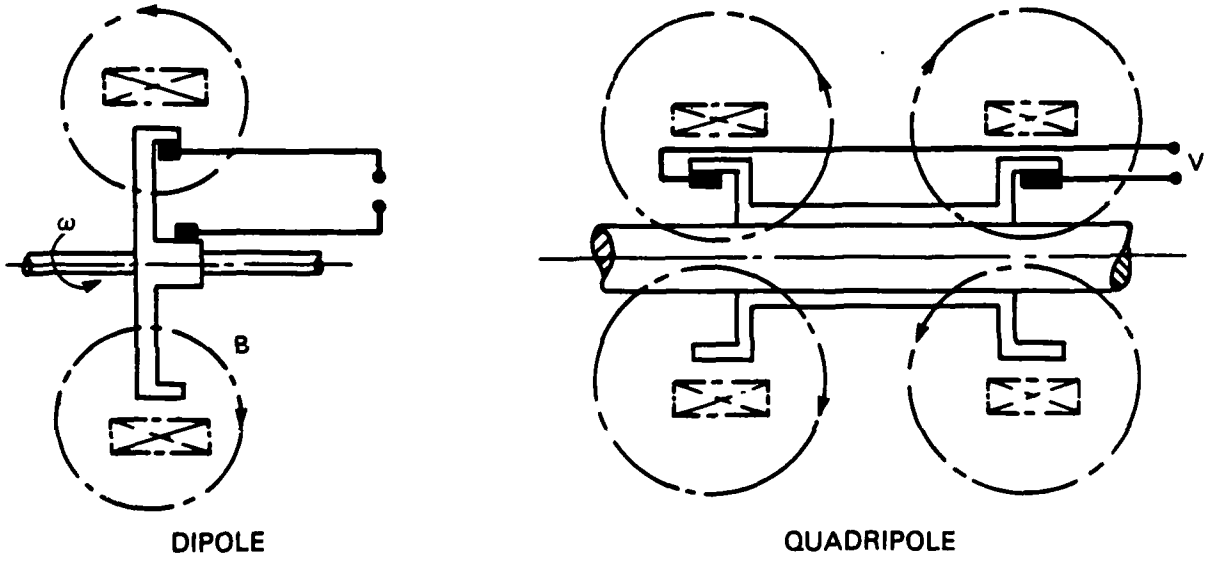

Figure 2 — Dipole and Quadripole Magnet Configuration

Conceptually, the field magnet might also be located between the rotor and stator portions of the machine. However, this would result in a complex interconnection problem within the machine, lengthen the current path, and contribute an additional, toroidal magnetic field in the magnet region due to the load current which would be detrimental to magnet performance.

There exist many more design considerations for the magnet related to the winding, cryogenic cooling, materials, stability, protection, and structure which have only an indirect bearing on the machine design per se. These considerations are described on page 23 and in an upcoming report.[8]

Rotor/Stator

The rotor and stator design are highly dependent on the current collector selection. If solid brushes are used, the rotor and stator may be segmented circumferentially and the segments interconnected in electrical series through the brush arrangement.[9] This arrangement requires commutation to take place between rotor and brushes to accomplish the voltage addition. The ability to conveniently generate reasonably high voltage with this arrangement makes it appear to be an attractive choice; however, the shortcomings of solid brushes becomes an overriding factor for high-speed, high efficiency machines as discussed below.

The use of a liquid metal as the current collection agent restricts the rotor/stator geometry to continuous channels at the current collector sites. Thus the stacked disk or concentric drum-type rotors or variations thereof are necessary. One alternative which could simplify construction would be to again segment the rotor and stator into bars, with groups of bars being connected to a continuous ring at the current collector sites.

At high speeds, the stresses in the rotor become large, and the selection of proper materials and construction techniques is important.

Secondary considerations in rotor/stator design include cooling methods, insertion and extraction of the liquid metal if necessary, sealing the inert atmosphere for liquid-metal purity maintenance, critical speed problems, connection to external current leads, assembly problems, and transferring reaction torque to the machine mounts.

Current Collectors

The selection of solid brushes of any type for a high power, high tip speed acyclic generator cn be ruled out for the following reasons. High power means a large brush contact area with resultant high friction

forces. The voltage drop across a solid brush contact can range from 0.1 to 2.5 volts depending on conditions of operation and materials.[10] At high currents this voltage drop translates to lower efficiency. A solid brush assembly running at high tip speeds will require frequent maintenance and replacement due to wear, an undesirable feature for shipboard equipment. The complexity and space requirements for solid brushes, especially if direct cooling is required, offer additional reason for rejection for the application of interest. Future improvements in solid brushes may change the above circumstances, but at least an order-of-magnitude improvement in current density, surface speed capability, and voltage drop would be required before they began to be competitive with liquid metals in acyclic machine applications.

The choice of liquid metals as a current collection mechanism leads to a number of problems separate from those of solid brushes. The magneto-hydrodynamic behavior of the liquid metal in a narrow circular channel, making contact with a high speed disk in the presence of intense magnetic fields and high current densities, is a theoretical problem of immense complexity. Any collector design must, of necessity, be the result of both theoretical and experimental effort. The primary losses in the liquid-metal current collectors are viscous drag, eddy currents, and resistive losses. In addition to minimizing these, one must also consider the stability of the liquid under high shear rates and magnetically induced forces. A general discussion and summary of problems associated with liquid-metal current collectors may be found elsewhere.[11]

Magnetic Shield

The magnetic shield for an acyclic machine should confine the magnetic flux to the interior of the machine without adding excess weight. In addition, the cylindrical symmetry of the field must be maintained in the rotating portion of the machine to avoid the generation of circulating currents in the rotor conductors. Therefore, a ferromagnetic shield should be designed to be operated at a high flux density everywhere within the shield material, and the shield should be as symmetric as possible with respect to the axis of rotation of the rotor. Computer calculated flux plots enable one to very accurately determine the optimum ferromagnetic shield configuration, including the effects of saturation, within the limits dictated by adequate mechanical design.

A secondary consideration in maintaining magnetic symmetry with respect to the ferromagnetic shield is the creation of unbalanced forces on the superconducting coil due to asymmetry or misalignment. At high flux densities, these forces may become very large resulting in the need for heavier magnet supports and a consequently larger cryogenic refrigeration load. This point is also applicable to any other ferromagnetic material used in machine construction.

The use of a secondary coil or set of coils for magnetic shielding may be attractive if size, cryogenic thermal efficiency, and large local magnetic fields external to the machine are not of paramount importance.

The only advantage of using a secondary superconducting coil set for magnetic shielding appears to be a possible weight reduction.

DESIGN REQUIREMENTS.

The design and performance requirements of a superconducting acyclic generator are dictated by the application. For a ship propulsion system application the following requirements are basic.

1. High Efficiency - Losses in the generator translate directly into fuel weight and thus decrease the payload or range of a ship. For low payload, high performance ships, such as a hydrofoil or surface effect ship (SES), this factor is especially important. Electric drive system efficiencies on the order of 95% are necessary if they are to be competitive with mechanical drive systems.

2. Magnetic Shielding - The stray magnetic fields of an unshielded superconducting magnet may be of the order of several kilogauss at a distance of two machine radii from the machine, and several gauss at distances of tens of feet from the machine envelope. To preclude the possibility of interference with other shipboard equipment, forces on nearby magnetic material or detection by magnetic ordinance, the generators should be shielded so that the stray magnetic fields are approximately the same as those of conventional generators of the same physical size, i.e., less than 100 gauss within a few inches of the machine envelope.

3. High-Speed Generator Operation - Since the intent of the development effort described here is to supply an alternative to mechanical drive elements insofar as possible, generators should be designed to run at gas turbine power shaft speed without gear reduction. This has the added advantage of minimizing generator size and weight, since rotational speed and generator size are inversely proportional at a given power level.

4. Compatibility with Shipboard Environment - All machine designs considered should be capable of being made compatible with shipboard environmental conditions including shock, vibration, temperature, motion, etc, without compromising the performance of the generator. Although model hardware may not incorporate all such features due to cost considerations, it should be convincingly demonstrated that such features can be feasibly included within the envelope of the generator design.

5. Capability of Extended Operation - The generator should be capable of continuous operation for extended periods of time without shutdown for maintenance, etc. Any periodic servicing required should be minimal and require a minimum downtime.

6. System Compatibility - The generator must be compatible with the superconducting motor to which it will supply power in terms of voltage and current output, and compatible with the prime mover which is an LM-100 gas turbine for the subject generator.

7. Capability of Operation under all Conditions of Speed and Torque - Sufficient design consideration must be given to a generator to allow operation over the full range of speeds dictated by system requirements, which may include zero speed and reverse under braking conditions. Reasonable design margin should be allowed for transient overload conditions.

LABORATORY MACHINE DESIGN

GENERAL DESCRIPTION

Superconductive acyclic generators tend to be high-speed machines as compared to motors because power density increases with speed and there are no intrinsic limitations on generator speed except those dictated by prime mover and mechanical constraints. Since current collector losses increase in proportion to total collector area and rotor tip velocity, and these losses represent the major source of inefficiency, there is a definite incentive to minimize the number of current collectors required in a generator. Examination of Figure 2 indicates that a dipole field coil requires two current collectors for each rotating element. However, the quadrupole configeration enables one to intercept the flux from two magnets with only two current collectors. Thus the quadrupole configeration should result in a more efficient generator with respect to current collector losses. The distinction between a drum- and disk-shaped rotor ceases to exist in a quadrupole machine because the drum-shaped rotor is exactly equivalent to two disks joined at their centers in terms of intercepting flux.

As a result of the above reasoning and the design options and considerations listed previously, the decision was made to design and construct a high-speed acyclic generator with an external quadripole superconducting field coil, using liquid-metal current collectors and a ferrous magnetic shield. A rough analysis indicated that this machine would result in a single rotor element having only two current collectors which would minimize the design and construction complexity. The conceptual arrangement of this generator is shown in Figure 3. The design parameters of the generator dictated by the LM-100 gas turbine prime mover selected and the already fixed superconducting motor characteristics are as follows.

1. Input-400 to 1,000 hp at 19,500 rpm rmp maximum.
2. Output-300 to 750 kVa at 30 Vdc.

The lesser numbers represent the nominal design point while the larger represent the maximum gas turbine capability.

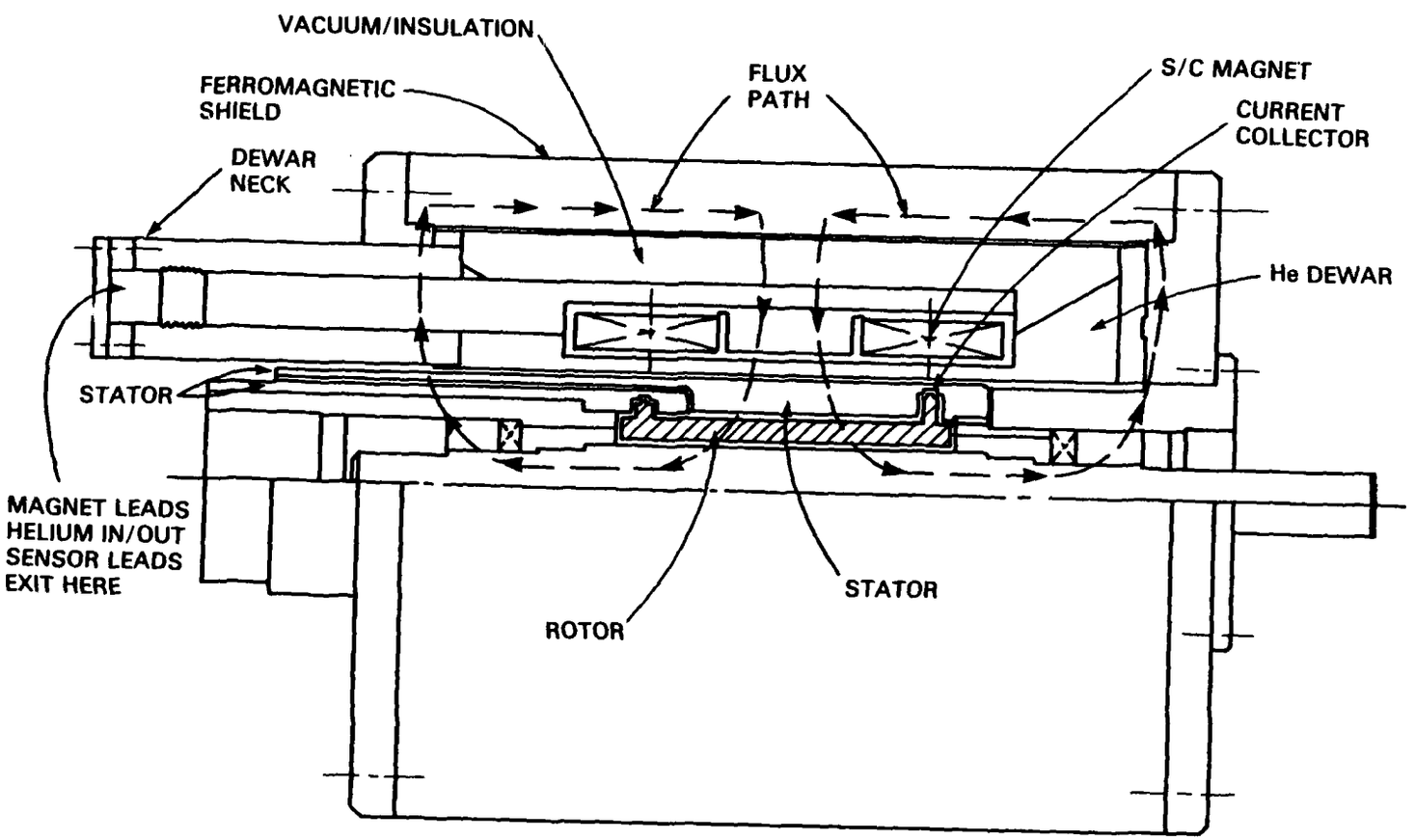

Figure 3 — Superconducting Acyclic Generator Conceptual Arrangement

The basic constraints established are:

1. Speed - 19,500 rpm
2. Current - 10,000/25,000 amps.
3. Voltage - 30 volts
4. Current Collectors - Liquid metal/Sodium Potassium (NaK)
5. Magnet Configuration - Quadripole
6. Rotor Location - Internal to magnet
7. Rotor Configuration - Drum with disk at ends for current collection
8. Shield - Ferromagnetic.

ELECTRICAL CIRCUIT DESIGN

The requirement that the generator provide 30 volts of output at 19,500 rpm dictates the rotor size for a given average magnetic field strength. The dimensions referred to are referenced to Figure 4. Note that all axial flux passing within the radius of the current collector is effective in producing voltage. Assuming an average magnetic field, $\overline{B}$, through the rotor, the rotor radius at the current collector site is determined from the following relationship derived directly from Equation (1)

$$V = \frac{nN}{60} \pi R^2 \overline{B} \tag{3}$$

or

$$R = \left(\frac{60\ V}{nN\pi B}\right)^{1/2}$$

where

V = Output voltage, 30 volts

n = No. of rotating elements, two (one for each magnet)

$\overline{B}$ = Average flux density through rotor, 3.5 Tesla

N = 19,500 rpm

R = rotor radius, m.

Hence R = 0.0647 m (2.5 in.). At this point, a choice in current collector configeration must be made, i.e., to rotate the channel or the disk as indicated in Figure 5. The rotating channel configuration appeared to be attractive from the standpoint of hydrodynamic stability of the liquid metal in the current collector. However, a rough analysis indicated that high stress concentrations in the channel and complexity of construction made this choice less attractive than the rotating disk stationary channel configuration which was chosen for

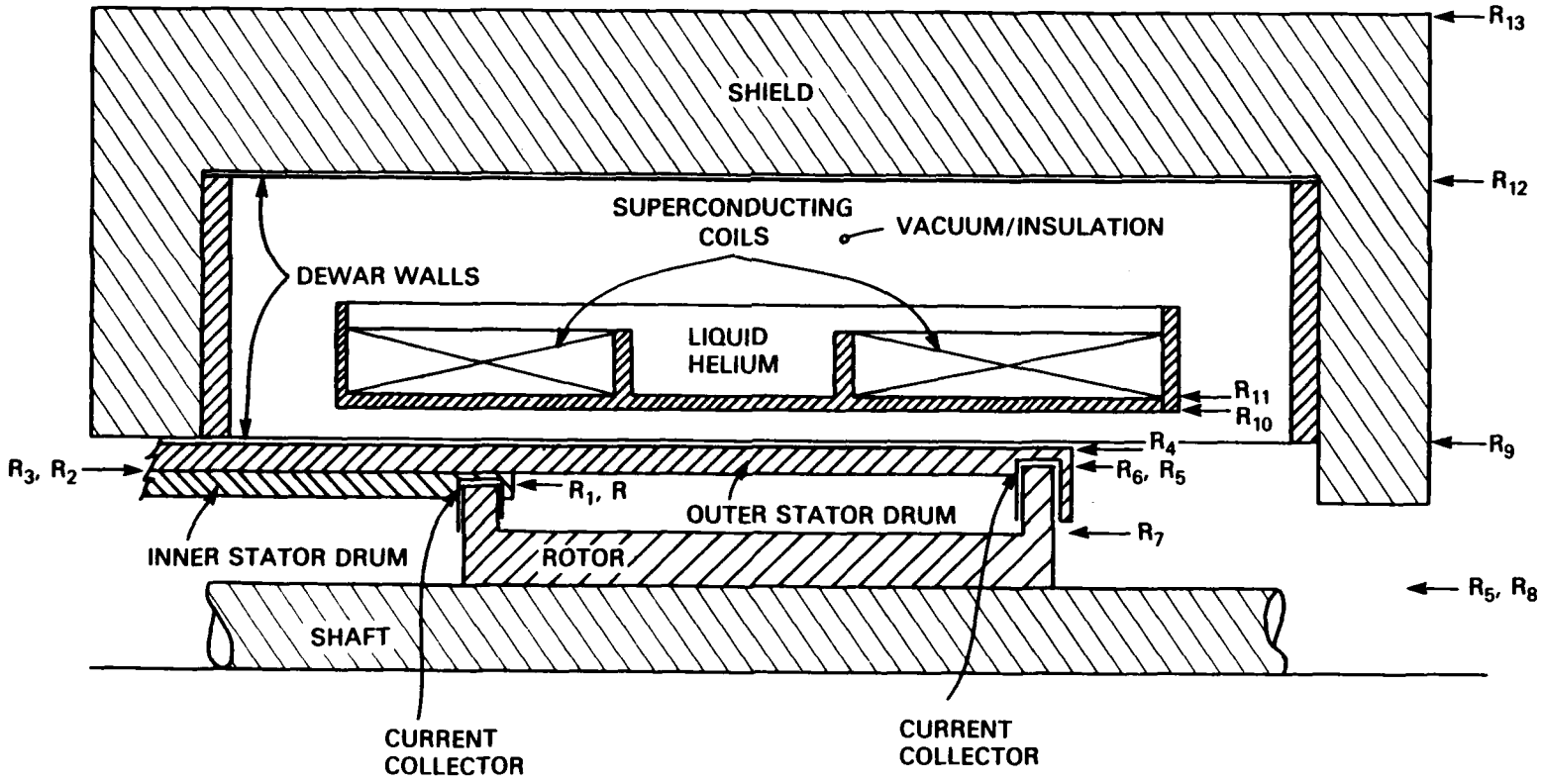

Figure 4 — Generator Nomenclature

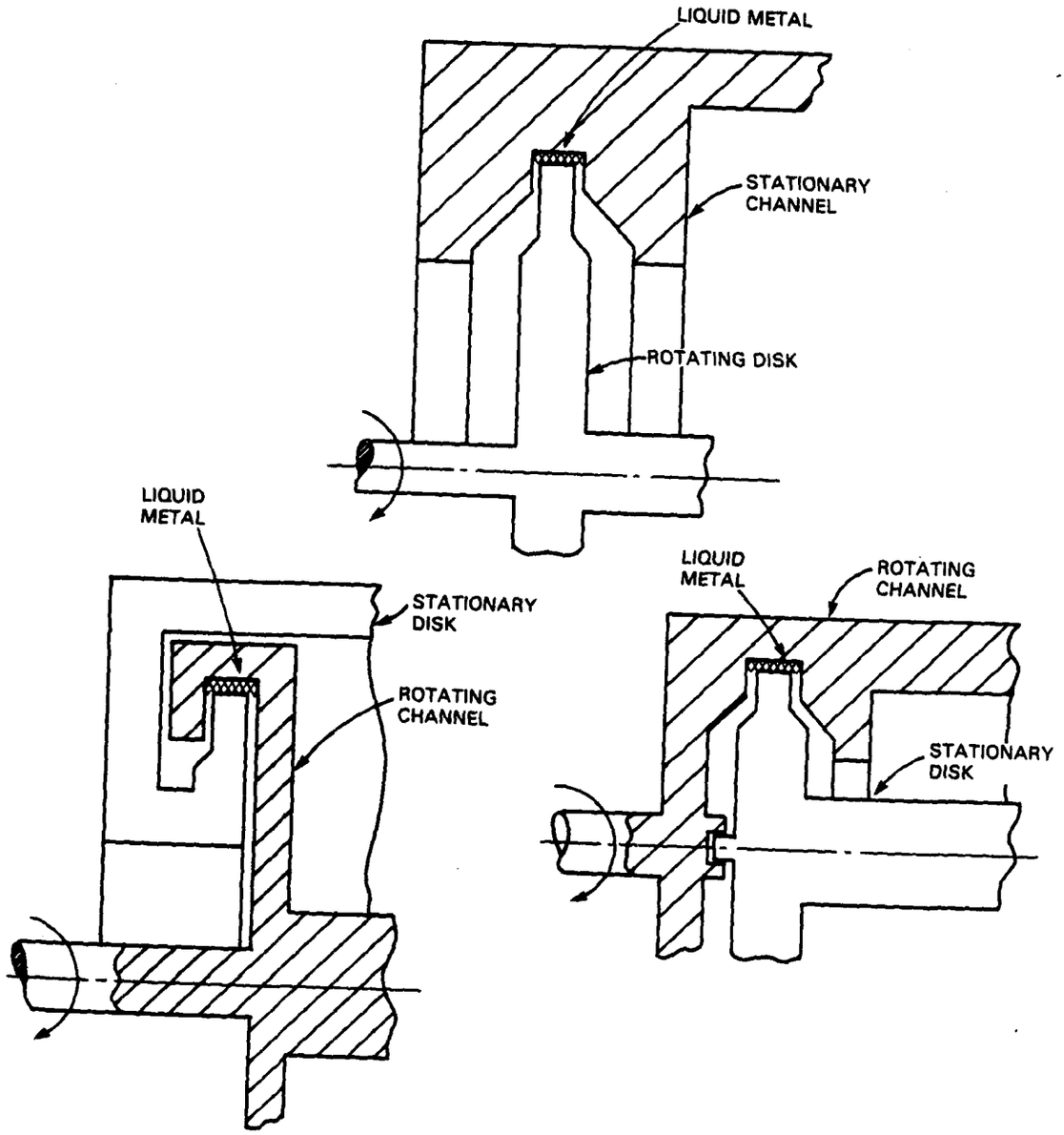

Figure 5 — Current Collection Configuration Rotating Disk and Channel

development. (In retrospect, this choice is not as clear and variations of a rotating channel design are presently being examined for possible future development.)

As is evident from Figure 4, the disk radius at one end of the rotor is slightly smaller to allow adequate space for the stationary current return path. The 6.35-cm (2.5-in.) radius was chosen as the smaller of the two disks as a conservative design measure. The liquid-metal-filled gap between rotor and stator was fixed at 0.0762 cm (0.02 in.). Thus the inner radius of the collector channel is $R_1 = R + 0.0762 = 6.426$ cm (2.530 in.).

The average current density in the rotor and stator was fixed at 232.5 amps/cm^2 with a maximum of 387.5 amps/cm^2 in dimensionally critical areas. One such area is the radial stator thickness directly above the current collector region.

The outer radius of the inner stator piece, R_2, is determined from

$$\pi (R_2^2 - R_1^2) = \frac{I}{J_{max}}$$

or

$$R_2 = \left(\frac{I}{\pi J_{max}} + R_1^2 \right)^{1/2}$$

where I = load current = 10,000 amps and J_{max} = 387.5 amps/cm^2. Therefore, $R_2 = 7.036$ cm (2.77 in.). If a 0.0254 cm (0.040 in.) insulation gap is allowed between the inner and outer stator paths, the inner radius of the outer stator, R_3, is then

$$R_3 = R_2 + 0.0254 = 7.061 \text{ cm } (2.780 \text{ in.})$$

The outer radius of the stator, R_4, is then given by

$$\pi (R_4^2 - R_3^2) = \frac{I}{J}$$

or

$$R_4 = \left(\frac{I}{\pi J} + R_3^2 \right)^{1/2}$$

where J = 232.5 amps/cm^2. Therefore, $R_4 = 7.976$ cm (3.14 in.). This defines the maximum required radius of the stator and thus the minimum dewar bore. The inner radius of the larger collector channel, R_5, is given by

$$R_5 = \left(R_4^2 - \frac{I}{\pi J_{max}} \right)^{1/2}$$

Therefore, R_5 = 7.442 cm (2.93 in.). Again, allowing a 0.0762 cm (0.02 in.) liquid-metal gap, the outer radius of the larger collector disk, R_6, is

$$R_6 = R_5 - 0.0762 = 7.366\,\text{cm}\ (2.90\,\text{in.})$$

The outer radius of the cylindrical or drum-shaped section of the rotor, R_7, was chosen to permit a 1.429-cm (0.563-in.) projection of the smaller disk into the channel to allow retention of liquid metal at zero speed. Thus, $R_7 = R - 1.429 = 4.923$ cm (1.938 in.). The inside radius of the drum section, R_8, is then

$$R_8 = \left(R_7^2 - \frac{I}{\pi J}\right)^{1/2}$$

$$R_8 = 3.244\,\text{cm}\ (1.277\,\text{in.})$$

Allowing 0.0762 cm (0.030 in.) for insulation, this results in a shaft radius, R_s, which appears to be adequate for the torque

$$R_s = 3.167\,\text{cm}\ (1.247\,\text{in.})$$

These calculated dimensions served as a design guide subject to modification due to the following thermal, mechanical, or magnetic calculations and analysis of losses in the current collectors. Both stator current paths were arranged to exit at the same end of the machine in order to effectively cancel the magnetic field due to load current, to prevent interaction of this field with the superconducting coil.

MAGNETIC CIRCUIT DESIGN

The magnetic circuit for the subject generator was designed using the dimensional requirements from the Electrical Circuit Design section, and a generous application of insight gained from previous magnet calculations. The following brief analysis was used as a first-cut estimate and later confirmed and specified accurately by computer calculations.

The maximum stator outside radius, R_4, is 7.976 cm (3.14 in.). Allowing a 0.159-cm (0.062-in.) gap, the inner dewar radius, R_9, is

$$R_9 = 8.133\,\text{cm}\ (3.202\,\text{in.})$$

Allowing 1.588 cm (0.063 in.) for the inner dewar wall thickness and 1.016 cm (0.4 in.) for vacuum and thermal insulation, the inner radius of the superconducting coil form, R_{10}, becomes R_{10} = 9.306 cm (3.664 in.). Allowing 0.37 cm (0.150 in.) for coil form thickness, the inner radius of the magnet winding, R_{11}, is R_{11} = 9.687 cm (3.814 in.).

The dimensions of the magnet winding, based on previous experience, were chosen such that the length of each coil in the quadripole pair was approximately equal to the mean winding radius, and the center-to-center distance between the coil pair was equal to the mean coil diameter. The thickness of the winding was chosen to be 2.54 cm (1 in.), again based on previous experience with similarly shaped coils. Then the individual coil dimensions are

Length	–	10.16 cm (4 in.) (each coil)
ID	–	19.385 cm (7.632 in.)
OD	–	24.465 cm (9.632 in.)
Separation	–	20.32 cm (8 in.) (center-to-center).

The outer radius of the dewar was fixed at R_{12} = 17.78 cm (7 in.) which allows a distance of approximately 5.08 cm (2 in.) between the outside radius of the magnet and the dewar jacket. This space is required for support structure and thermal insulation. The shield thickness was determined by assuming that essentially all of the magnet flux was carried by the shield without complete saturation. Assuming an average field of 4.5 T through the entire magnet bore, the flux carried by the shield would be 4.5 x R_{11}^2 = 0.133 Wb. Since the shield begins at the outer dewar radius, R_{12}, the maximum field through the iron shield is assumed to be 1.8 T. The shield outer radius, R_{13}, is given by

$$\pi (R_{13}^2 - R_{12}^2) = \frac{0.133\ Wb}{1.8\ Wb/m^2}$$

$$R_{13} = \left(\frac{0.133}{1.8\,\pi} \pm R_{12}^2\right)^{1/2}$$

$$R_{13} = 0.234 \text{ m } (9.21 \text{ in.})$$

The dewar length was fixed at 55.88 cm (24 in.) to allow adequate room for coil support, and approximately 5.08 cm (2 in.) of iron was allowed at each end for further shielding. It was also decided to construct the shaft of magnetic material which should enhance the flux distribution in the rotor area. This assumption and the above estimates were confirmed using the TRIM* computer program, which calculates the exact flux distribution including the effects of iron saturation. The results of this calculation are shown in the flux plot in Figure 6, and the values of interest are given below for a magnet current of 135 amps.

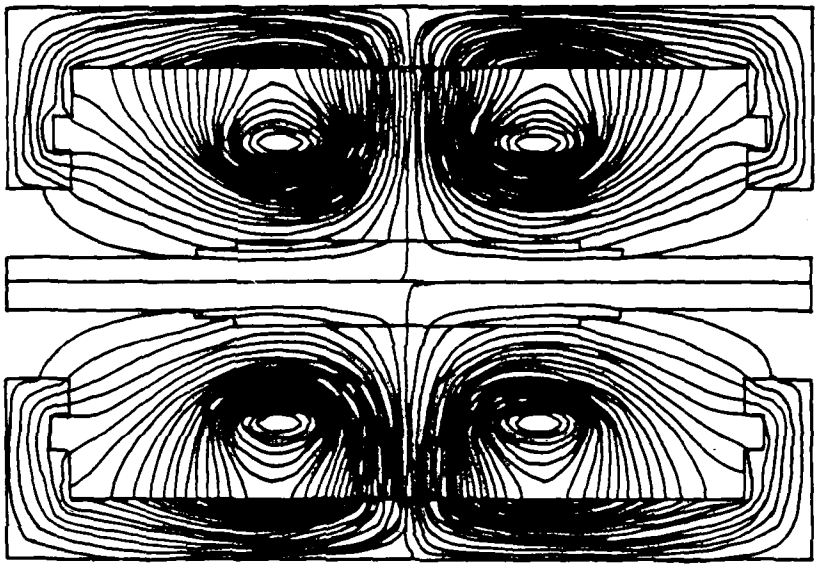

Figure 6 — Generator Flux Plot

Ampere turns in coil	–	742,500
Maximum field in coil	–	58 kG
Flux through small disk	–	0.0611 Wb
Flux through large disk	–	0.0779 Wb
Total flux intercepted	–	0.139 Wb.

Since the flux required through both rotor disks combined to produce 30 volts at 19,500 rpm is

$$\phi = \frac{60\ V}{N}$$

where N = rpm and ϕ = flux, or

$$\phi = \frac{(60)\ (30)}{19{,}500} = 0.0923\ \text{Wb}$$

*Magnetic analysis procedure using relaxation technique to solve two-dimensional magnetic field problems (developed at Argonne National Laboratory).

It is clear that the coil is quite adequate to produce the flux required if the operating point of the superconducting wire is within the critical current/field limitations. The 742,500-amp turns per coil was selected on the basis of using 5,500 turns per coil at 135-amp current. As can be seen in Figure 7, this operating point is below the critical $I - H$ curve. Note that this operating point was selected somewhat arbitrarily and is not consistent with the design requirements. The actual operating point of the magnet derived from the 0.0923-Wb requirement detailed above, assuming a linear field-current relationship, and accounting for the large disk at one end is only 89.64 amps to produce 30 volts at 19,500 rpm. This then determines the actual operating point of the magnet. Note that the selection of an operating point for the superconducting coil is somewhat arbitrary since it was not determined a priori but as a consequence of several assumptions, and preselected design parameters. Since the actual operating point is somewhat lower than the one initially assumed, it would be possible to reduce the amount of wire in the superconducting coil. However, since the machine size and weight is not particularly sensitive to small variations in the coil size, parameters assumed and calculated above were retained, which should provide a comfortable margin in the superconducting coil performance. Further details relating to the superconducting coil design are given in the section entitled "Superconducting Magnet."

LIQUID-METAL CURRENT COLLECTOR DESIGN

Theoretical analysis of the behavior of liquid-metal current collectors is an extremely complex problem, particularly where high magnetic fields are present. Previous reports[10-12] provide detailed consideration of the effects to be considered, so only a brief treatment is given here. Calculation of liquid-metal current collector losses is included elsewhere in this report.

Several loss mechanisms are present in the subject current collector situation. Consider the following and Figure 8. Assume a disk tip velocity, $\vec{V}$; axial magnetic field, $\vec{B}a$; radial magnetic field, $\vec{B}_r$; and a load current in the radial direction of current density, $\vec{J}$. The principal loss mechanisms are as follows.

1. Viscous loss resulting from purely hydrodynamic effects.
2. Viscous loss resulting from magneto-hydrodynamic forces on the liquid metal proportional to $\vec{J} \times \vec{B}_a$.
3. Joule losses resulting from the liquid-metal resistivity proportional to $\vec{J}^2$.
4. Joule losses resulting from circulating currents which are created by the voltage generated across the finite width of the collector disk rotating in the magnetic field, $\vec{B}_r$, and overlap of the liquid metal down the sides of the collector disk which shorts out the voltage generated by the disk rotating in the axial field, $\vec{B}_a$.
5. Viscous losses resulting from the circulating currents giving rise to a change in velocity via an interaction with the axial magnetic field.

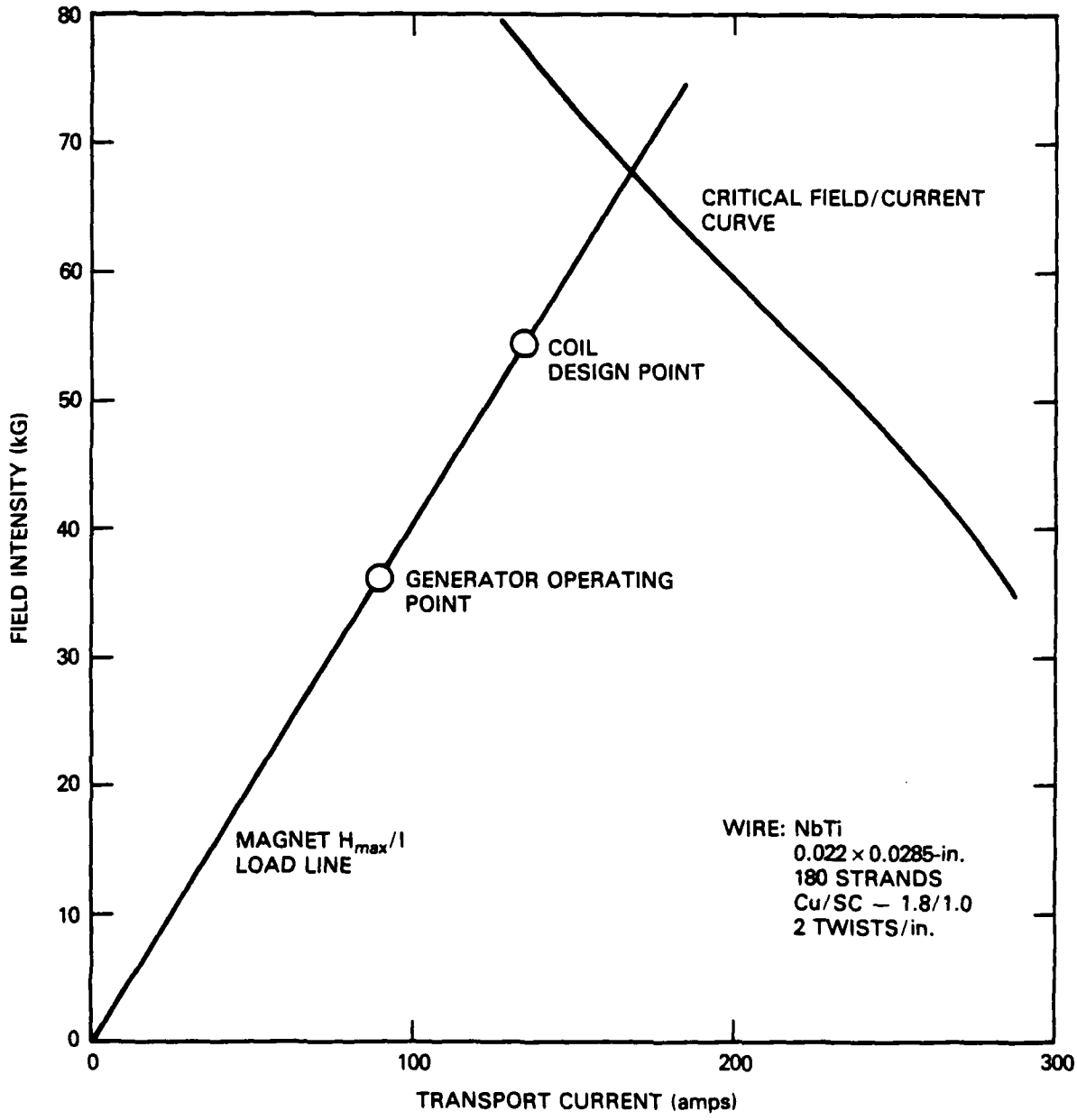

Figure 7 — Superconducting Wire Properties (Measured Short Sample at 4.2 K)

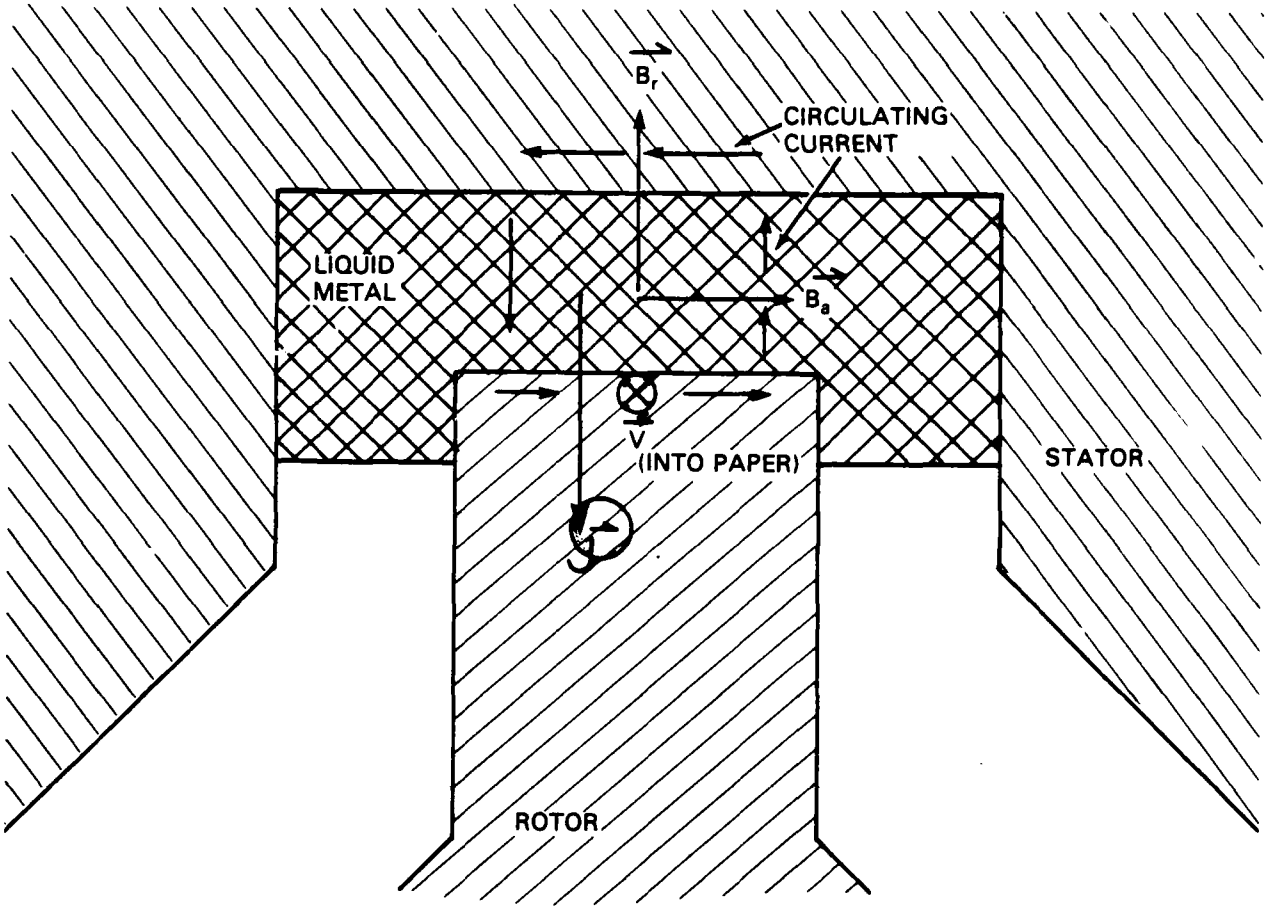

Figure 8 — Current Collector Geometry and Nomenclature

The viscous losses and circulating current losses are likely to predominate in a high-speed generator, since they are first order effects and increase with tip velocity. Since viscous losses are proportional to the surface area in contact with the liquid metal and circulating current losses are proportional to the width, it is logical to minimize the total collector area by making the disk width very narrow, which results in a high current density, $\vec{J}$. This tradeoff may be carried to the point where the ohmic losses in the liquid metal begin to dominate. A disk tip width for the generator of approximately 0.457 cm (0.18 in.) was selected initally, resulting in a current density of 542.5 amps/cm^2 in the collector region at a 10,000-amp load current. At the projected 25,000-amp level, this results in about 1356.2 amps/cm^2 which appears to be a reasonable limit. It is expected that the optimum collector width will have to be determined experimentally.

Another important factor in the current collector design is the collector geometry. Since the circulating currents are proportional to the radial component of the magnetic field, or, to be more exact, the component of field perpendicular to the collector disk tip, this loss component may be minimized by locating

and shaping the disk tip so that it is parallel to the local magnetic field vector everywhere on its surface, thus negating any perpendicular field component.

The collector geometry is also a factor in the stability of the moving collector fluid at high rotor tip speeds. In order to assure hydrodynamic stability, the collector geometry must be designed to cause any portion of the liquid which tends to be ejected from the collector to be returned to the active region.

A significant effort is presently being brought to bear on these problems, and details of the final generator collector geometry will be fixed at the latest possible time using the best results available at that time. (See Appendix A for most recent results.)

The current collector losses are estimated in a following section using the analysis procedures of Rhodenizer.[12] These calculations indicate an expected loss of approximately 5 kW per collector site. As indicated, the collector sites and stators are split in half axially for assembly purposes.

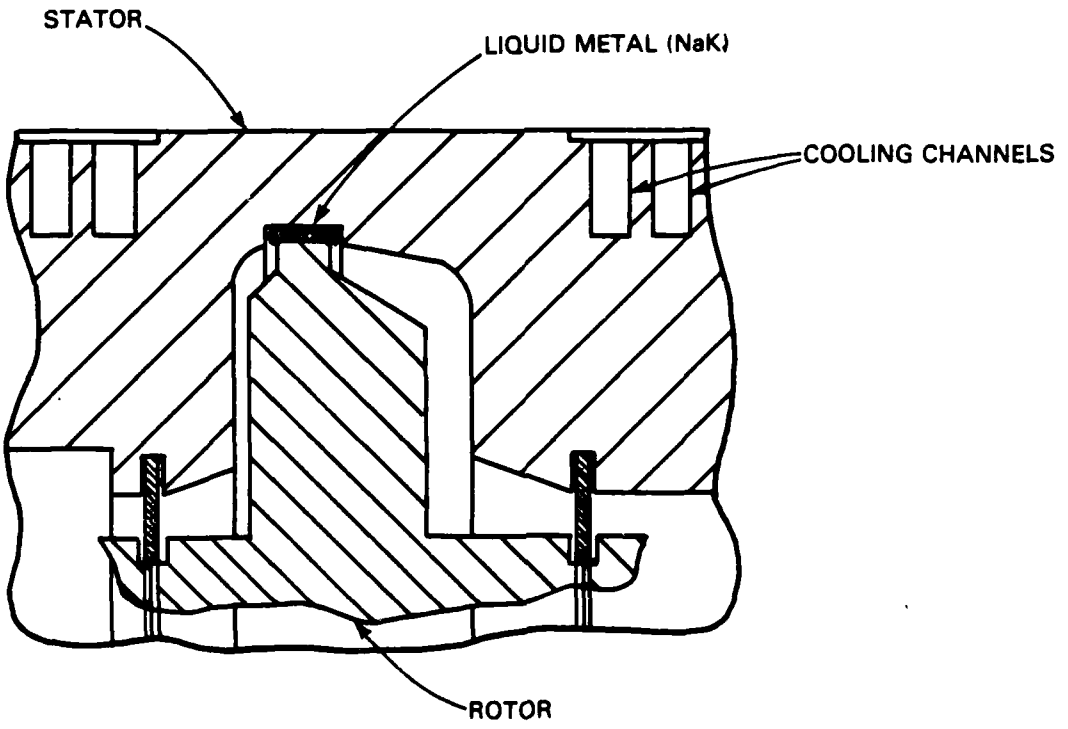

Figure 9 — Liquid-Metal Current Collector For Superconducting Acyclic Generator

Figure 9 is an enlarged cross section of the generator collector as presently designed. The sodium potassium liquid metal is inserted into each collector region via a tube running axially through the stator. A redundant fill tube has also been included to allow insertion of a thermocouple and separate access for

clean up procedures. In addition, the second NaK fill tube to each collector will allow circulation or replacement of NaK if necessary. The center line of the collectors are located approximately 0.5 cm (0.2 in.) outboard of the center line of each magnet. Computer calculations indicate that the radial component of the magnetic field in the collector region is a minimum at this point.

SUPERCONDUCTING MAGNET

The superconducting magnet for the superconducting generator was designed and constructed at Annapolis. From the outset of the design effort, the magnet was assumed to be a lightweight, very high current density device, which led to rather severe requirements on the magnet structure and winding. The generator design assumed a magnet capable of carrying a current density of over 28,000 amps/cm^2 overall. Prior to final detailed design of the magnet itself, a test program was conducted to determine suitable wire size, shape, winding techniques, and other details of construction methods. The results of this test program are included in an upcoming report.[8]

The generator magnet consists of two solenoids 19.35-cm ID x 24.43-cm OD x 10.16 cm long (7.62 x 9.62 x 4 in.). These two coils are wound on a common coil form with an 20.32-cm (8-in.) distance between centers. The opposite currents in each solenoid create a quadripole field distribution. The magnet was designed for an operating current of 135 amps and a theoretical critical current of 160 amps. The superconducting wire selected consists of 180 NbTi alloy strands imbedded in a copper matrix, with a copper to superconductor ratio of 1.8 to 1.0. The wire is twisted two times per inch to increase stability. As a result of the experimental test program, it was determined that wire with a rectangular cross section resulted in a very homogeneous winding with improved mechanical integrity, neater layer-to-layer transitions, and improved packing factor as compared to round wire. The wire was therefore specified to have a rectangular cross section of 0.5588 x 0.7239 mm (0.022 x 0.0285 in.) with a 0.0203-mm (0.0008-in.) formvar insulation thickness. An enlarged cross section of this wire is shown in Figure 10.

The coil form was constructed from a 316 stainless steel forging in a single piece, to eliminate the uncertainty associated with the strength of welds at helium temperature. The coil form is a highly stressed structure with a calculated maximum stress of 131 x 10^6 N/m^2 in some sections due to the 178,000-N (40,000-lb) force between coils at a 135-amp magnet current. The average magnetically induced hoop stress in each coil was calculated to be 51.7 x 10^6 N/m^2 (7500 psi) at a 135-amp current. Therefore, a great deal of effort was expended to devise a suitable technique for preventing relative motion of the magnet wires, since even very small relative motions may cause a coil quench due to the frictional heat generated. The winding technique includes regulation of the wire tension during winding, changing tension to account for stress relief of the inner wire layers when additional layers are added, inserting a layer of fiber glass cloth between layers

during construction, and vacuum impregnation of the entire coil after winding is completed. A 0.254 cm thick (0.10-in.) layer of epoxy impregnated fiber glass is wound on the outer diameter of the magnet to increase the resistance of the magnet to hoop stresses.

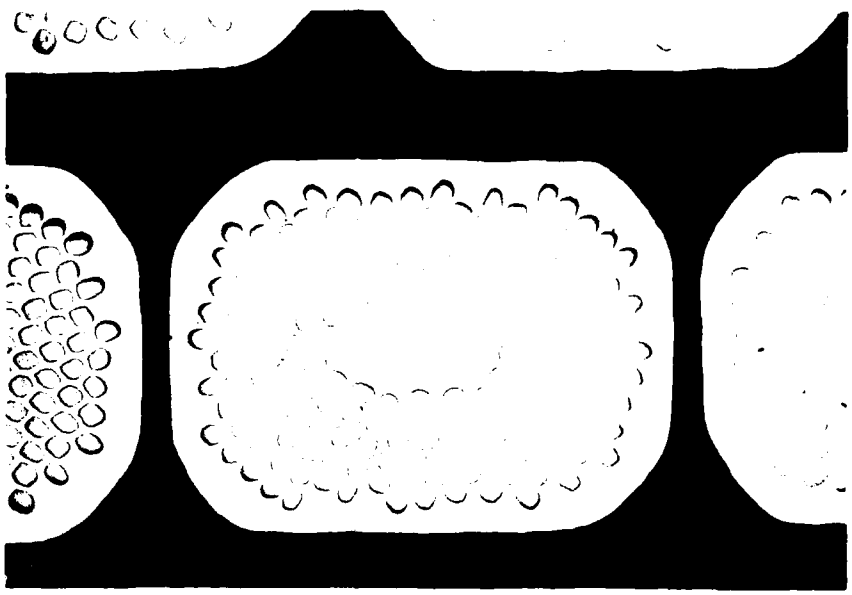

Figure 10 Superconducting Wire Cross Section

A test coil equivalent to one half of the generator magnet was wound and tested using the above procedures. After complete potting, the magnet quenched at 150 amps as compared to a calculated critical current of 158 amps. Training was observed in the magnet, but appeared to be permanent in that the measured quench current never decreased after warming to room temperature, recooling, and retesting. The inability of the test magnet to reach full critical current is at least in part attributable to some slight damage which occurred during repotting process, which was required as a result of a construction error. These results provided sufficient confidence to go ahead with the generator coil winding. Figure 11 shows the generator coil during various stages of construction and testing. Figure 12 is a cross section of the test coil which was cut apart after testing for visual inspection. Note the absence of any voids between wires, indicating the complete impregnation of the coil.

Figure 13 is a photograph of the generator coil form, indicating the region occupied by the windings. Figure 14 is a picture of the completed coil. Figure 15 is a view of the generator coil in a test fixture. The tie bolts shown serve as a substitute for the sheet metal can which will be welded to the coil form to form the helium reservoir. The tie bolts or can provide additional restraint against the force between the coils.

Figure 11a Winding Procedure

Figure 11 (Continued)

Figure 11b Completed Coil Prior to Vacuum Impregnation

Figure 11 (Continued)

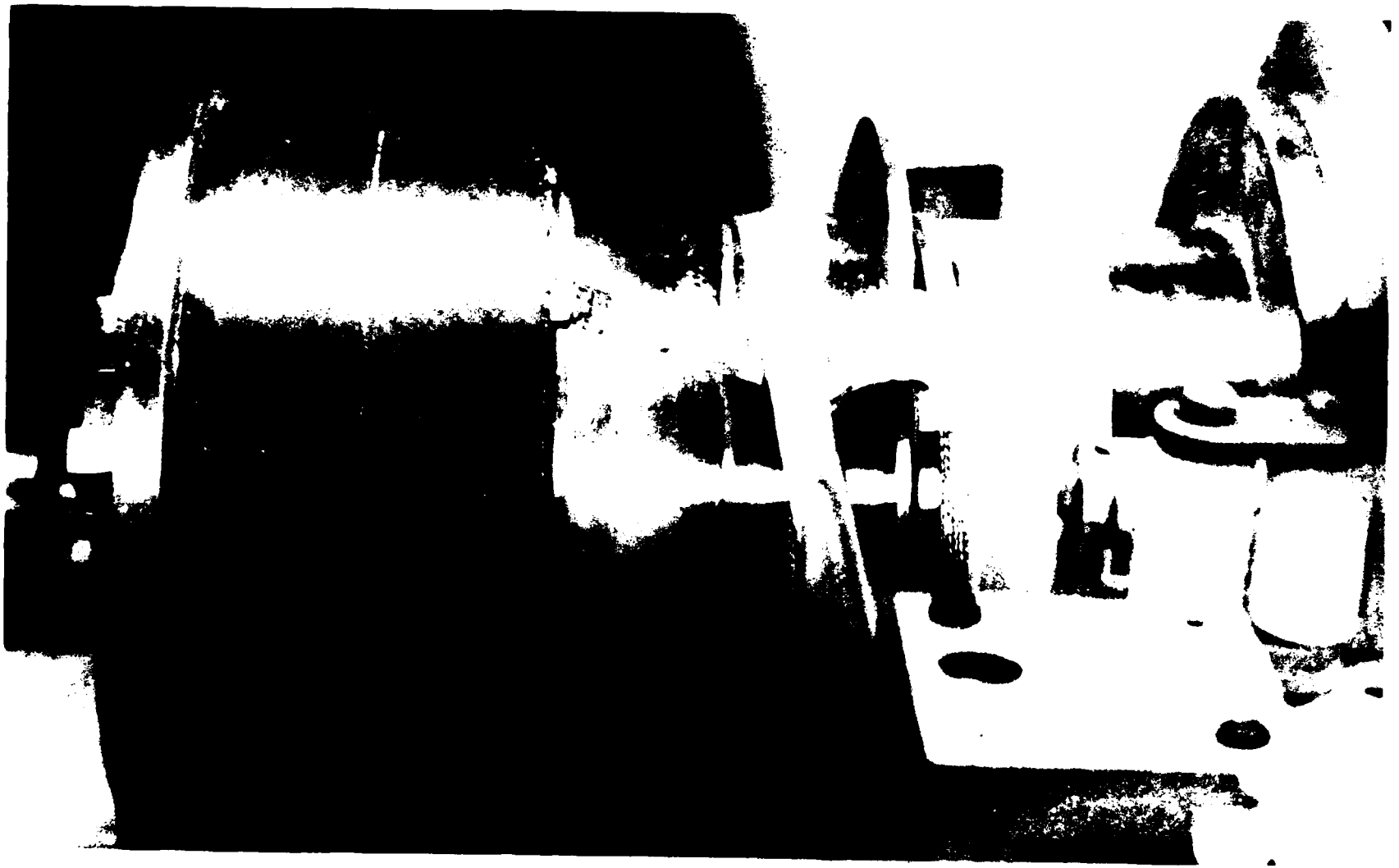

Figure 11. Completed Coil Head After Vacuum Pressure Impregnation

Figure 5 — Current Collection Configuration Rotating Disk and Channel

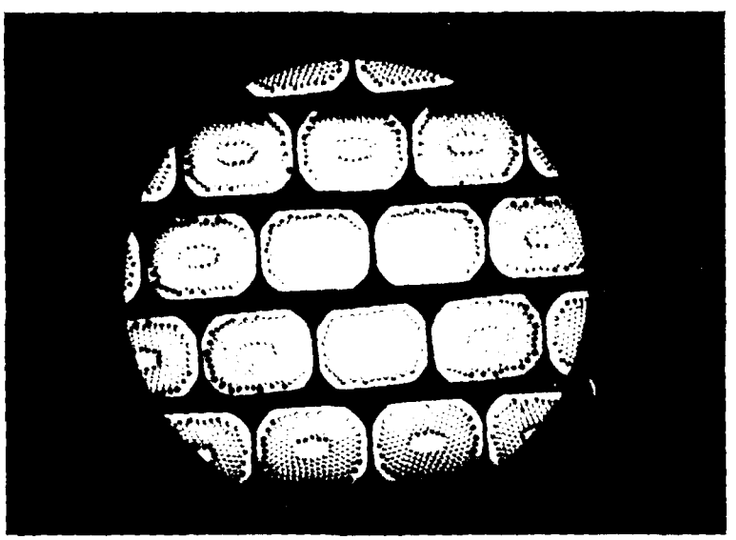

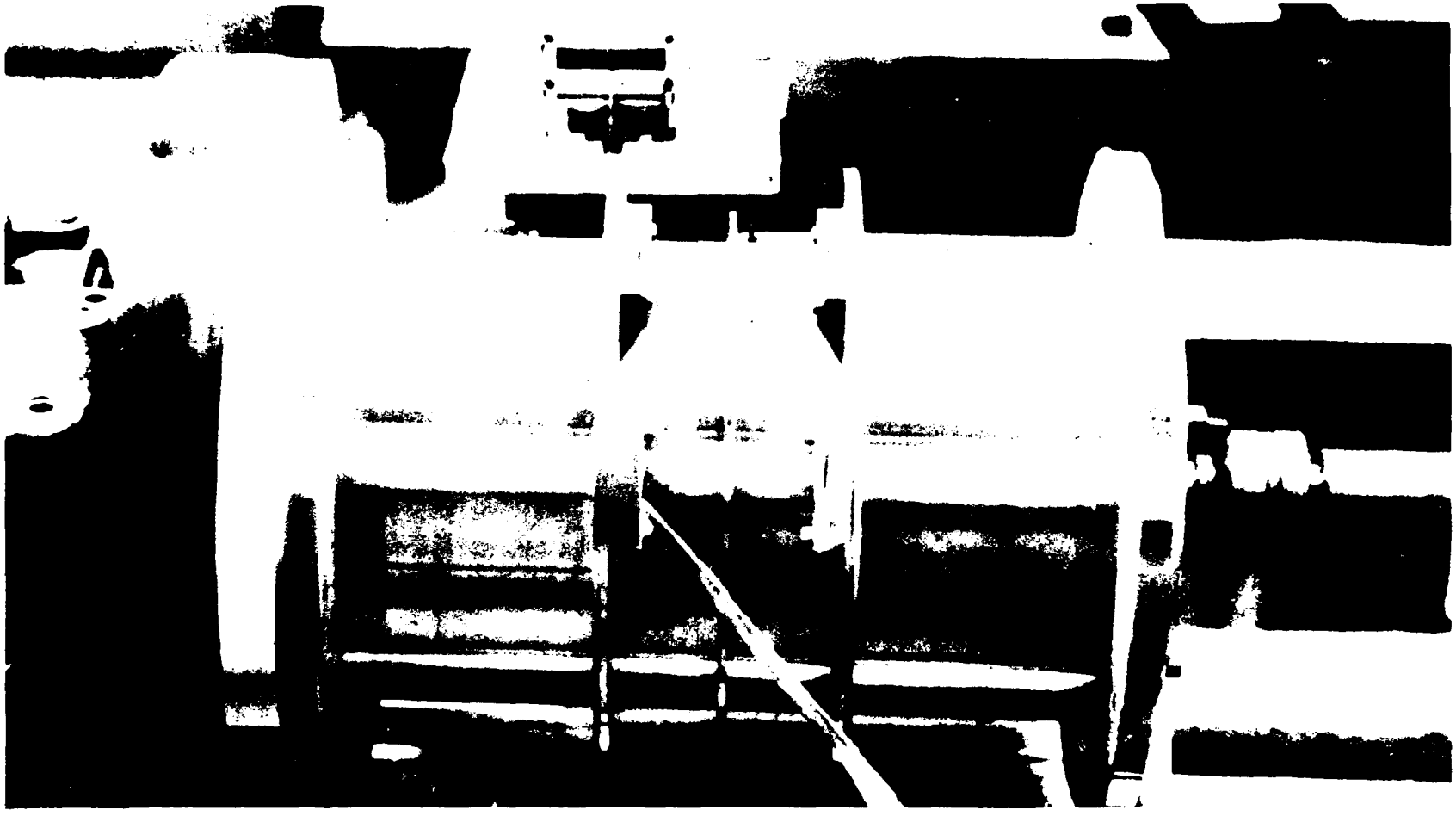

Figure 13 Generator Coil Form

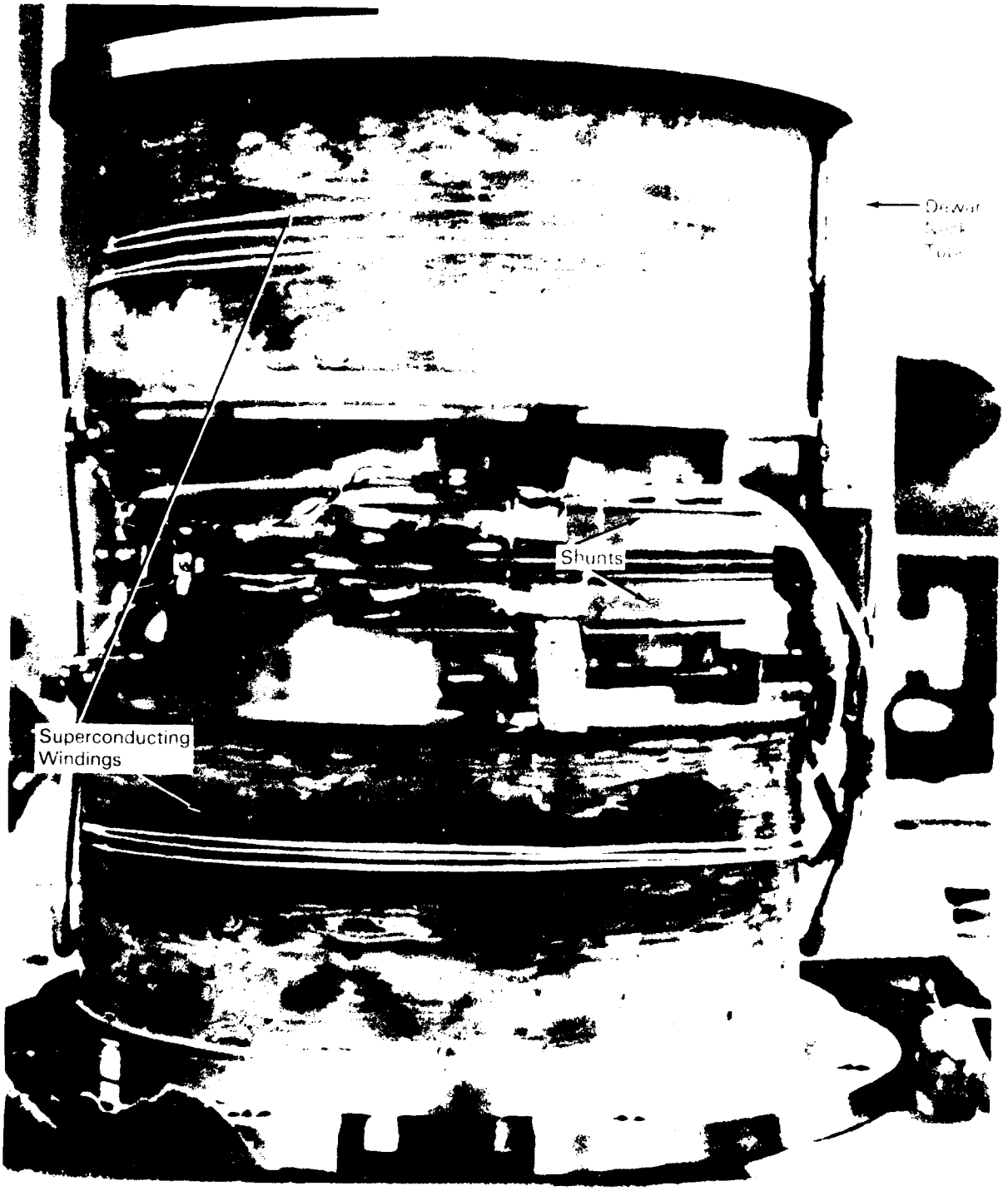
Shunts
Superconducting
Windings

Figure 15. Generator Coil in Test Fixture

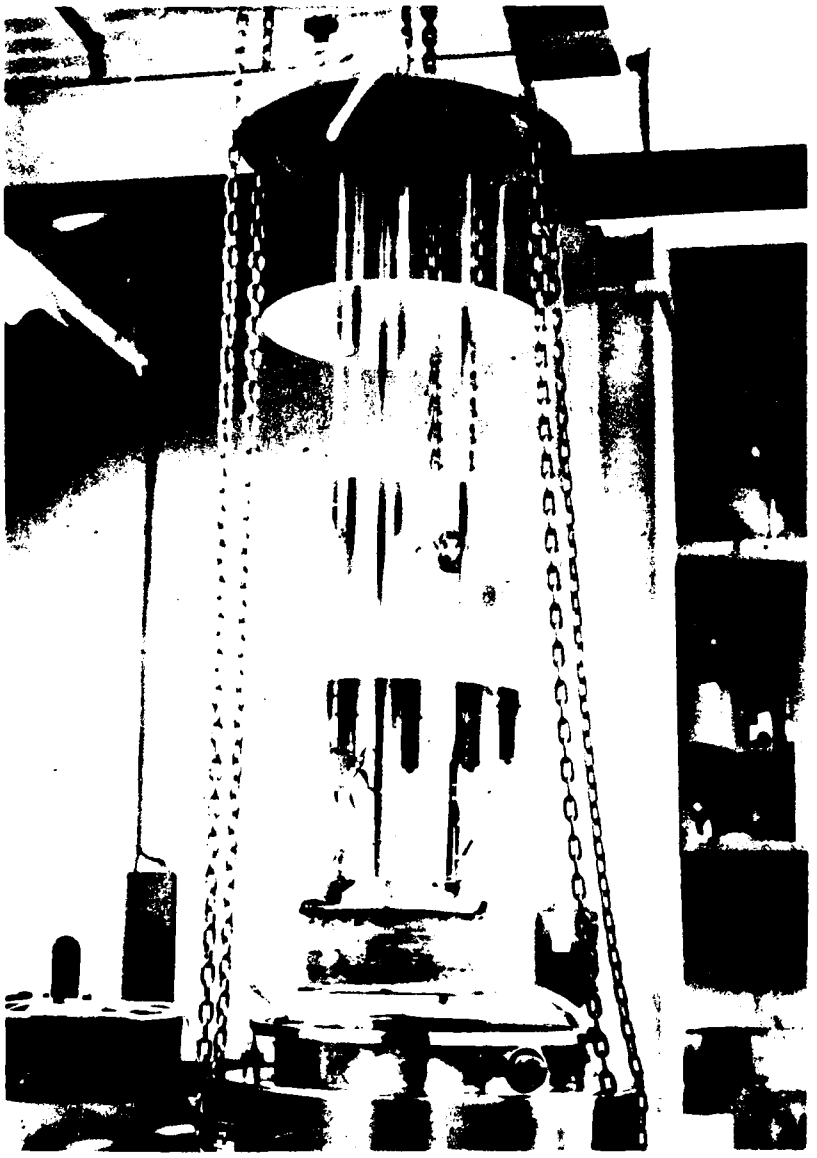

The generator coil was tested in the setup shown in Figure 16. After several quenches due to training, a steady superconducting current of 135 amps was carried by the coil without quenching. A maximum current of 145 amps was put through the coil. No effort was made to go beyond this current due to the rapid increase in forces, and fear of damage to the coil form structure due to these forces. The calculated critical current of the magnet is 160 amps.

Judging from the experience gained from the test coil, each half of the generator coil, and the entire generator coil, no additional training of the generator coil is expected. The vital statistics of the generator magnet are summarized in Table 1.

The superconducting coil was designed to provide the required flux as an air core magnet at a nominal current of 135 amps. Additional magnetic calculations indicate that, when the effect of iron present in the generator is accounted for, and an accurate flux plot made, the required magnet current to produce 30 volts is only 89.64 amps. The magnet as designed and constructed thus has more than adequate margin in terms of flux-producing capability. Further details of the magnet/dewar system are contained in the following section.

TABLE 1 — GENERATOR MAGNET PARAMETERS

Wire	
Size	0.588 x 0.723 mm (0.022 x 0.0285 in.)
S/C Material	NbTi
Copper S/C Ratio	1.8/1.0
Twists	0.8 cm (2 in.)
Insulation	0.020 mm (0.0008 in.) formvar
Coil	
Coil Form Material	316 Stainless Steel
Size of Windings (Each)	19.35-cm ID x 24.43-cm OD x 10.16-cm Long (7.62 x 9.62 x 4 in.)
Center-to-Center Spacing	20.32 cm (8 in.) on axis
No. of turns	5500 (each coil)
Design Current	135 amps
Nominal Operating Current	89.6 amps
Calculated Critical Current	160 amps (air care)
Max Field in Windings	5.8 T at 135 amps
Inductance	11 H
Total Stored Energy	100.2 kJ at 135 amps
Potting Material	Epoxy (with fiber glass between layers)
Packing Factor (Bare Wire)	0.766
Current Density (Overall) at 135 Amps	28,500 amps/cm^2
Current Density in Superconductor at 135 Amps	104,000 amps/cm^2
Stainless Steel Shunts	Two on each coil, 2 ohms each

DEWAR SYSTEM

The dewar system for the superconducting generator performs two functions. It must provide sufficient thermal insulation to keep the magnet at liquid helium temperature, and at the same time restrain the magnet from moving relative to the generator structure due to shock, vibration, and magnetic forces. These two requirements are basically incompatible; i.e., the more support required for the magnet, the greater the heat leak into the liquid helium region. The dewar system design is therefore a compromise between these requirements. The dewar system was specified by the Center in terms of dimensions and mechanical requirements. The detailed design was done by an outside contractor, Develco, Incorporated, Mountain View, California. For the particular case of the subject generator, the resonant frequency of the magnet support system in the dewar became the principal design problem. Due to the 19,500 rpm speed of the generator, no resonant frequencies were allowable below 350 Hz. This requirement, however, led to a very stiff support system design which had a calculated heat load equivalent to 8 ℓ/hr of liquid helium. It was determined that a support system which had a resonant frequency below 75 hz would be acceptable, because the generator would usually operate above this resonance. In the interest of minimizing the heat load, the second option was chosen for construction. (Subsequent analysis of different magnet support techniques indicate that a high frequency support system might be constructed with a reasonable heat leak using thin metallic or fiber-glass-epoxy composite conical supports. Details of such a system are under investigation and will be reported later.) Another requirement of the magnet support system is that the magnet be precisely located with respect to the shield to prevent unbalanced magnetic forces from creating additional stress in the supports. The support system was therefore designed so that each support was adjustable to allow accurate centering of the magnet under operating conditions.

The general layout of the dewar system is shown in Figure 17. The helium vessel is formed by the coil with a 0.16-cm-thick (0.062-in.) stainless steel shell welded around the outer flanges. Access to the cold region is gained through an axial neck tube located near the outer radius of the magnet and enclosed by a bump in the helium vessel outer wall.

This assembly is supported by a series of eight rods, four extending from each end of the coil form face to the outer dewar end flange, as shown in Figure 18. These rods are 0.381 cm in diameter and 12.7-cm long (0.150 and 5 in.). The support rod material is Ti-6Al-4V alloy which has very high yield strength and relatively low thermal conductivity. Each of these rods is attached to an externally adjustable lever mechanism to allow adjustment of the coil location within the dewar. The helium vessel is surrounded with several layers of superinsulation consisting of alternate layers of aluminized mylar and thin nylon material, which reduces considerably the heat leak into the dewar due to thermal radiation. Included in the insulation system are two thin copper radiation shields located within the layers of superinsulation. Each of these shields is heat-sinked to the cold helium vapor escaping from the helium vessel. These shields are also thermally

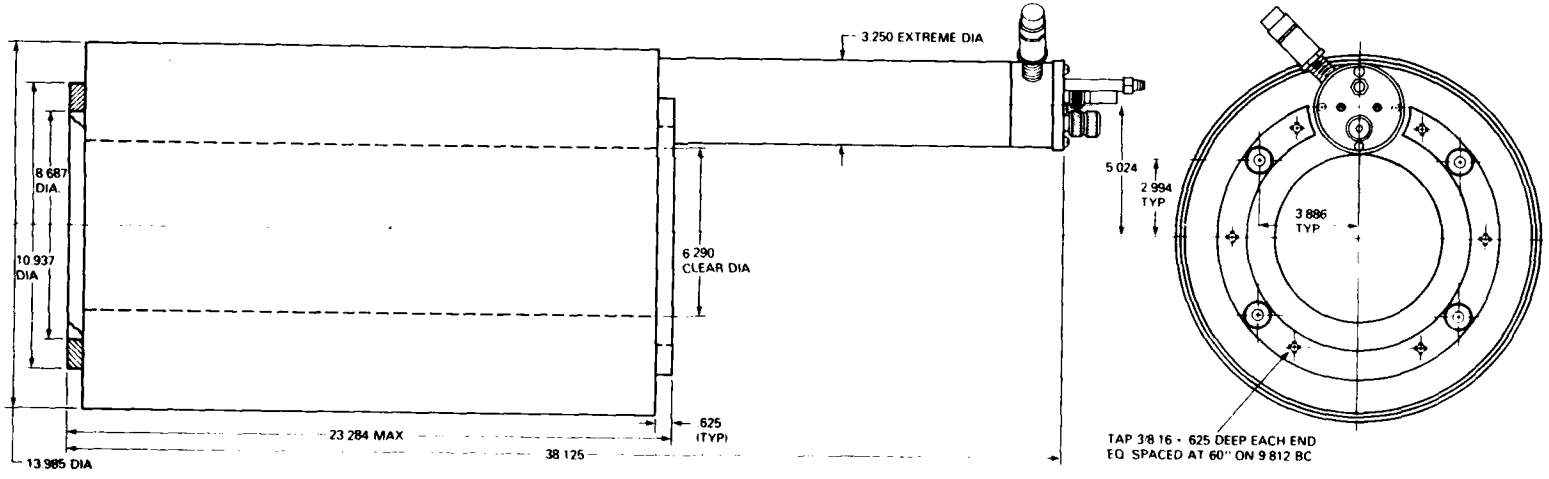

Figure 17 – Dewar System General Layout

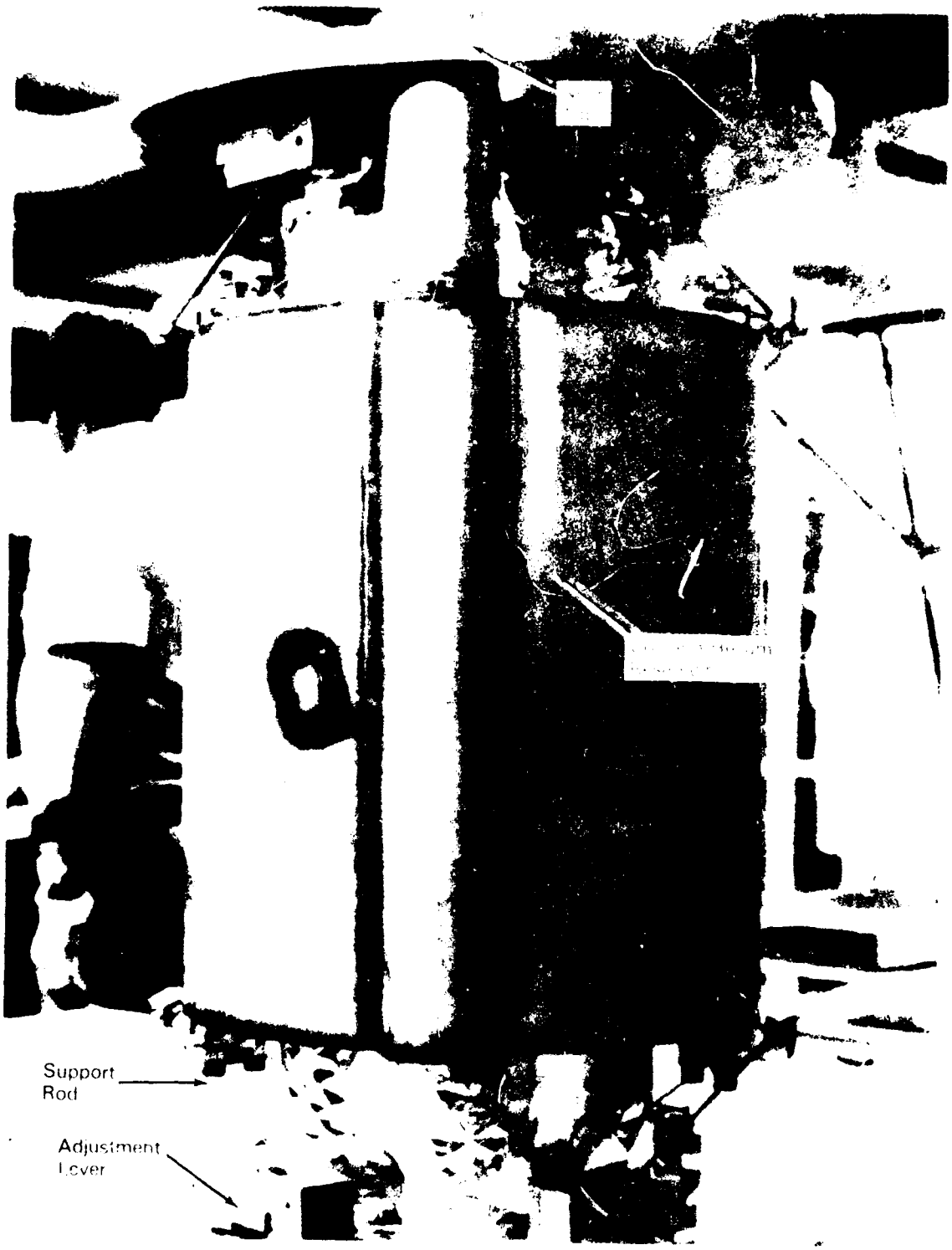
Support Rod
Adjustment Lever

shorted to the magnet support rods at precalculated distances along their length. The copper radiation shields thus perform two functions. First, they intercept thermal radiation entering through the dewar walls, convert it to heat, and eject this heat to the cold helium boil-off gas. Second, they intercept heat coming down the magnet support rods and transfer it also to the helium boil-off gas. Ideally, the amount of heat entering the liquid helium causes just enough cold gas to be generated to absorb the heat removed by the vapor-cooled shields and warm the gas to room temperature, thus utilizing the entire refrigeration capability of the helium. An additional heat leak, due to the current leads for the superconducting magnet, must also be taken into account when trying to obtain such a heat balance. Cold helium gas is also used to intercept heat coming down these leads. The thermal design of the dewar system attempted to strike the above balance between liquid helium and gaseous helium heat interception. The resulting design indicates a theoretical consumption of 0.7 ℓ/hr of liquid helium including 0.4 ℓ/hr due to the current leads, although actual performance is somewhat greater due to the limitations of construction techniques.

Figure 19 shows the completed dewar. The dewar neck extends axially through the generator magnetic shield between the inner and outer radii of the dewar. All connections to the interior of the dewar are contained within the diameter of the neck to allow disassembly of the generator without interrupting the dewar vacuum jacket. The coil current is carried through two vapor-cooled leads. The current leads are threaded at the cold end to allow insertion and removal if necessary. A fixture mounted on the coil form shown in Figure 20 contains threaded sockets for the current leads and a receptacle for the helium transfer line. The arrangement is such that the transfer line may be pulled back a fraction of an inch to allow the liquid helium to enter the top of the helium vessel rather than at the bottom through the extension tube shown in Figure 20. This prevents helium gas entrapped in flowing liquid from bubbling through the liquid already present which would increase the boil-off rate, especially if a transient volume of warm gas were to come through the transfer line, e.g., when changing helium supply dewars. The superconducting coil is instrumented with temperature and liquid level sensors to aid in controlling the coil temperature and helium flow rate.

The thermal and mechanical analysis of the dewar system are included in Appendix B. Table 2 is a summary of pertinent dewar system characteristers.

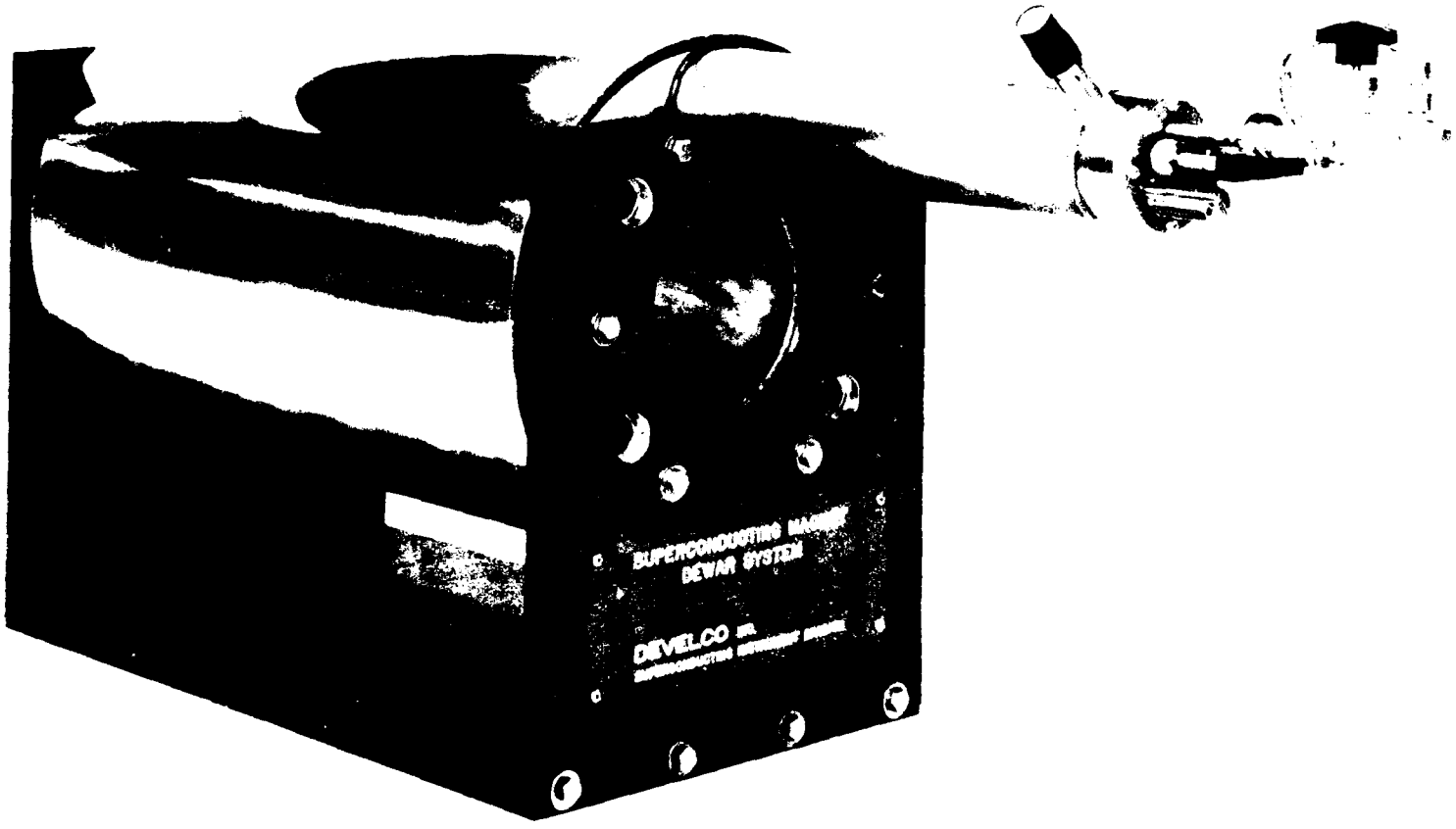
SUPERCONDUCTING MAGNET
DEWAR SYSTEM
DEVELCO INC.

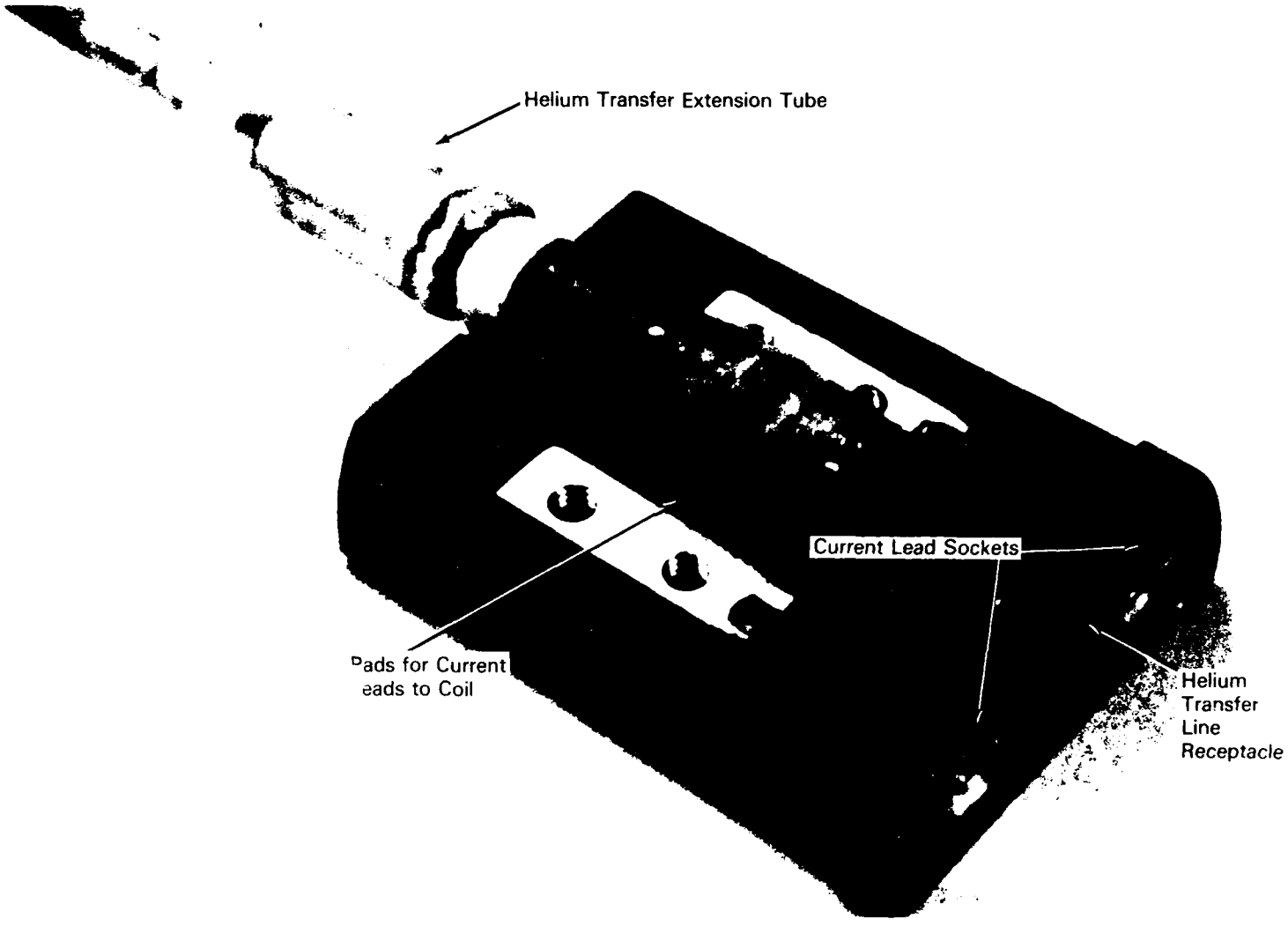

Figure 20 – Magnet Current Lead Termination

TABLE 2 — GENERATOR DEWAR PARAMETERS

Physical	
Outside Diameter, cm (in.)	35.56 (14.00)
Inside Diameter, cm (in.)	16.03 (6.312)
Overall Length, cm (in.)	96.84 (38 1/8)
Length of Dewar Section, cm (in.)	59.14 (23.284)
Neck Tube Offset, cm (in.)	12.76 (5.024)
Neck Tube Clear Diameter, cm (in.)	8.26 (3.250)
Weight (Including Magnet), kg (lb)	88.43 (195)
Mechanical	
Maximum g-Load (Weakest Direction), g	15
Maximum g-Load (Radial Direction), g	27
Maximum g-Load (Axial Direction), g	28
Resonant Frequency, Hz	
Radial	88
Axial	87
Torsional	143
Maximum Torsional Load, N•m (ft-lb)	2650 (1956)
Suspended Weight, kg (lb)	45.53 (100.4) operating
Thermal	
Liquid Helium Consumption (Operating), l/hr.	1 ¼ at 135 amps
Electrical Monitors	
Magnet Voltage	5 monitor points
Liquid Helium Level	2
Calibrated Magnet Temperatures	Two germanium resistors
Rough Magnet Temperature	5 Copper Constantan Thermocouples

EFFICIENCY AND LOSSES

This section delineates the anticipated loss mechanisms in the superconducting generator and an estimate of their magnitude at the nominal operating points. The identifiable intrinsic loss mechanisms are:

P_B – Bearing friction

P_S – Seal friction

P_W – Windage

P_{CX} – Liquid-metal current collector losses

P_J – Joule heating in conductors.

Bearings

No analysis was conducted of bearing losses during design. Estimates obtained from suppliers indicate that, with proper lubrication, each bearing should have a frictional loss of 150 W. This estimate is based on the use of 50-mm bore, extra light series, angular contact bearings, with an axial preload of 400 N and a radial load of 156 N at 19,500 rpm, using oil-mist lubrication. Assuming a velocity-squared dependence of the loss, and two bearings

$$P_B = 7.5 \times 10^{-7} N^2 W \tag{4}$$

where N = rpm. At 19,500 rpm, P_B = 300 W.

Seals

Seal friction losses are difficult to calculate with any degree of confidence. Since all seals used in the generator are noncontacting types, the only loss associated with seals should be windage friction at any significant speed. An admittedly arbitrary penalty of 50 W at 19,500 rpm has been assessed each seal for estimation purposes. This loss may be attributed to rubbing friction at low speeds and windage at high speeds. For four seals, this results in an assumed power loss relationship

$$P_S = 5.26 \times 10^{-7} N^2 W \tag{5}$$

assuming a square law velocity dependence and four seals. At 19,500 rpm, P_S = 200 W.

Windage

Only windage losses in the cover gas will be considered, because clearances elsewhere in the machine are large enough so that windage should be negligable in comparison. Assuming an argon cover gas at 2 atmospheres, the windage loss may be calculated after establishing the nature of the flow.
The following constants and variables are relevant to the calculation.

f = Fanning friction factor = 0.007

N = rpm

N_r = Reynolds number

D_h = Hydraulic diameter

$\overline{V_c}$ = Average fluid velocity

A_s = Surface area in contact with gas = 0.075 m^2

G_r = Rotor stator clearance = 7.6×10^{-4} cm

P_w = Windage power loss

μ_A = Absolute viscosity of argon = 0.24×10^{-4} $N/m\text{-}s$

P_A = Argon density at 2 atmospheres = 4.22 kg/m^3.

Assuming $\overline{V_c}$ is one half the rotor tangential velocity and a rotor radius of 0.0523 m,

$$\overline{V_c} = 2.74 \times 10^{-3} N/m\text{-}s.$$

The hydraulic diameter is taken as twice the rotor stator clearance

$$D_h = 2 G_r = 1.52 \times 10^{-3} m.$$

The Reynold's number is

$$N_r = \frac{P_A \overline{V}_c D_h}{\mu_A} = 0.732 N.$$

At N = 19,500 rpm, N_r = 14,280. Thus turbulent flow may be expected at most operating speeds. Under these conditions, power loss is given by

$$P_W = \mu_A f \overline{V}_c A_s = 4.56 \times 10^{-11} N^3 W. \quad (6)$$

At N = 19,500 rpm, P_W = 338 W.

An enlarged view of a generator current collector is shown in Figure 21. Making reference to the nomenclature in Figure 21 and Table 3, the following analysis is applied to the current collector losses.

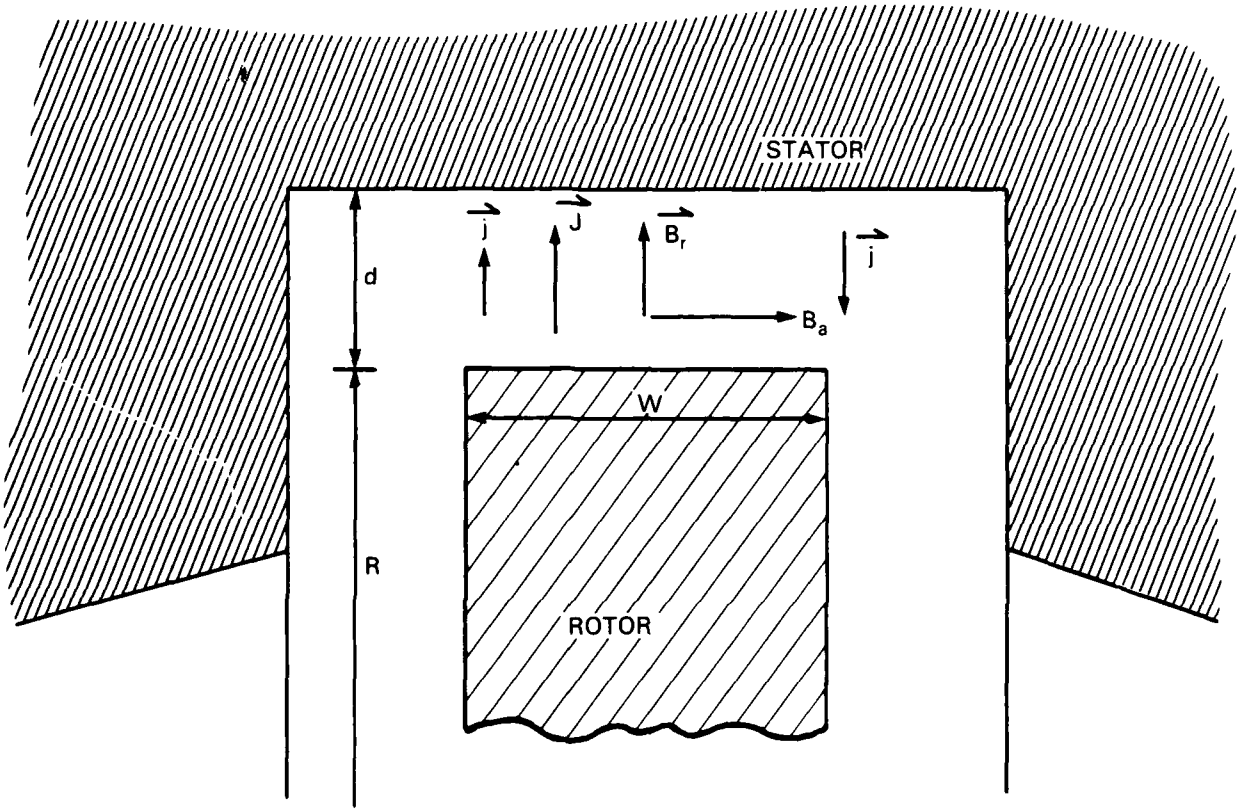

Figure 21 — Liquid-Metal Current Collector Details

This analysis follows that developed previously.[12] An a-priori assumption has been made that none of the liquid metal is in contact with the sides of the rotating disk in the current collector. This assumption is based on the fact that any liquid in contact with these surfaces would be subjected to a centrifugal force tending to accelerate it radially outward toward a region where the rotational velocity of the fluid is lower, i.e., toward the stationary wall of the collector channel. Since there is no force to oppose the resulting pressure gradient, the liquid should form a surface profile similar to that indicated in Figure 22. At sufficiently high speed, one might extend this reasoning to conclude that the liquid would completely separate from the rotor tip. Proper shaping of the collector geometry and a sufficient amount of *NaK* in the collector should prevent this from occurring. For purposes of this analysis, it will be assumed that only the disk tip is in contact with the liquid and that all losses occur at this interface.

TABLE 3 LIQUID METAL CURRENT COLLECTOR PARAMETERS

P_{cc}	Ohmic power loss due to load current
J	Current density in liquid metal
d	Collector radial gap, 5.08 x 10 $^{-4}$ m
A_c	Collector tip surface area, 1.82 x 10 $^{-3}$ m^2
σ	Conductivity of *NaK*-78, 2.2 x 10^6 *ohm/m*
I	Generator load current
N_r	Reynolds number
ϱ_{NaK}	*NaK* - 78 density, 850 kg/m^3
$\overline{V}$	Average fluid velocity
D_h	Hydraulic diameter in collector
η_{NaK}	*NaK* viscosity, 4.7 x 10 $^{-4}$ kg/m·s
N	Generator rpm
P_{cv}	Viscous drag power loss in collector
f	Fanning friction factor, 0.007
Ba	Axial component of generator field in collector region, 3.24 T at I_f = 89.64 amps
P_{MHD}	Viscous drag power loss due to MHD effects
P_{cc}	Circulating current losses in collector
W	Collector disk tip width, 4.57 x 10 $^{-3}$ m
B_r	Radial component of field in collector, 0.1 T at I_f = 89.64 amps
P_{ccv}	Viscous drag power loss due to circulating currents
I_f	Field current in magnet

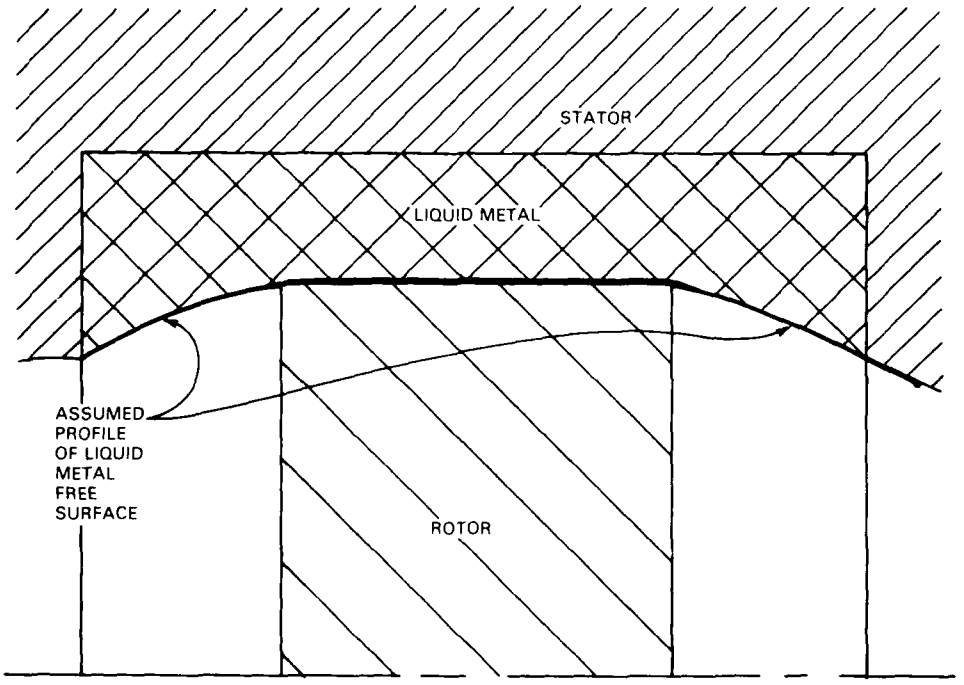

Figure 22 Liquid Metal Free Surface Profile

The loss mechanisms treated are listed and described in detail below.

1. Ohmic losses in liquid metal due to load current.
2. Viscous losses in liquid due to mechanical rotation.
3. Viscous losses in liquid due to velocity introduced by load. Current interaction with the axial magnetic field.
4. Ohmic losses due to circulating currents caused by motion of liquid metal interacting with the radial magnetic field component.
5. Viscous losses in liquid due to velocity inparted by interaction of circulating currents and the axial magnetic field component.

Ohmic losses due to load current

Assuming that the load current flows radially from the disk tip, the ohmic loss for two collectors is given by

$$P_{co} = 2\frac{J^2 d}{\sigma} A_c.$$

Since $J = I/A_c$

$$P_{co} = 2\frac{I^2 d}{A_c \sigma} = 0.254 \times 10^{-6} I^2 W. \tag{7}$$

At the operating points, P_{co} = 25 W at I = 10,000 amps and 156 W at I = 25,000 amps.

Viscous loss due to mechanical rotation

The Reynolds number for the flow in the collectors is given by

$$N_r = \frac{\rho_{NaK} \overline{V} D_h}{\mu_{NaK}}.$$

$\overline{V}$, the average fluid velocity, is assumed to be half the disk tip velocity. For a rotor radius of R = 0.07 m,

$$\overline{V} = 1/2\,(2R)\frac{N}{60} = 3.66 \times 10^{-3} N m/s.$$

Thus, $N_r = 10.05\,N$. For N greater than 1000 rpm, turbulent flow is indicated. Since the generator will seldom, if ever, run below this speed, turbulent flow will be assumed. For turbulent flow, the viscous loss for two collectors is expressed as

$$P_{cv} = 2\,\varrho_{NaK} f\,\overline{V}^3 A_c. \tag{8}$$

Using the given values,

$$P_{cv} = 1.06 \times 10^{-9} N^3\ W.$$

At 19,500 rpm, $P_{cv} = 7860\ W$.

Viscous drag due to MHD effects

Due to the strong axial component of the magnetic field in the collector site, and the radial direction of the load current, there is a net Lorentz force on the liquid metal tending to retard the fluid velocity with respect to the rotor tip. This results in a larger velocity differential between the rotor and bulk fluid and a resultant increase in the viscous drag. The parameter which determines the relationship to be used is[12]

$$\delta = \frac{2\,B_a\,Jd}{4f\,\varrho_{NaK}\,\overline{V}^2} = \frac{2\,B_a\,Id}{4f\,\varrho_{NaK}\,A_c\,\overline{V}^2}$$

but

$$B_a = 0.0348\,I_f\,T.$$

Thus

$$\delta = 60.7\,\frac{I\,I_f}{N^2}. \tag{9}$$

As can be seen, the parameter, δ, is dependent on the relative magnitude of current and speed. Since δ is essentially the ratio of the Lorentz force on the liquid to the viscous drag, if δ is greater than one, the bulk fluid velocity is actually opposite to that of the rotor; if δ is less than one, the bulk fluid velocity is in the same direction as the rotor. The governing relationships for these cases for the power loss due to MHD effects are

$$\delta < 1\text{:}\ P_{MHD} = P_{cv}(3\,\delta^2) = 1.17 \times 10^{-5}\,\frac{I^2\,I_f^2}{N}\,(W) \tag{10}$$

$$\delta > 1: P_{MHD} = P_{cv}\left(2(1+\delta)(2\delta-1)^{1/2} - 1\right) \tag{11}$$

or

$$P_{MHD} = P_{cv}\left(F(\delta)\right).$$

At the operating point, $I = 10^4$ amps, 19,500 rpm and $I_f = 89.64$ amps

$$\delta = 0.143, F(\delta) = 0.0614$$

and $P_{MHD} = 482$ W. At $I = 25{,}000$ amps, $P_{MHD} = 3016$ W.

Ohmic loss due to circulating currents

Eddy currents will be generated by the rotation of the finite width collector disk interacting with the radial component of the magnetic field at the disk tip. This interaction produces a voltage gradient along the width of the disk which is short-circuited by the liquid-metal stator path, giving rise to a circulating current. Since this current flows radially in the collector gap, it will interact with the axial field component to produce a Lorentz force on the liquid. Unless this latter effect is accounted for, the circulating current calculated would be overestimated in magnitude. A self-consistent calculation yields the following result for the ohmic eddy current loss

$$P_{cc} = P_{cv}\left[2\frac{d/\sigma}{\dfrac{B_a^2 d^2}{2f\varrho_{NaK}\overline{V}}}\frac{B_r^2 W^2}{B_a^2 d^2}\right]. \tag{12}$$

As pointed out previously,[12] the last term in the brackets must be less than 1 for the analysis which leads to the above relationship to be valid. Using the given values from Table 3

$$\frac{B_r W}{B_a d} = 0.2776.$$

Thus we may use the above equation for the case of the generator since this ratio will not change. An effort was made during generator design to minimize B_r in the collector site by proper location of the collectors relative to the magnet. Ideally, the radial field component could be lower than the value used here, but due to the finite resolution of the field calculations, a conservative estimate was used. Using the values given, the circulating current ohmic power loss is

$$P_{cc} = P_{cv}(1.49 \times 10^{-3})\frac{N}{I_f^2} = 1.58 \times 10^{-12}\frac{N^4}{I_f^2}.$$

For N = 19,500 rpm, P_{cc} = 28.4 W.

Viscous loss due to circulating currents

As mentioned above, the circulating currents interacting with the axial field generate a Lorentz force on the liquid which results in an additional viscous drag similar to the P_{MHD} term calculated above. The magnitude of this loss is given by

$$P_{ccv} = \left[P_{cv}\frac{B_r^2 W^2}{B_a^2 d^2}\right] = 8.16 \times 10^{-11} N^3 W. \quad (13)$$

At 19,500 rpm, P_{ccv} = 605 W.

For completeness, the magnitude of the circulating current may be calculated from

$$j(x) = \frac{4f\varrho \overline{V}^2}{B_a d}\ \frac{(B_r X)}{(B_a d)}$$

where x is the distance measured axially from the center line of the collector disk tip. Since $J(x)$ is in opposite directions on either side of this center line, the integration need only be from $x = 0$ to $x = w/2$ or

$$i_c = 2\pi R \int_{x=0}^{x=w/2} j(x)\,dx.$$

Carrying out the calculation, one finds

$$i_c = 5.48 \times 10^{-4}\frac{N^2}{I_f} \text{ amps.}$$

At 19,500 rpm, I_f = 89.64 amps and i_c = 2367 amps.

One may appreciate the value of the axial field in reducing the eddy currents by calculating the magnitude of i_c without accounting for the Lorentz interaction. For this case one obtains

$$i_c' = 1.48 \times 10^5 \text{ amps.}$$

Assuming that the parameter, δ, is less than 1 over the range of operation, a complete expression for the collector losses may be written as:

$$P_c = P_{co} + P_{cv} + P_{MHD} + P_{cc} + P_{ccv}$$

or substituting the above results with load current, rpm, and field current as the variables

$$P_c = 0.254 \times 10^{-6} I^2 + 1.14 \times 10^{-9} N^3 + \left[1.17 \times 10^{-5} \frac{I^2 I_f^2}{N}\right] + 1.581 \times 10^{-12} \frac{N^4}{I_f^2} W \tag{14}$$

for $\delta \leq 1$. For $\delta > 1$, the term in brackets becomes

$$\left[1.06 \times 10^{-9} N^3 \left(2(1 + \delta)(2\delta - 1)^{1/2} - 1\right)\right].$$

For the design operating points at N = 19,500 rpm for $I = 10^4$ amps, P_c = 9,000 W, and at $I = 2.5 \times 10^4$ amps, P_c = 11,665 W.

Joule Losses in Conductors

The Joule loss in the conductors of the rotor and stator are a simple function of load current, geometry, and conductor material. To a good approximation, the conductor cross section is constant through the generator internal electric circuit. Thus

$$P_J = \frac{I^2 \varrho_{cu} L}{A_1}$$

where

ϱ_{cu} = Copper resistivity = $1.7 \times 10^{-8}\ \Omega - m$

L = Length of electrical circuit = 1.08 m

A_1 = Cross section of copper in circuit = $4.3 \times 10^{-3}\ m^2$.

Therefore

$$P_J = 4.29 \times 10^{-6} I^2 W. \tag{15}$$

At the design operating points, $P_J = 429\ W$, at $I = 10^4$ amps, and 2681 W, at $I = 2.5 \times 10^4$ amps.

Efficiency

The efficiency is plotted as a function of rpm and load current in Figure 23. These curves are derived from the calculations in this section and do not include parasitic losses such as coolant pumping power, refrigeration, and magnet excitation. Total power loss, P_T is thus given by

$$P_T = P_B + P_S + P_W + P_C + P_J.$$

Assuming a 30-volt output at nominal field current and 19,500 rpm, the power output, P_g, as a function of current, speed, and field current is

$$P_g = 1.71 \times 10^{-5} I_f I N.$$

The efficiency, η, is then

$$\eta = 100 \left(1 - \frac{P_T}{P_g}\right) \%.$$

Using the previously derived expressions, and assuming operating conditions such that the assumptions previously made are valid, the efficiency is given by

$$\eta = 100 - \left(7.47 \frac{N}{I_f I} + 6.93 \times 10^{-3} \frac{N^2}{I_f I} + 9.25 \times 10^{-6} \frac{N^3}{I I_f^3} + \left[68.4 \frac{I_f I}{N^2}\right] + 26.5 \frac{I}{I_f N}\right) \tag{16}$$

for $\delta \leq 1$. For $\delta > 1$, the term in brackets becomes

$$6.2 \times 10^{-3} \frac{N^2}{I_f I} \left(2(1 + \delta)(2\delta - 1)^{1/2} - 1\right)$$

Where $\delta = 60.7\ I_f\ I/N^2$.

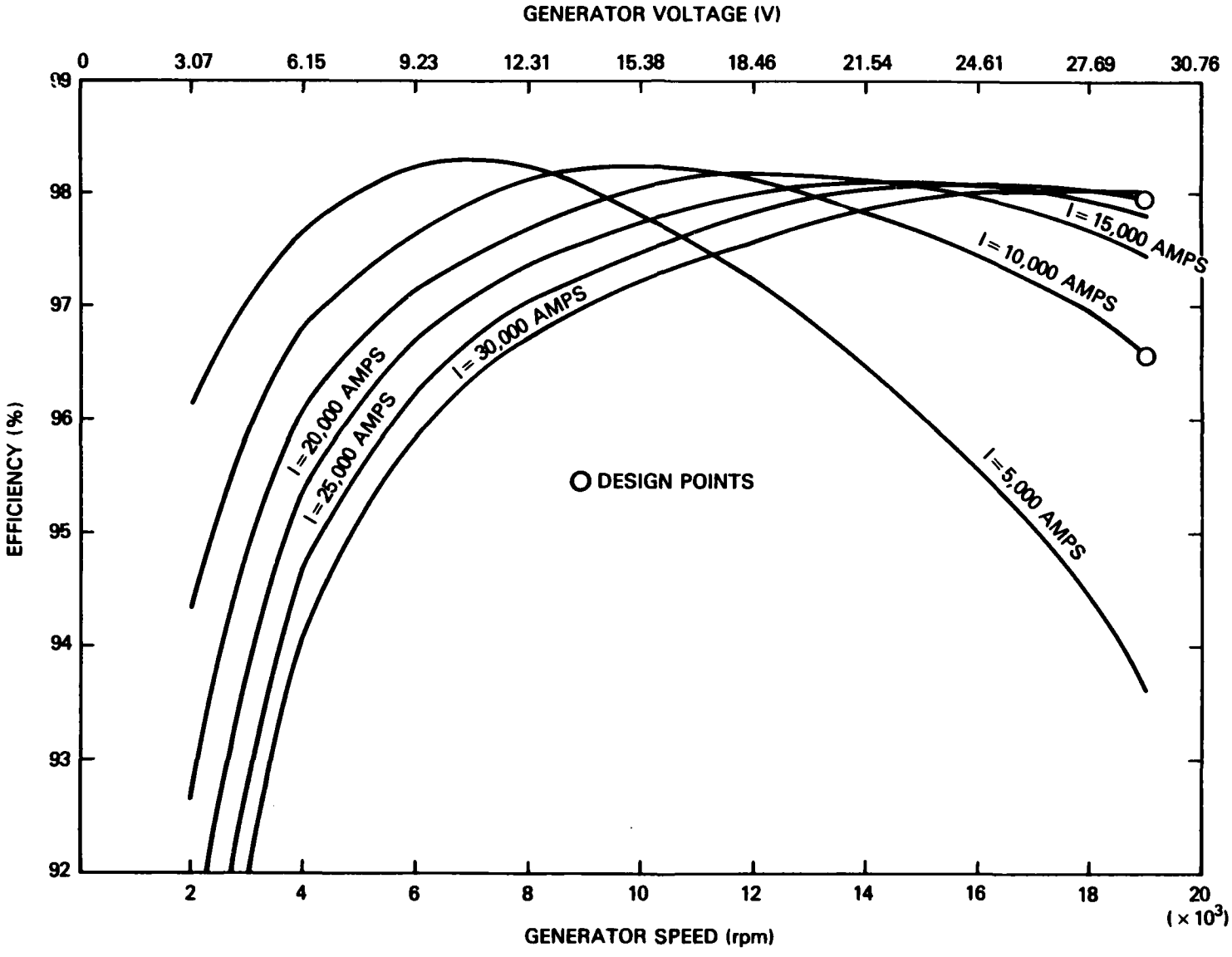

Figure 23 – Generator Efficiency Characteristics (Field Current 89.64 amperes)

THERMAL ANALYSIS/COOLANT SYSTEM

As indicated in the previous section, the major source of heat in the superconducting generator is the liquid-metal current collectors; therefore, the coolant system was designed to carry the coolant as close to these sources as possible to prevent large thermal gradients. A silicone-based fluid (Coolanol)™ was selected as the coolant because of its compatibility with *NaK*. However, it may be possible to use water as the coolant fluid with a high degree of confidence since little opportunity exists for leaks into the *NaK* region.

The basic problem in design of the coolant system was to provide sufficient surface area in a small volume to allow the required heat transfer to occur at reasonable temperature differentials. The analysis proceeded by assuming a particular configuration and fluid flow, then analyzing the resulting temperature and pressure distribution. Several iterations of this process yielded a satisfactory solution which is presented below. Figure 24 indicates the general layout of the coolant loops through the generator, each of which encompasses one half of a collector. As indicated, four separate loops are present in the generator. The coolant loop parameters and numerical values are listed in Table 4.

Coolant channels are arranged such that coolant enters the stator axially through a milled channel to the coolant channel which is slotted to increase the heat transfer area. The coolant travels through this channel 180 degrees around the stator parallel to the collector channel, crosses the collector channel, and returns 180 degrees in the opposite direction, then exits via a return channel similar to the inlet. This arrangement is indicated in Figure 25. The assumption is made that all heat generated in the rotor is transferred to the coolant through the liquid metal, so the heat flow path is as indicated in Figure 26.

The temperature drop, ΔT_1, from the rotor center to the current collector is given by

$$\Delta T_1 = \frac{\dot{q} L_2}{2 K_{cu}}$$

where $\dot{q}$ is the joule heat generated per unit volume in the rotor due to load current, i.e.,

$$\dot{q} = J^2 \varrho_{cu} = \frac{I^2}{A_{cu}^2} \varrho_{cu}$$

Thus

$$\Delta T_1 = \frac{I^2 L_2^2 \varrho_{cu}}{2 K_{cu} A_{cu}^2} \tag{17}$$

or

$$\Delta T_1 = 2.35 \times 10^{-8} I^2 - {}^\circ\text{C}.$$

™Coolanol is a registered trademark of the Monsanto Corporation.

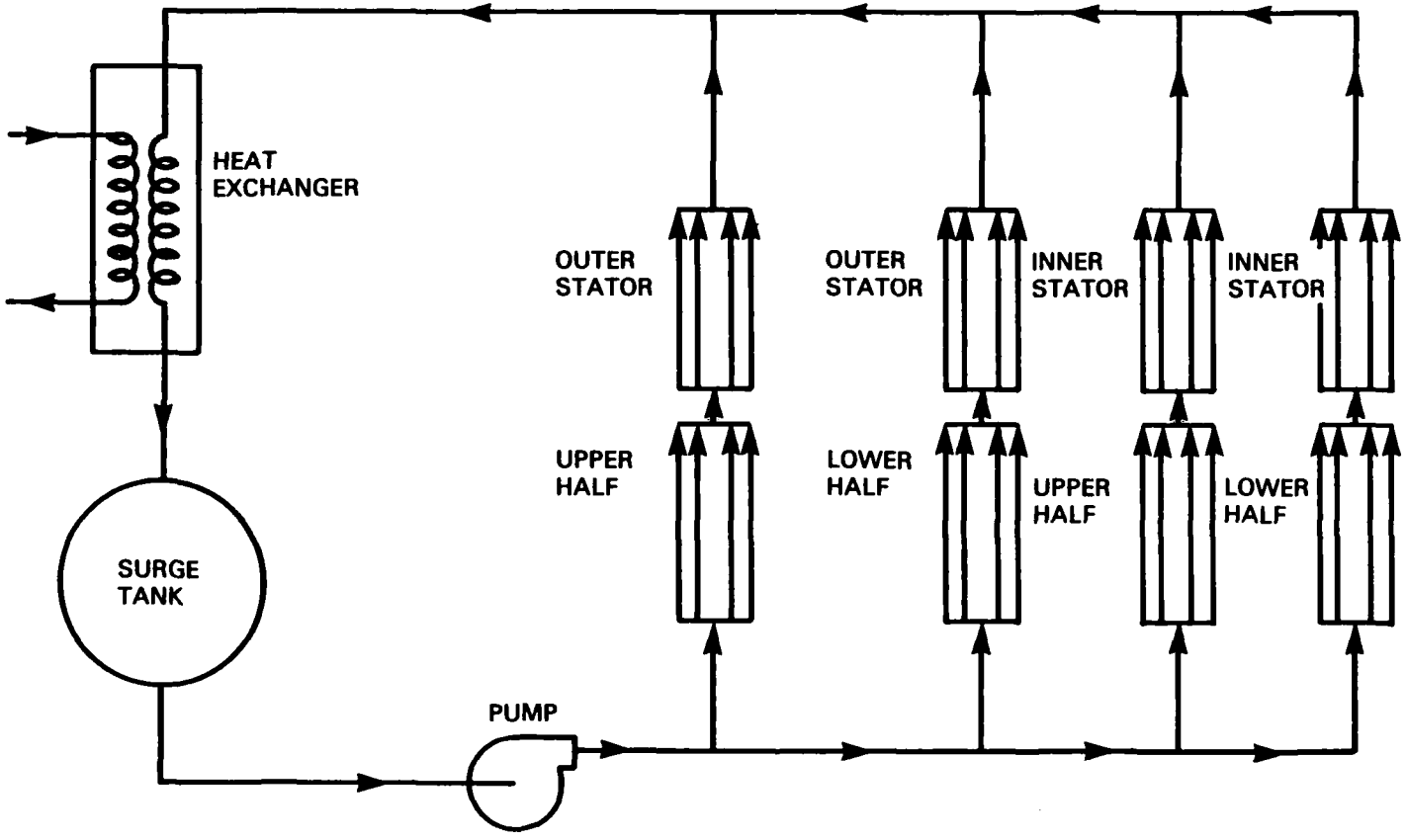

Figure 24 — Generator Coolant System Schematic

TABLE 4 — COOLANT LOOP PARAMETERS

A_x	Coolant channel cross section, $7.548 \times 10^{-5}\ m^2$
P_W	Coolant channel wetted parameter, $0.0757\ m$
ℓ	Coolant channel length, $0.381\ m$
A_w	Coolant channel surface area, $P_w \times \ell = 0.0288\ m^2$
d_h	Hydraulic diameter of coolant channel, $4A_x/P_w = 3.99 \times 10^{-3}\ m$
$\dot{M}$	Coolant mass flow, kg/s
$\dot{Q}$	Heat flux, J/s
C_p	Specific heat of coolant - Coolanol, 1504 $J/kg - °C$ - water, 4200 $J/kg - °C$
ϱ_c	Coolant density - coolanol, 910 kg/m^3 - water, 1000 kg/m^3
μ_c	Absolute viscosity - coolanol, $22.4 \times 10^{-4}\ kg/m\text{-}s$ - water, $28.2 \times 10^{-4}\ kg/m\text{-}s$
K_f	Coolant thermal conductivity - coolanol, 0.116 $W/m\text{-}°C$ - water, 0.675 $W/m\text{-}°C$
K_{cu}	Thermal conductivity (copper), 393 $W/m\text{-}°C$
D_h	Feed and return line hydraulic diameter, $8.45 \times 10^{-3}\ m$
A_f	Feed and return line cross section, $8.06 \times 10^{-5}\ m^2$
L	Feed and return line total length, $0.914\ m$
L_1	Average distance between coolant and collector channel, $0.019\ m$
A_{cu}	Average copper cross section, $3.87 \times 10^{-3}\ m^2$
L_2	Distance from rotor center to collector, $0.127\ m$
ϱ_{cu}	Resistivity of copper, $1.72 \times 10^{-8}\ \Omega\text{-}m$

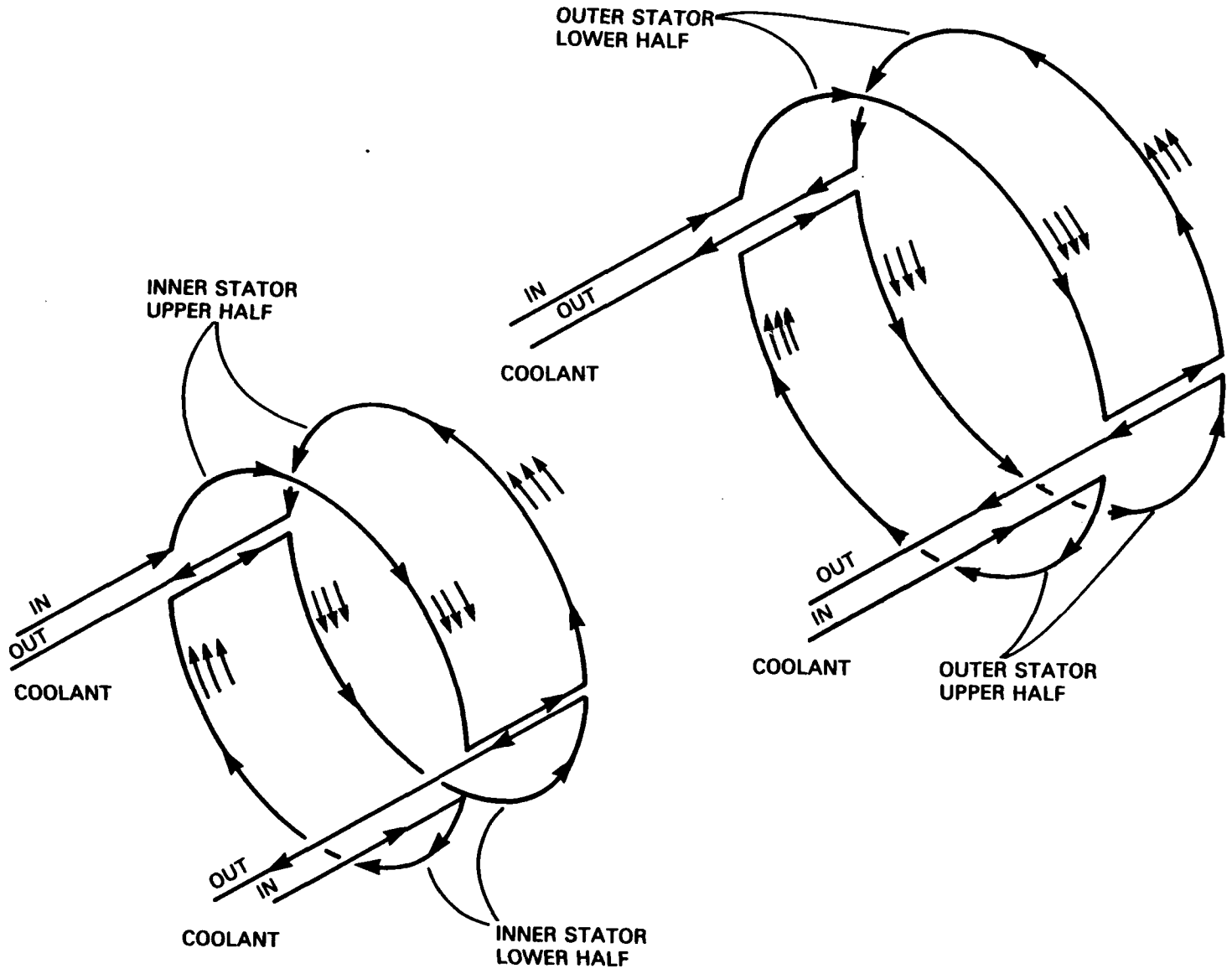

Figure 25 — Generator Coolant Loop Geometry

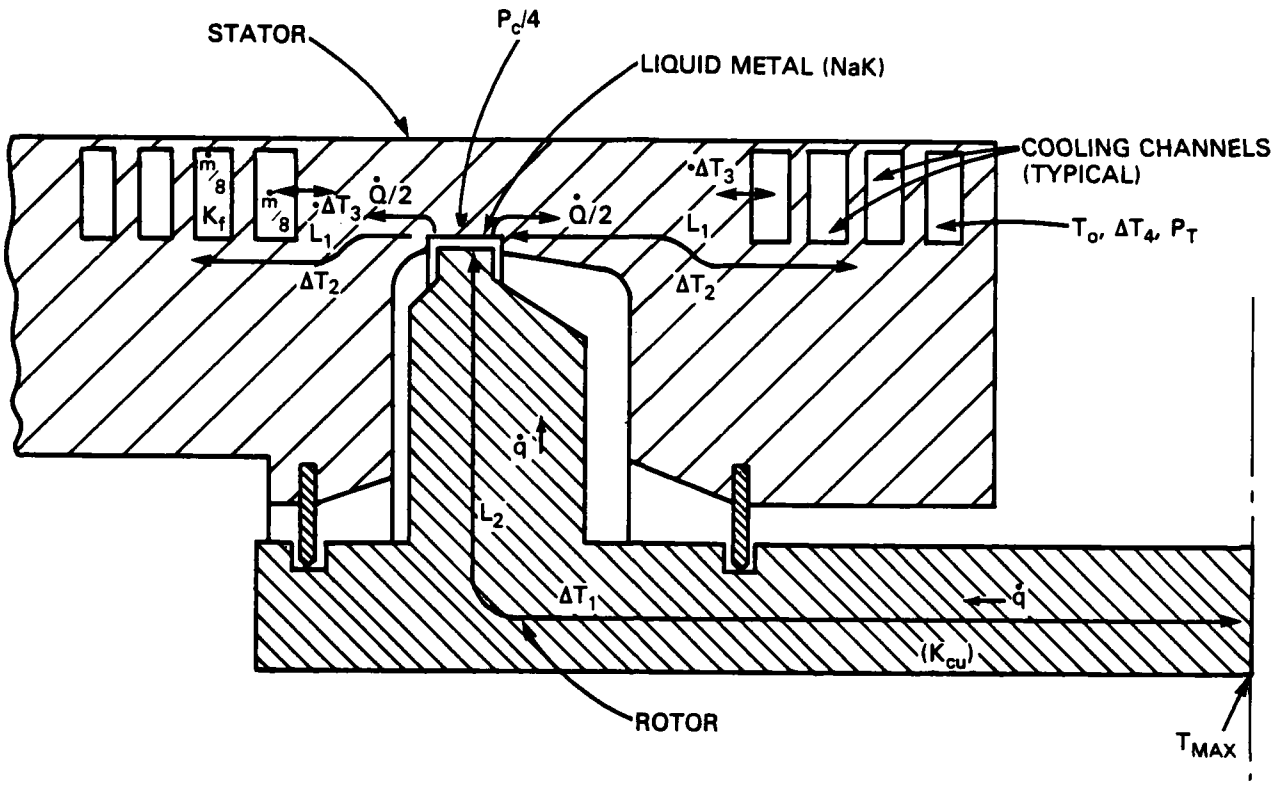

Figure 26 — Heat Flow Path in Generator (Typical Section)

Since the flow of liquid metal in the collector channel is turbulent, no temperature gradient is assumed between the rotor disk tip and the stator channel. If $\dot{Q}$ is the total heat generated by the current collector and rotor ohmic heating, the temperature drop between the coolant channel and liquid metal is given by

$$\Delta T_2 = \dot{Q} L_1 / K_{cu} A_{cu} = \dot{Q} (0.0125)\ ^\circ C.$$

$\dot{Q}$ may be expressed as a function of operating variables as described in the previous section on current collector losses.

$$\dot{Q} = 1/2\, I^2 \varrho_{cu} \frac{L_2}{A_{cu}} + \frac{P_c}{4}$$

where P_c is given by Equation (14) and the factor of 1/4 is present, since $\dot{Q}$ represents only the heat intercepted by one of the coolant loops of which four are present. Collecting the numerical values, one obtains

$$\dot{Q} = 0.343 \times 10^{-6} I^2 + 0.285 \times 10^{-9} N^3 + 0.293 \times 10^{-5} \frac{I^2 I_f^2}{N} + 0.395 \times 10^{-12} \frac{N^4}{I_f^2}.$$

Thus

$$\Delta T_2 = 4.2 \times 10^{-9} I^2 + 3.56 \times 10^{-12} N^3 + 3.66 \times 10^{-8} \frac{I^2 I_f^2}{N} + 4.94 \times 10^{-15} \frac{N^4}{I_f^2}. \tag{18}$$

The temperature differential across the coolant channel wall, ΔT_3, is given by

$$\Delta T_3 = \dot{Q}/h_f A_w$$

where h_f is the film coefficient. When turbulent flow is indicated, as will be shown later, the film coefficient takes the form

$$h_f = 0.023 \left(\frac{K_f}{d_h} \right) R_e^{0.8} P_r^{0.33}$$

where R_e = Reynolds number and P_r = Prandtl number.

$$R_e = \frac{\varrho_c V_c d_h}{\mu_c}$$

but

$$V_c = \frac{\dot{m}}{\varrho_c A_x}$$

Thus

$$R_e = \frac{\dot{m} d_h}{\mu_c A_x} = 2.36 \times 10^4 \dot{m} \tag{19}$$

and

$$P_r = \frac{C_p \mu_c}{K_f} = 29.0. \tag{20}$$

Substitution yields

$$h_f = 6399 \dot{m}^{0.8}.$$

Thus

$$\Delta T_3 = \frac{0.434}{\dot{m}^{0.8}} \Delta T_2. \tag{21}$$

The temperature rise in the coolant, ΔT_4, is given

$$\Delta T_4 = \frac{\dot{Q}}{\dot{m} C_p} = \frac{0.053}{\dot{m}} \Delta T_2. \tag{22}$$

If the collant inlet temperature is T_0, then the temperature distribution in the generator is

Coolant inlet	$= T_0$
Coolant outlet	$= T_0 + \Delta T_4$
Stator channel	$= T_0 + \Delta T_4 + \Delta T_3$
Liquid metal	$= T_0 + \Delta T_4 + \Delta T_3 + \Delta T_2$
Rotor center (hot spot)	$= T_0 + \Delta T_4 + \Delta T_3 + \Delta T_2 + \Delta T_1$.

Maximum machine temperature at hot spot is thus

$$T_{max} = T_0 + 2.35 \times 10^{-8} I^2 + \left(1 + \frac{0.434}{\dot{m}^{0.8}} + \frac{0.053}{\dot{m}}\right)$$

$$\times \left(4.2 \times 10^{-9} I^2 + 3.56 \times 10^{-12} N^3 + \left[3.66 \times 10^{-8} \frac{I^2 I_f^2}{N}\right] + 4.94 \times 10^{-15} \frac{N^4}{I_f^2}\right) \tag{23}$$

for $\delta \leq 1$. For $\delta > 1$, the term in brackets becomes

$$3.312 \times 10^{-12} N^3 \left(2(1 + \delta)(2\delta - 1)^{1/2} - 1\right)$$

Where $\delta = 60.7\ I I_f / N^2$.

Figure 26 is a plot of hot spot temperature versus flow rate for the nominal operating points of the generator.

The pressure drop through the coolant loop is the sum of the drop through the feed and return lines, and the coolant channel. The pressure drop in the coolant channel is given by

$$\Delta P_c = f \frac{\ell}{d_h} \frac{\varrho_c V_c^2}{2}$$

where f is the friction factor, assumed to be 0.03, the other factors have been previously identified. Since $V_c = \dot{m} / \varrho_c A_x$

$$\Delta P_c = \frac{f \ell \dot{m}^2}{d_h 2 A_x^2 \varrho_c} = 2.76 \times 10^5 \dot{m}^2 \ (N/m^2) \ (= 40 \dot{m}^2 psi). \tag{24}$$

The pressure drop in the feed and return lines is given by

$$\Delta P_f = f\frac{L}{D_h}\frac{\varrho_c V_f^2}{2} = f\frac{L\dot{m}^2}{D_h 2\,\varrho_c A_f^2} \tag{25}$$

or

$$\Delta P_f = 1.37 \times 10^5 \dot{m}^2 \left(\frac{N}{m^2}\right) \quad (= 19.9\,\dot{m}^2\,psi).$$

Total pressure drop through the coolant system is given by

$$P_T = P_c + P_f$$

$$P_T = 4.13 \times 10^5 \dot{m}^2 \tag{26}$$

which is also plotted in Figure 27. With the data presented, an operating point can be selected consistent with the temperature rise capability of the generator. Results are also given for the use of water in place of Coolanol as the coolant fluid. The advantages of using water are evident from the results shown.

The following are modified relationships for the indicated equations for water used as the coolant

$$R_e = \frac{\dot{m}\,d_h}{\mu_c A_x} = 1.87 \times 10^4 \dot{m} \tag{19a}$$

$$P_r = \frac{C_p \mu_c}{K_f} = 6.28 \tag{20a}$$

$$h_f = 0.023\left(\frac{K_f}{d_h}\right) R_e^{0.8} P_r^{0.33} = 18657\,\dot{m}^{0.8}$$

Therefore

$$\Delta T_3 = \frac{0.149}{\dot{m}^{0.8}}\Delta T_2 \tag{21a}$$

$$\Delta T_4 = \frac{0.019}{\dot{m}}\Delta T_2 \tag{221}$$

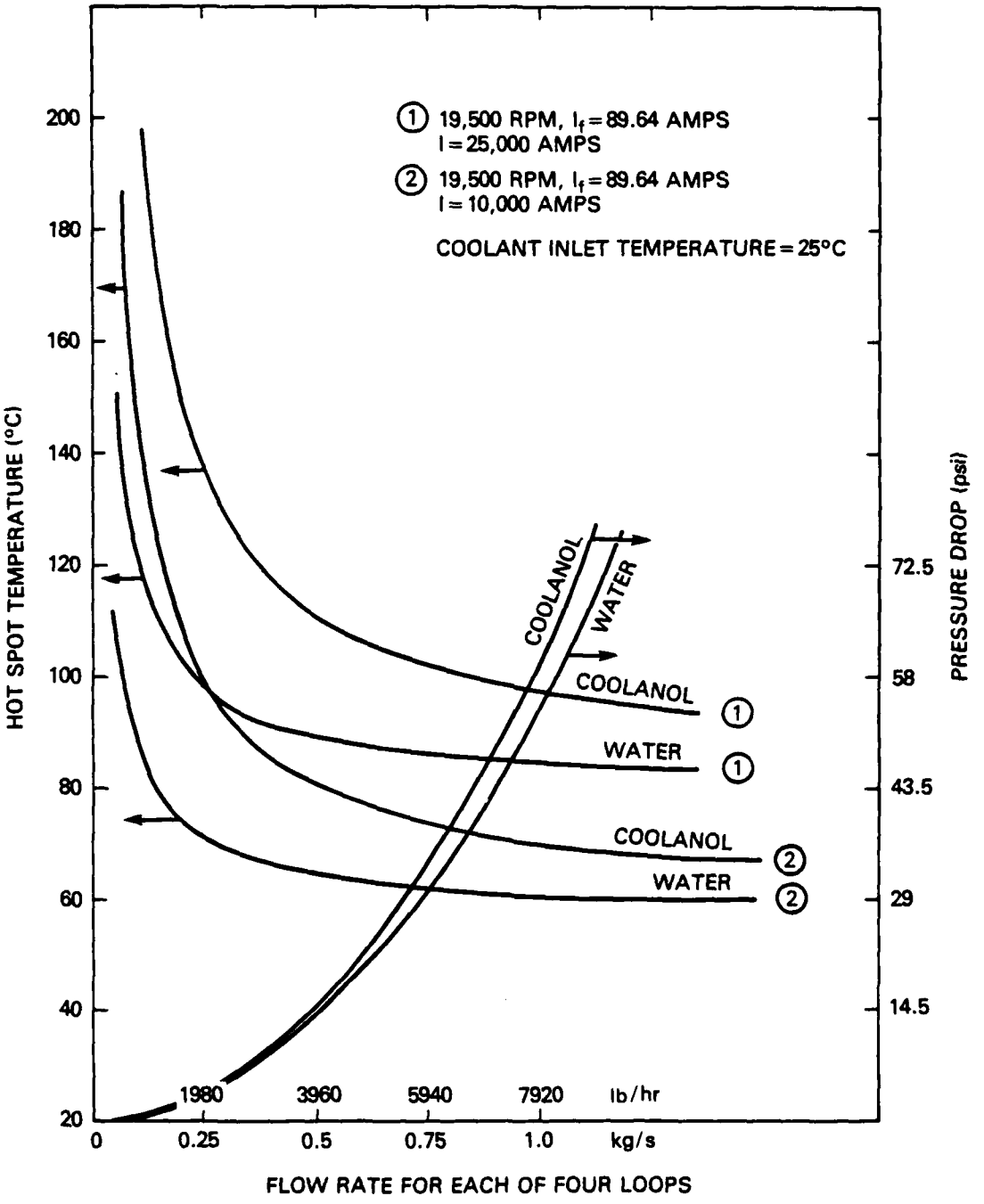

Figure 27 — Generator Hot Spot Temperature and Coolant Loop Pressure Drop at Nominal Design Points.

Maximum machine temperature at hot spot for water cooling is then

$$T_{max} = T_0 + 2.35 \times 10^{-8} I^2 + \left(1 + \frac{0.149}{\dot{m}^{0.8}} + \frac{0.019}{\dot{m}}\right) \tag{23a}$$

$$\times \left(4.2 \times 10^{-9} I^2 + 3.56 \times 10^{-12} N^3 + \left[3.66 \times 10^{-8} \frac{I^2 I_f^2}{N}\right] + 4.94 \times 10^{-15} \frac{N^4}{I_f^2}\right)$$

for $\delta \leq 1$. For $\delta > 1$, the term in brackets becomes

$$3.312 \times 10^{-12} N^3 \left(2(1 + \delta)(2\delta - 1)^{1/2} - 1\right)$$

Where $\delta = 60.7 \frac{I I_f}{N^2}$.

$$\Delta P_c = f \frac{\ell \dot{m}^2}{d_h 2 A_x^2 \varrho_c} = 2.51 \times 10^5 \dot{m}^2 \left(\frac{N}{m^2}\right) \tag{24a}$$

$$= (36.1 \dot{m}^2 \text{ psi}).$$

$$\Delta P_f = f \frac{L \dot{m}^2}{D_h 2 \varrho_c A_f^2} = 1.247 \times 10^5 \dot{m}^2 \left(\frac{N}{m^2}\right) \tag{25a}$$

$$= (18.1 \dot{m}^2 psi)$$

$$P_T = 3.76 \times 10^5 \dot{m}^2 \left(\frac{N}{m^2}\right) \tag{26a}$$

The flow rates shown in Table 5 are for the entire machine, i.e., four times those indicated in Figure 27 which represents only one of the four coolant loops which are connected in parallel.

No credit has been given to the coolant feed and return lines for heat removal. A brief analysis indicates their effect on the cooling capability of the system could be substantial, on the order of 20%, but a detailed thermal analysis has not been undertaken.

TABLE 5 — COOLANT FLOW RATE AND GENERATOR TEMPERATURES AT SELECTED DESIGN POINTS

Output (kw)	300	750
Current (amps)	10,000	25,000
Voltage (V)	30	30
Speed (rpm)	19,500	19,500
Coolant	Water	Water
Flow Rate (kg/s)	1.0	1.0
Coolant Inlet Temperature (°C)	25	25
Coolant Outlet Temperature (°C)	27.3	28.4
Maximum Stator Temperature (°C)	40	45.3
NaK Temperature (°C)	68.4	83.9
Maximum Rotor Temperature (Hot Spot) (°C)	70.6	98.6
Coolant Pressure Drop (psi)	5	5

Note: Tabular data at other operating points may be found in Appendix C.

MECHANICAL ANALYSIS

The majority of the noncryogenic components in the generator are not highly stressed. Only the copper rotor, at a speed of 19,500 rpm, experiences forces significant with respect to its yield strength. The critical speed of the rotor shaft bearing system is also of importance. Computer programs were written to treat each of these problems.

The rotor stress calculation, although straightforward, requires the solution of several simultaneous equations, each describing the forces on a thin annular section of the rotor. The program applies to symmetric disk-like shapes of nonuniform thickness, a good approximation to the disk-shaped ends of the generator rotor. Thus the stresses in each of the two end sections and the center cylindrical section of the copper rotor were calculated separately. The program can also account for internal and external pressure on the rotor, which enables shrink-fit stresses and pressure due to an external wrap of high strength material to be included in the calculation. The results of the rotor stress analysis, which were obtained after several

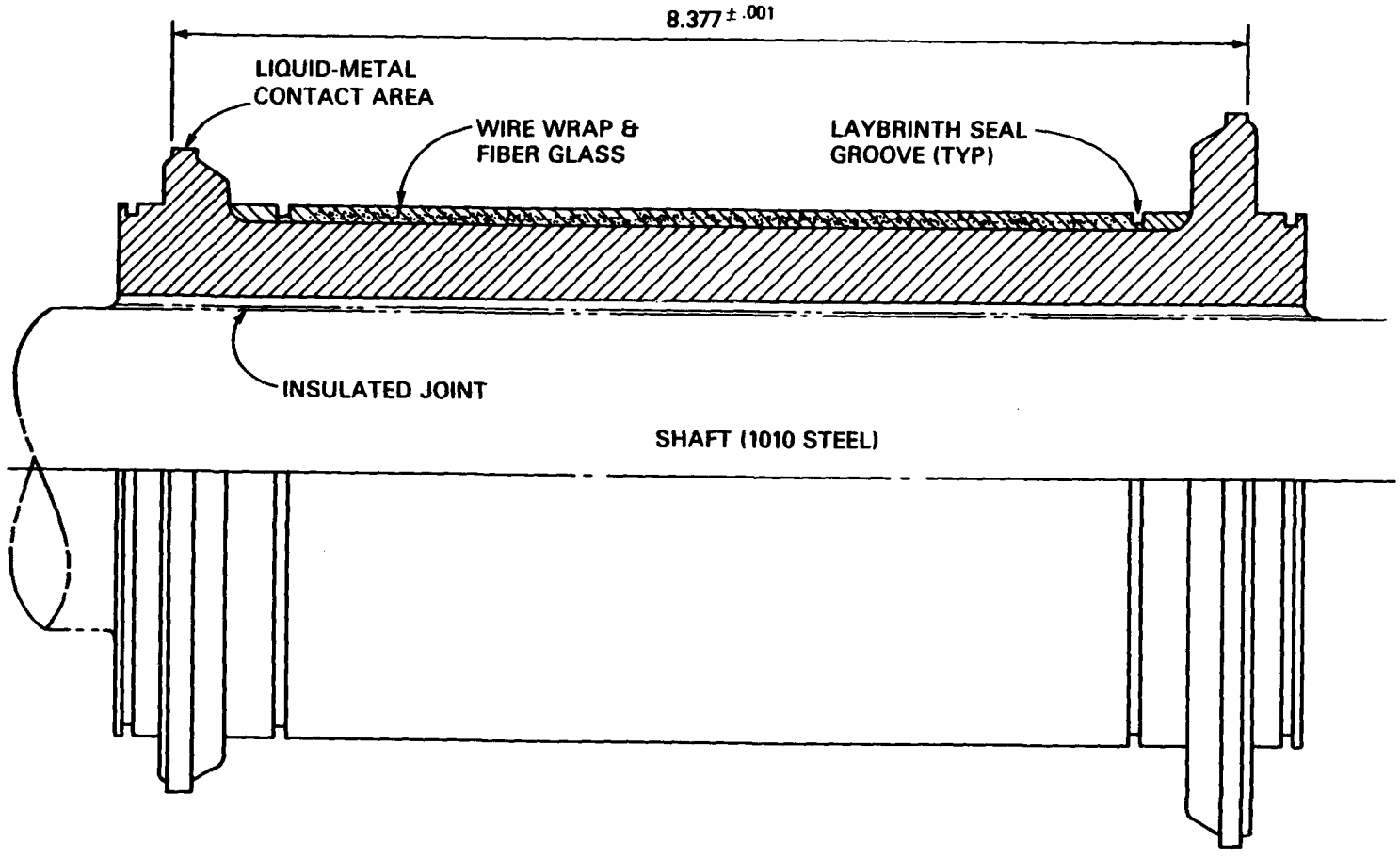

Figure 28 — Generator Rotor Geometry

iterations, are given below. These results were obtained for a rotor of the shape shown in Figure 28 consisting of two copper disks joined at their centers by a hollow thick-walled copper tube. The center tubular section of the rotor will be over wrapped with high strength stainless steel wire to a thickness of 90 mils which will then be epoxy impregnated to prevent loosening of the wire. The wire wrap will provide sufficient external pressure under all anticipated conditions of thermal expansion and rotational stresses to maintain sufficient frictional force between rotor and shaft to transfer the torque required. The disks at each end of the center section are not required to transfer torque directly to the shaft but only to the center section of the rotor; therefore, a heavy shrink fit for these sections of the rotor is not required. In order to assure the adequacy of the rotor design, the rotor stress calculation was made for the combinations of rotational speed, and temperature encountered during operation, and also for conditions encountered during construction to assure that the copper was never stressed beyond its yield point. For purposes of analyzing thermal effects, a maximum temperature differential between rotor and shaft of 100°F was assumed to exist. Zirconium copper alloy was selected as the rotor material because of its yield strength of above 2.62×10^8 Nt/m^2 and electrical conductivity of about 90% IACS. The results of the stress analysis are summarized in Table 6.

TABLE 6 — RESULTS OF ROTOR STRESS ANALYSIS

Condition*	Equivalent Internal Pressure** (N/m^2)	Maximum Stress*** (N/m^2)
Shrink Fit	4.37×10^7	1.24×10^8
Wire Wraps	4.37×10^7	4.02×10^7
Spin to 20,000 RPM	1.57×10^7	1.7×10^8
100-Degree Differential T	3.45×10^6	1.7×10^8

* The conditions are sequentially additive.
** For cylindrical section of rotor only.
*** Highest stress present in all of rotor.

The internal radius of the cylindrical section of the rotor is 3.43 cm (1.35 in.) and the length of this section is 17.15 cm (6.75 in.) giving a surface area contact of 369.5 cm^2 (57.2 in^2) to resist the rotor torque.

Assuming a coefficient of friction of 0.3 between rotor and shaft, and the worst-case condition from Table 6 of 3.45×10^6 N/m^2 contact pressure between rotor and shaft, the torque required to cause the rotor to slip on the shaft is 1445 $N\text{-}m$. Since the torque at full turbine output of 1226 hp at 19,500 rpm is 459 $N\text{-}m$, there is a safety factor of about 3 in the calculated design.

The critical speed of the rotor was calculated using a computer program capable of accounting for distributed masses, varible elastic modulii, and bearing stiffness. The shaft rotor bearing system was designed to a first critical speed of 24,000 rpm. The mechanical design for the magnet support system is described in Appendix B.

AUXILIARY SYSTEMS DESIGN

The following paragraphs are a description of several subsystems necessary to the proper operation of the generator described herein.

Cover Gas System

Liquid sodium potassium (*NaK*), which is used in the liquid-metal current collectors, is an extremely reactive material. Therefore, great care must be exercised to remove oxygen, water vapor, or any other substances which may react with the *NaK* from the region of the current collectors. This is accomplished first by careful materials selection in construction of the generator, and second, by maintaining a very pure inert atmosphere inside the generator. Purified inert gas is used to maintain a positive pressure inside the generator in the region of the collector sites. Rotating shaft seals prevent excess leakage of the cover gas from the machine. There are commercially available purifiers which use various resins capable of purifying gas to 1 ppm water and oxygen. However, present plans do not include using these devices for actual generator operation.

The use rate of the inert gas is expected to be less than a few cubic centimeters per minute, this rate being dependent on the performance of the rotating seal system described later.

The cover gas system will consist of a source of inert gas (e.g., argon), a pressure regulator, a purifier to remove oxygen and water vapor, a flowmeter to monitor flow rate, and sensors to monitor and detect the

level of oxygen and water vapor in the cover gas. An overpressure of approximately 15 psi will be maintained within the generator.

Bearings and Seals

Due to the high-speed operation of the generator, the bearing and seal selection is not trivial. The initial design called for the use of hydrodynamic journal bearings. A manufacturer's analysis indicated that these would operate satisfactorily but required a large oil flow rate to remove the 3.5 to 4 kw of heat generated by each bearing at top speed of 19,500 rpm. In addition to efficiency considerations, the large oil flow rate increases the likelihood that oil could migrate through the seal system to the interior of the machine. After substituting angular contact ball bearings for the journals, and using air-oil mist for lubrication, the bearing-generated heat was calculated to be approximately 150 W per bearing. Due to the high-speed, high precision ABEC-7 bearings are required. A bearing test stand has been fabricated to aid in determining the exact lubrication requirements, operating temperature, losses, and expected life for the generator bearings.

The shaft seals on the generator must confine the inert cover gas to the interior of the machine with minimal leakage, and also prevent the migration of the bearing lubricant into the inert gas region. To accomplish this, a double seal arrangement shown in Figure 29 will be used, with a buffer region of dry air between the seals. The inboard seal is a hydrodynamic carbon face seal. This seal is required to run in a completely dry atmosphere and thus requires a special grade of carbon to be used. During operation, there is no contact between the seal face and the runner because the seal is designed to create a very thin cushion of gas between these mating pieces. With proper design, this seal should last indefinitely.

The secondary outboard seal is essentially a labyrinth formed by a stationary channel pressed into the bearing housing, and a reinforced carbon ring which fits closely around the shaft and in the channel. In operation, the carbon ring may or may not rotate with the shaft, depending on the thermal expansion present. The pressure differential across the seal forces the ring to one side of the channel creating a very narrow gap for leakage. This type of seal is capable of very high-speed operation, but its leak rate is somewhat higher than a face seal. The selection of the labyrinth for the secondary seal is the fact that the oil-mist lubrication present would prevent proper operation of the hydrodynamic face seal and lead to excessive frictional heat generation; whereas, the labyrinth seal will operate satisfactorily in the presence of the oil mist.

In order to prevent oil migration through the seal system, a positive pressure gradient will be maintained through the seal system with the highest pressure being that of the inert cover gas, the dry air buffer gas being at a lower pressure, and the oil-mist lubricant entering the bearing area at an even lower pressure. Present plans call for these pressures to be 15, 10, and 5 psi, respectively.

The pertinent bearing and seal information is listed in Table 7.

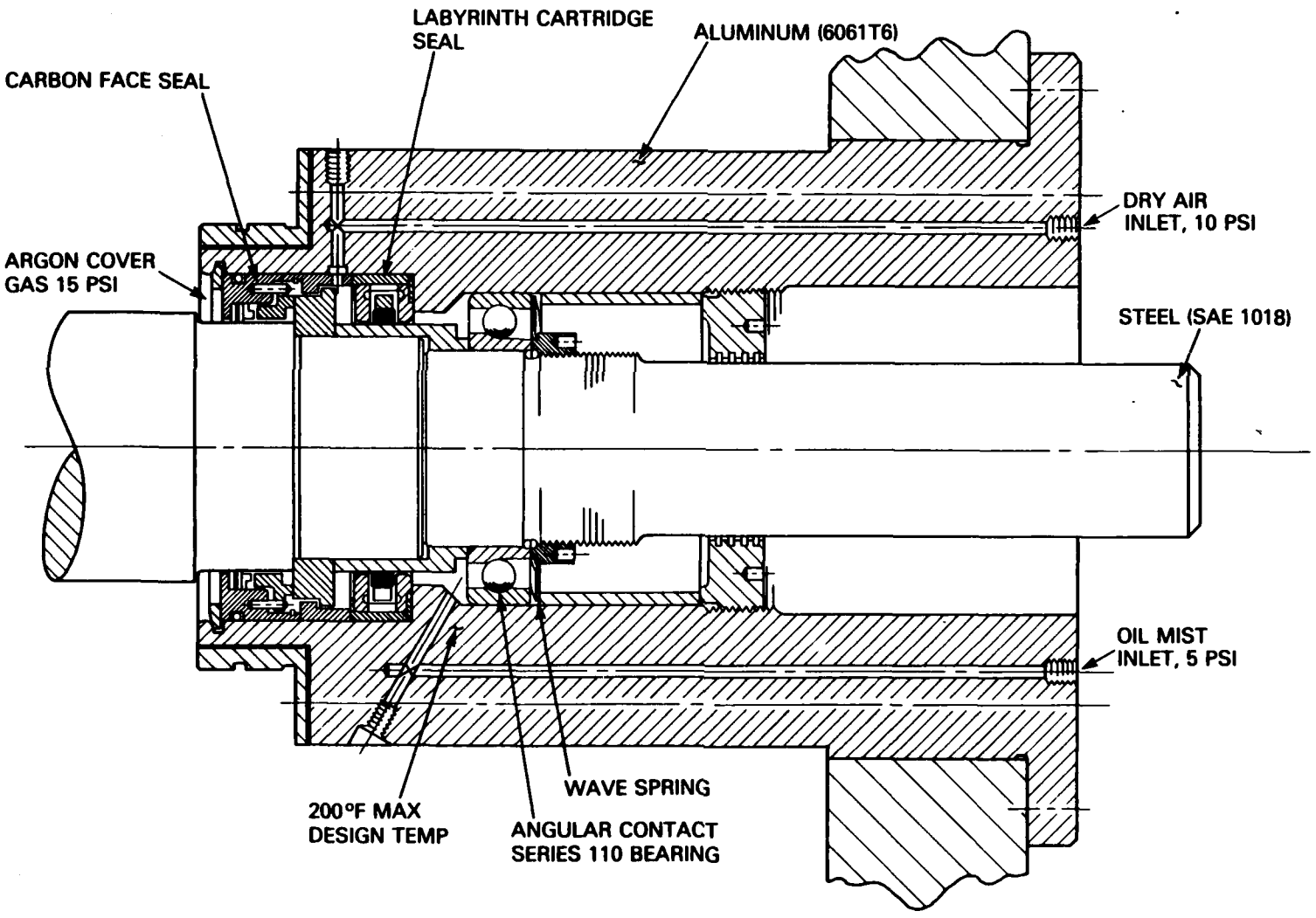

Figure 29 — Generator Bearing and Seal Arrangement

TABLE 7 — BEARING AND SEAL PARAMETERS

Bearing	
Type	Size 110, 15-degree angular contact
Power Consumption	0.15 kW at 19,500 rpm
Lubricant	Air-oil mist
Inboard Seal	
Type	Dry carbon face-type with hydrodynamic lift pads
Size	7.62-cm (3-in.)
Power Consumption	Negligable
Pressure Drop	5 psi across seal face
Leak Rate	Less than 20 cm^3/min
Outboard Seal	
Type	*Carbon ring labyrinth*
Size	6.35 cm (2.5 in.) at carbon ring ID
Power Consumption	Negligable
Pressure Drop	5 psi across seal
Leak Rate	Less than 14 g/min air

Cryogenic System

The cryogenic system requirements for initial operation of the superconductive acyclic generator are relatively simple. Since longterm operation is contemplated using bulk helium, provision must be made for accurately controlling helium flow rate to the magnet from a helium storage vessel. This will be accomplished by maintaining a constant pressure of approximately 1 psi on the supply vessel and controlling the liquid helium flow rate by adjusting the back pressure in the magnet dewar by means of a throttling valve in the boil-off gas line external to the magnet dewar. A helium level detector in the magnet dewar is used to observe the liquid level. Future plans call for servo control of the throttle valve with control signal derived from the level detector which will allow long-term unattended operation. Ultimately, the intention is to connect the generator to a closed-cycle liquifier wherein the boil-off gas is returned to the liquifier for reuse.

Due to the anticipated very low heat leak (approximately 1.25 l/hr) of the generator dewar, a low-loss helium transfer line is being designed to connect the magnet dewar to the helium supply dewar because conventional transfer line losses would dominate the system losses.

TABLE 8 — SUPERCONDUCTING GENERATOR INSTRUMENTATION

Parameter	Range	Sensor	Location
Magnet Temperature	300 - 4.2K	Germanium resistance thermometer	Two places, top and bottom of coil form
Magnet Temperature	300 - 4.2K	Type T, TC	Five places, two on each coil and one near helium exhaust
Helium Level	1/2 to full	S/C wire level detector	Two places, either side of coil
Coil Voltage	0 - 10 Vdc	Voltmeter	Four places each coil
Coil Current	0 - 135 amps	Shunt	In series with current leads outside dewar
Support Rod Tension	0 - 300 lb	Load cell	At external attachment point of each support rod
Internal Helium Pressure	0 - 2 psi	Pressure gage	At helium vent on dewar
Helium Supply Pressure	0 - 4 psi	Pressure gage	Helium supply dewar
Helium Boil-off Rate	0 - 5 ℓ/hr	Flowmeter	Helium Vent on magnet dewar
Helium Exhaust Temperature	300 - 70K	Type T, TC	Helium Vent on magnet dewar
NaK Temperature	50° - 250°F	Type T, TC	Two locations each probe in collector channel
Stator Temperature	50° - 150°F	Type T, TC	Two locations on stator
Bearing Temperature	50° - 250°F	Type T, TC	Two locations, each bearing
Coolant Inlet Temperature	50° - 150°F	Type T, TC	Two locations, each inlet
Coolant Outlet Temperature	50° - 150°F	Type T, TC	Two locations, each outlet
Coolant Flow Rate	0 - 1 kg/s	Flowmeter	At coolant pump
Coolant Pressure	0 - 50 psig	Pressure gage	Coolant inlet
Cover Gas Pressure	0 - 15 psi	Pressure gage	Cover gas inlet
Cover Gas Flow Rate	0 - 1 ft^3/hr	Flowmeter	Cover gas inlet
Generator Voltage	0 - 35 V	Voltmeter	Across generator terminals
Generator Current	0 - 30,000 amps	Shunt	In series with X-mission live
Torque	0 - 300 ft-lb	Torquemeter	On drive shaft
RPM	0 - 20,000 rpm	Magnetic rpm sensor	Torquemeter
Buffer Gas Pressure	0-10 psi	Pressure gage	Two locations, each inlet
Buffer Gas Flow Rate	0-10 ft^3/min	Flowmeter	Two locations, each inlet
Oil-Mist Pressure	0-10 psi	Pressure gage	Two locations, each bearing cavity
Oil Flow Rate	0-50 drop/min	Visual	Oil-mist generator

Instrumentation and Controls

Because of the experimental nature of this generator, all parameters of interest will be measured, both in the cryogenic section and room temperature sections of the machine. Table 8 is a listing of the parameters to be measured and their expected range.

The parameters in Table 8 will be monitored on a more or less continuous basis. Of course, several other items such as internal resistance and *NaK* volume will be measured during testing procedures by appropriate means.

Control of the superconducting generator will be exercised by field control to regulate the voltage/rpm ratio and turbine throttle control to regulate power output. Field changes will be made at a maximum rate of 15 amps/min, while turbine throttle control should be almost instantaneous. Governors and/or interlocks on the turbine will prevent overspeed due to loss of load. The field current will be supplied by a power supply capable of constant charge rate and current regulated. Interlocks built into the power supply will automatically shut it down if a quench occurs. Other interlocks to protect the overall system will be incorporated later as a result of further analysis of the control problems for the motor-generator turbine system.

DESIGN PERFORMANCE

The test program for the subject superconducting generator includes initial testing in the laboratory with a resistive load. These tests are to be followed by system tests in which the generator will supply power to a superconducting motor[7] loaded by a dynamometer. Ultimately this system will be put on a test craft as an electric propulsion system. The superconducting motor has a nominal rating of 400 hp with a projected capability of 1000 hp. The LM-100 gas turbine to be used as the prime mover for these tests is capable of delivering power throughout this range. The design operating point of the generator was therefore selected at 300 kw, with later thermal analysis indicating that load current could be increased to the 750-kw level without thermally overstressing the machine. Water will be used as the coolant.

Two operating points were chosen for detailed analysis, 300 kw/30 V/10,000 amp output and 750 kw/30 V/25,000 amp output. Both operating points are at a speed of 19,500 rpm. Since critical speed rather than torque dictated shaft size, and magnet design is dictated by voltage, the only limitation at the higher power is the increased thermal load due to the higher load current. The calculated generator performance parameters at these two operating points are listed in Table 9.

TABLE 9 — SUPERCONDUCTING GENERATOR OPERATING POINT PERFORMANCE ESTIMATES

	400 HP	1000 HP
Machine Performance		
Input		
Rotor Speed (rpm)	19,500	19,500
Torque (ft-lb)	108	270
Power (hp)	400	1,000
Output		
Terminal Voltage (V)	30	30
Load Current (amps)	10,000	25,000
Power (kW)	300	750
Power Density		
kW/m^3	2,770	6,927
kW/kg	0.545	1.36
Efficiency (%)	96.67	97.97
Magnetic Circuit Data		
Magnet		
Field Current (amps)	89.64	89.64
Maximum Field (T)	3.85	3.85
Rotor - Intercepted Flux (Wb)	0.0923	0.0923
Shield (G)		
Maximum Flux Density	18,000	18,000
Stray Field at 6 In.	30	30
Electric Circuit Data		
Current Density (A/cm^2)		
Rotor	232.5	232.5
Stator	232.5	581.3
NaK	1,100	2,750
Local Maximum	387.5	968.8
Circuit Resistance (10^{-6} ohms)	4.29	4.29
Machine Losses		
Electric Circuit, Ohmic (kW)	0.429	2.68
Bearings (kW)	0.30	0.30
Seals (kW)	0.20	0.20

TABLE 9 — (Continued)

	400 HP	1000 HP
Machine Losses (Continued)		
Collectors (kW)		
Ohmic	0.025	0.156
Viscous	7.86	7.86
MHD	0.482	3.02
Circulating Current	0.028	0.028
Viscous Loss from Circulating Current	0.605	0.605
Collector, Total	9.0	11.7
Windage (kW)	.34	.34
Total Loss (kW)	10.2	15.1
Thermal Design Data		
Coolant		
Flow (Water) (kg/s)	1.0	1.0
Pressure Drop (psi)	5	5
Inlet Temperature (°C)	25	25
Outlet Temperature (°C)	27.3	28.4
Maximum Temperature (°C)		
Stator	40	45.3
NaK	68.4	83.9
Rotor	70.6	98.6
Structural Design Data		
Size (m)		
Diameter	0.457	0.457
Length (Shield)	0.66	0.66
Weight (kg)	550	550
Stress - Rotor Tensile Maximum (N/m^2)	1.7×10^8	1.7×10^8
Critical Rotor Speed (rpm)	24,000	24,000

The performance of the generator will obviously change as a function of operating conditions. The intent of the following curves is to show a portion of these dependencies to indicate the performance of the generator under off-design conditions. In reality, a shipboard generator would run at full power only a small fraction of the time. Therefore, performance must be reasonable, especially in terms of efficiency over the entire range of operating conditions. The curves of Figures 30 through 41 present a more complete picture of the potential of this type of machine and the operating conditions under which the best performance may be realized; e.g., whether it is better to lower the speed or field current to reduce voltage and maintain maximum efficiency. This does not, however, take into account the variables introduced by other elements in a propulsion system which must ultimately be included in any system analysis to determine the optimum operating conditions.

Figure 42 is included as a performance model in that the efficiency is plotted against power output, where it is assumed that the load is a motor/propellor system which follows a cubic power versus speed relationship, and a constant generator field.

CONCLUSIONS AND PLANS

The foregoing design description of a superconductive acyclic generator indicates that no barrier problems exist to the successful construction and performance of this generator. The dewar system performance is particularly attractive and indicates the feasibility of attaining very low cryogenic heat leaks in full-scale systems. An artist's rendering of the final generator design, showing construction details, is shown in Figure 43.

To the best of the writer's knowledge, this generator will represent a unique liquid metal current collector situation. The combination of unflooded collectors, high current densities, high tip speed, and high axial magnetic fields has not existed in any machine or test situation to date. As the current collectors are one of the most advanced concepts in the generator design, the test results should be extremely useful in the design of future machines and as an indication of the validity of the theoretical treatment of this problem. It is fully intended to experimentally evaluate the current collector performance early in the testing phase and to change the geometry or electrical insulation in the collector region if warranted.

Present plans are to evaluate the generator under no-load conditions, i.e., open circuit and short circuit, immediately after construction. The next phase of testing will include operation into a dummy load with a gas turbine prime mover driving the generator. Assuming success in these tests, the generator will then be run as part of a system to include a gas turbine prime mover, generator, water-cooled transmission lines, the superconducting motor described elsewhere,[7] and a water brake dynamometer load. The final testing phase will consist of the installation of the entire system described above, with the exception of the

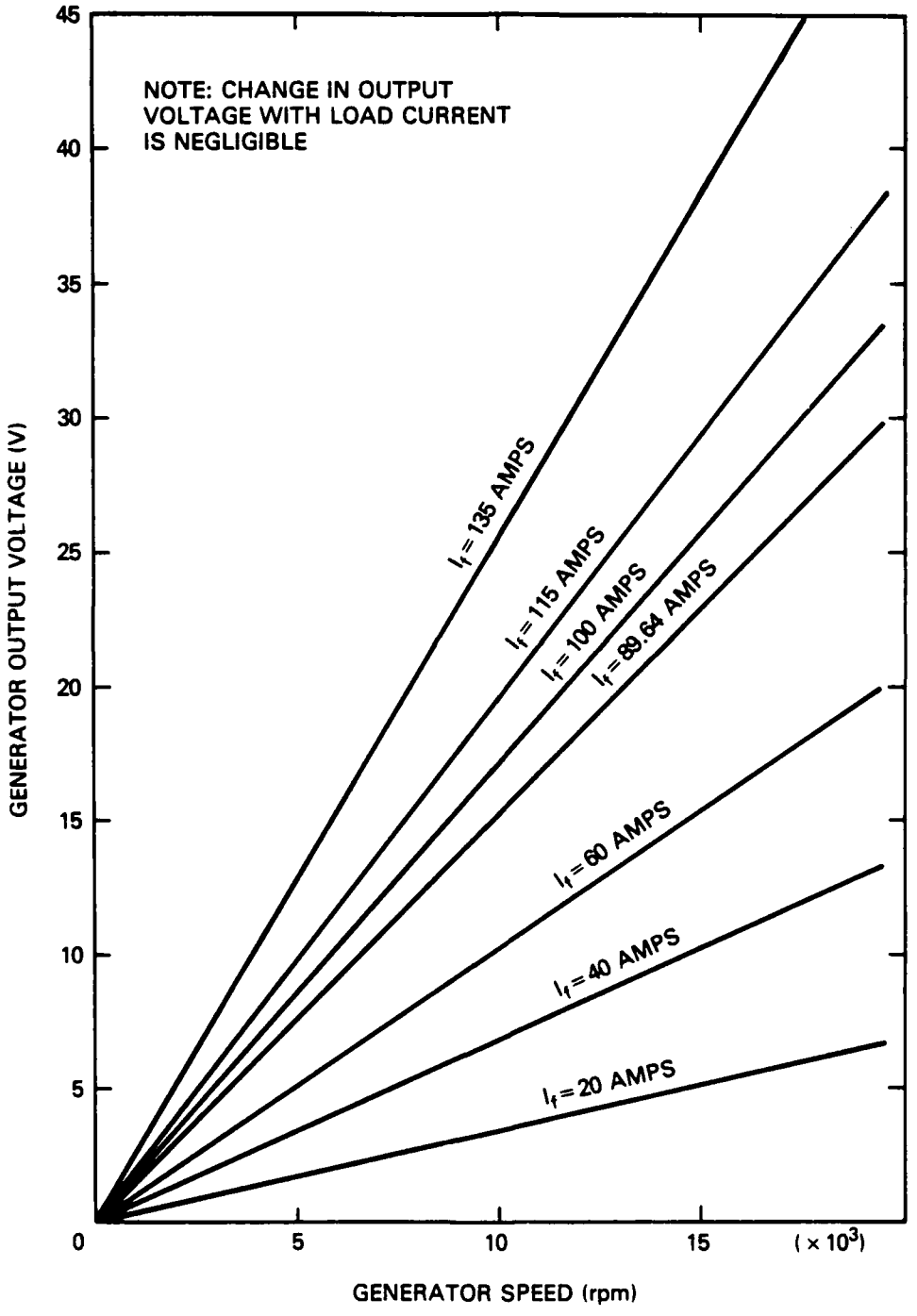

Figure 30 — Generator Output Voltage Characteristics

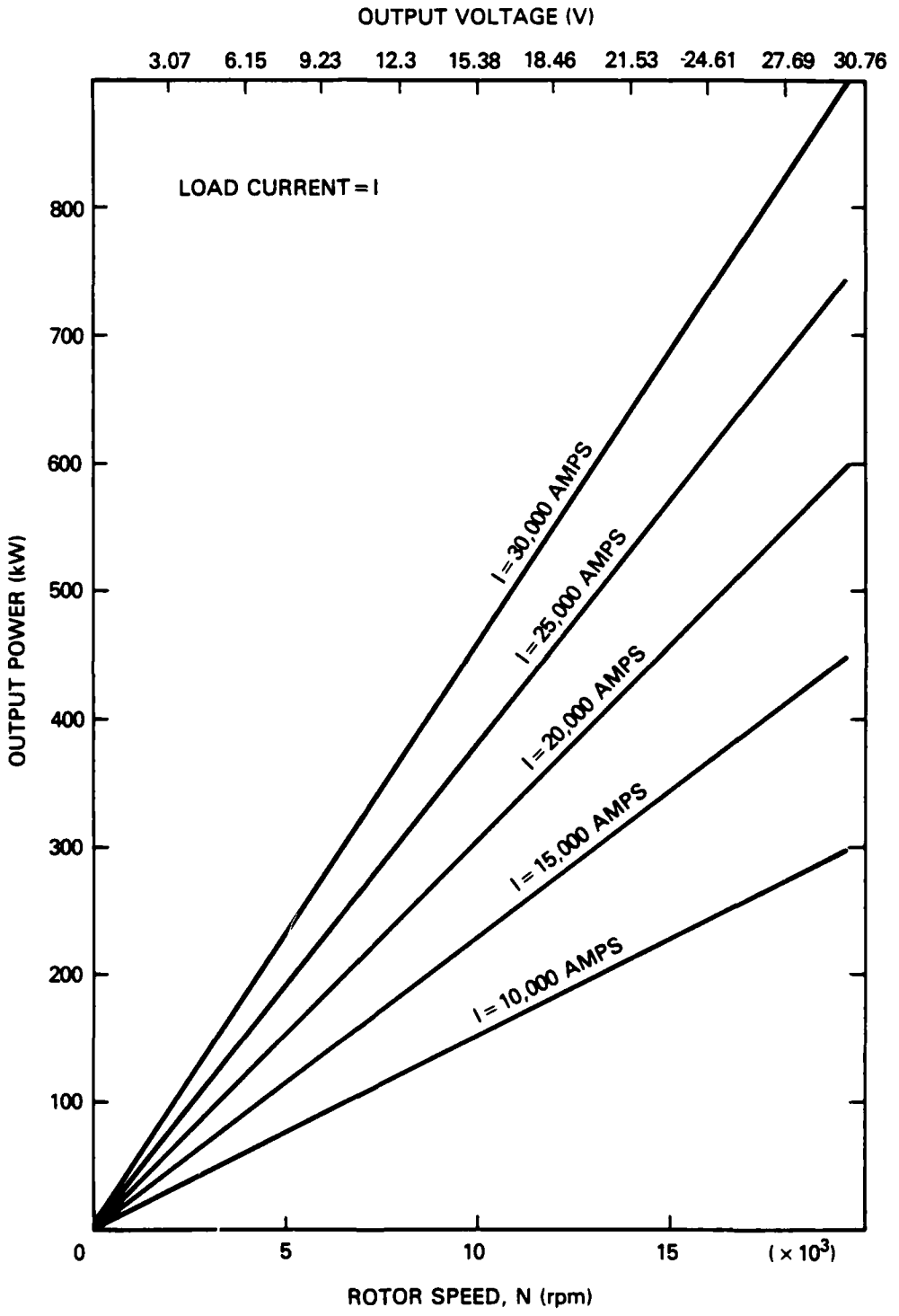

Figure 31 — Generator Output Power Characteristics (89.64-Ampere Field Current)

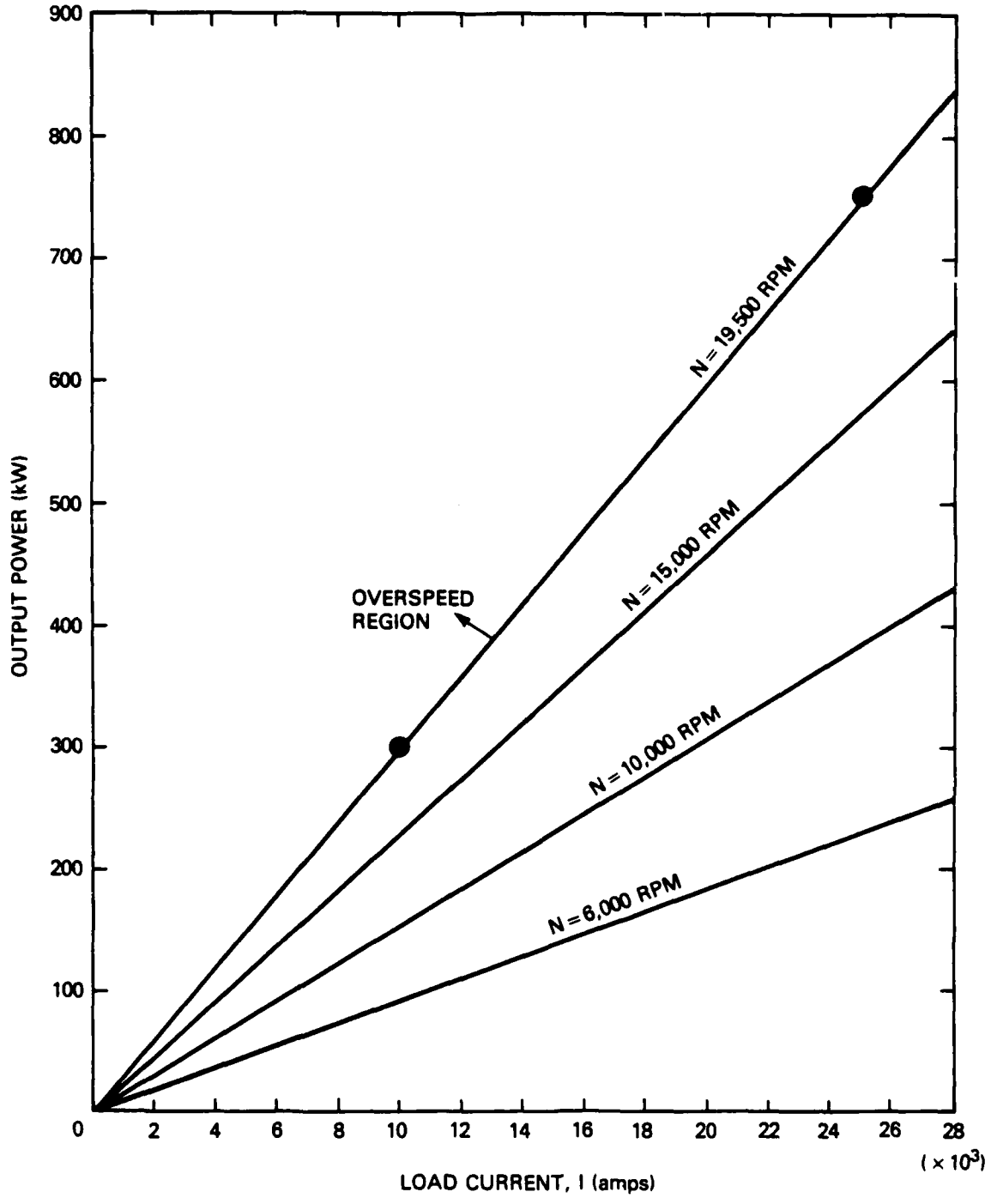

Figure 32 — Generator Output Power Characteristics (89.64-Ampere Field Current)

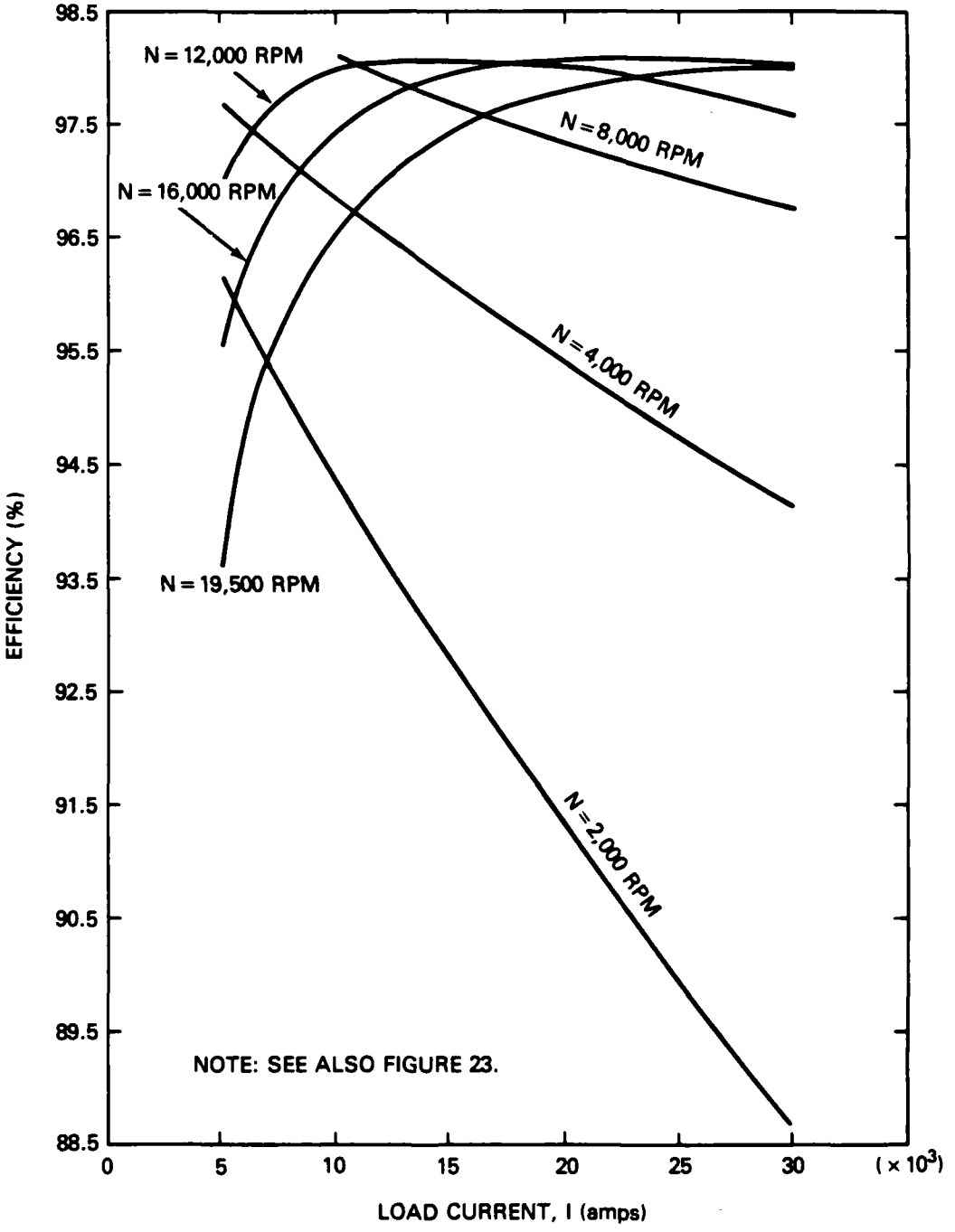

Figure 33 — Generator Efficiency Characteristics (89.64-Ampere Field Current)

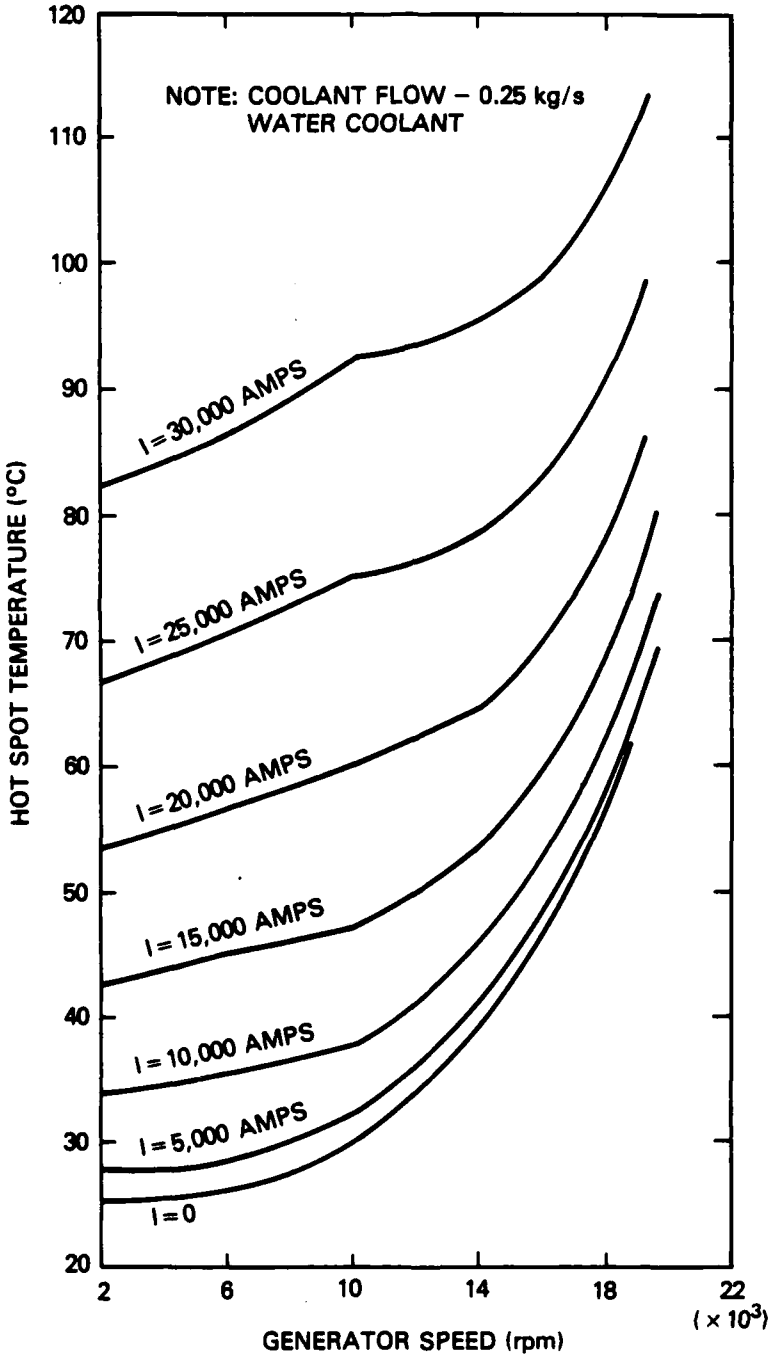

Figure 34 — Generator Thermal Characteristics (89.64-Ampere Field Current)

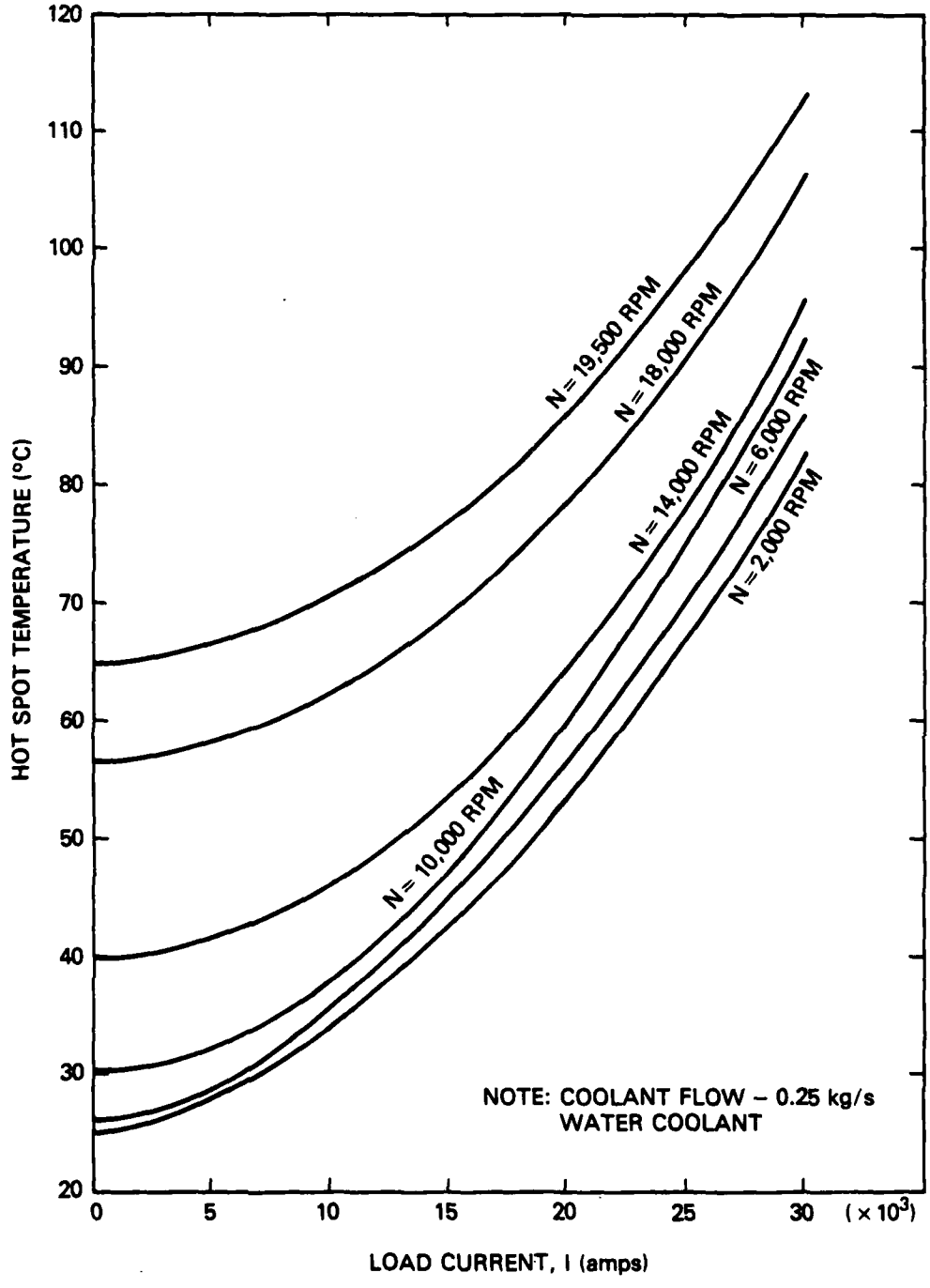

Figure 35 - - Generator Thermal Characteristics (89.64-Ampere Field Current)

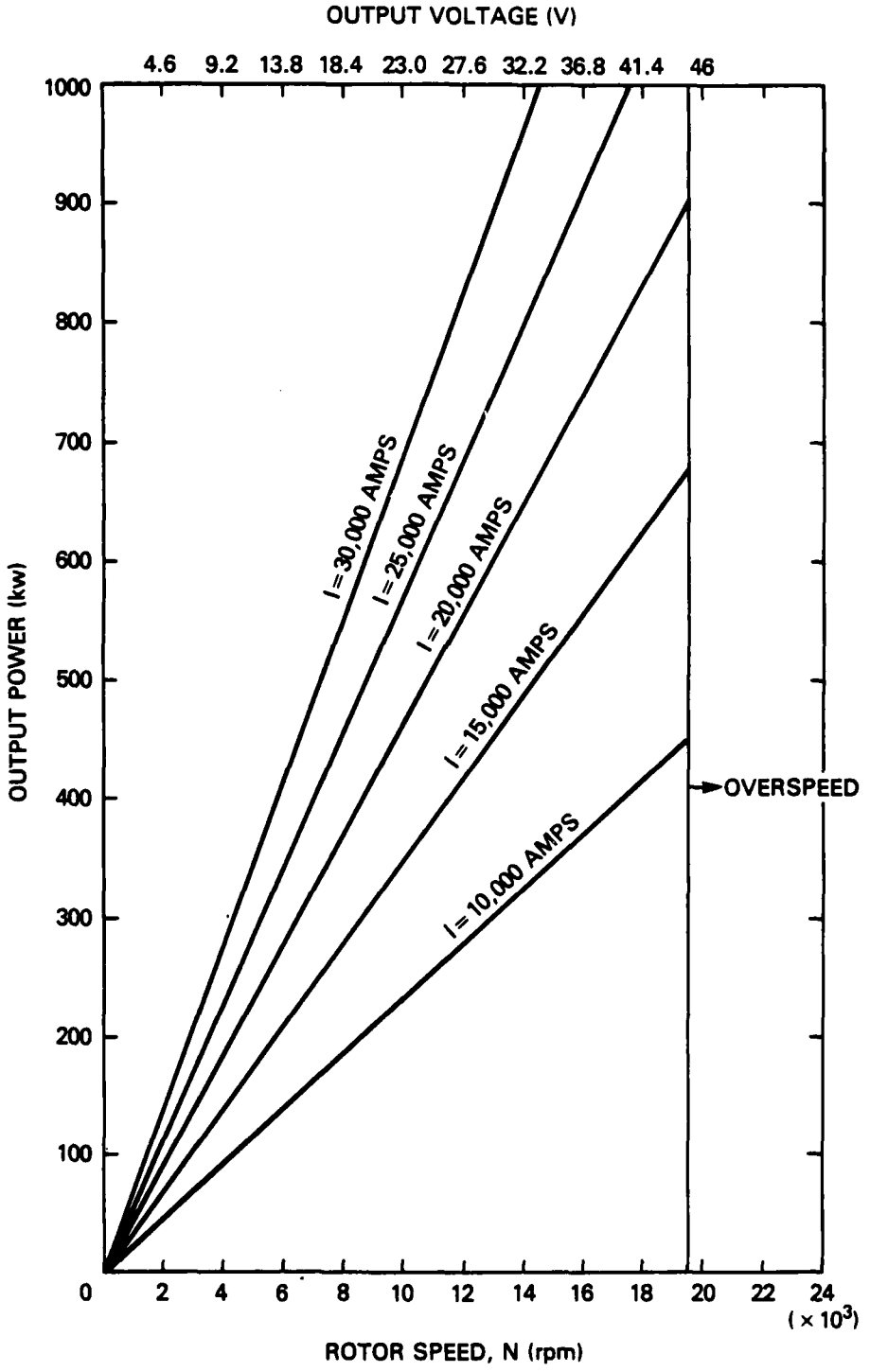

Figure 36 — Generator Output Power Characteristics (135-Ampere Field Current)

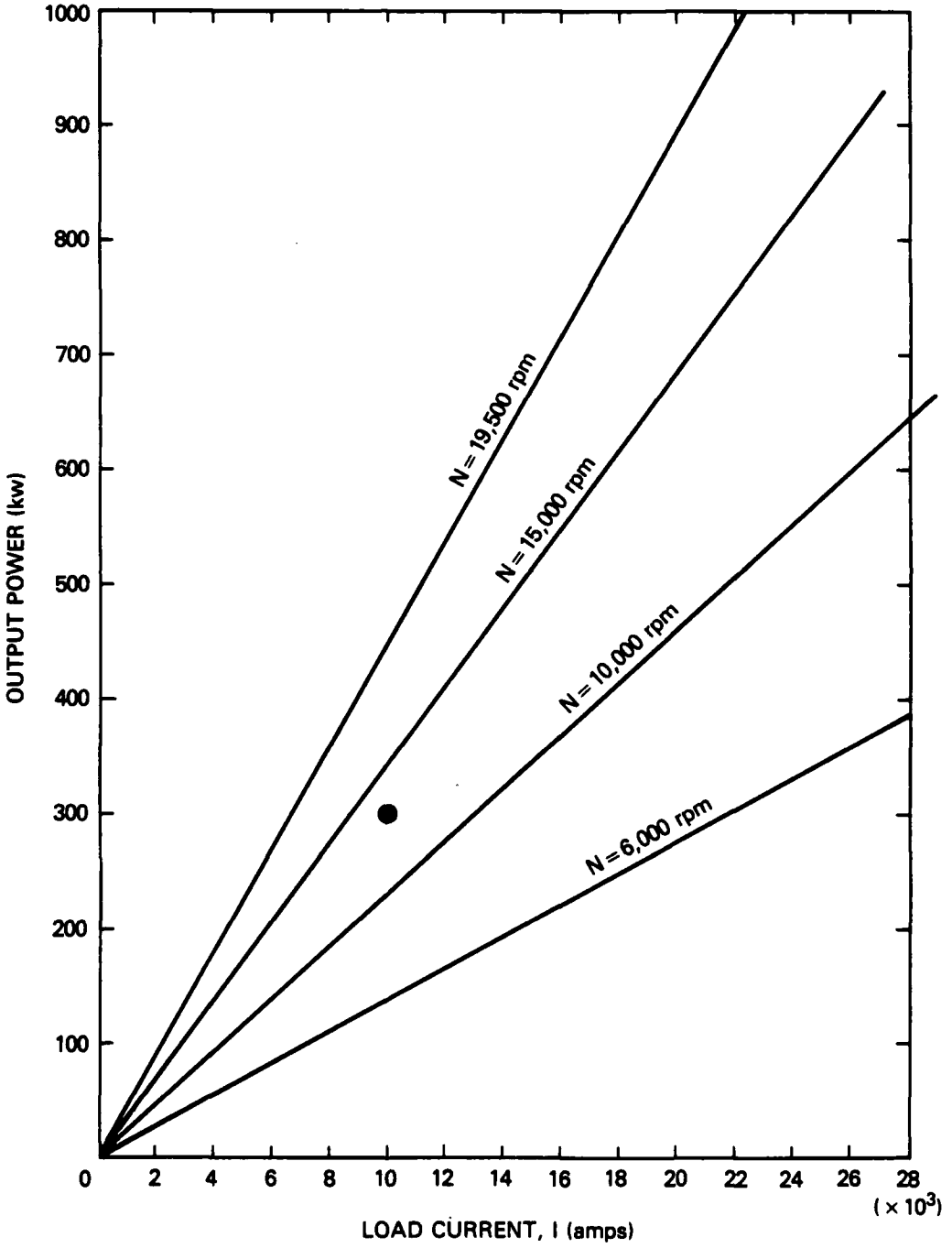

Figure 37 — Generator Output Power Characteristics (135-Ampere Field Current)

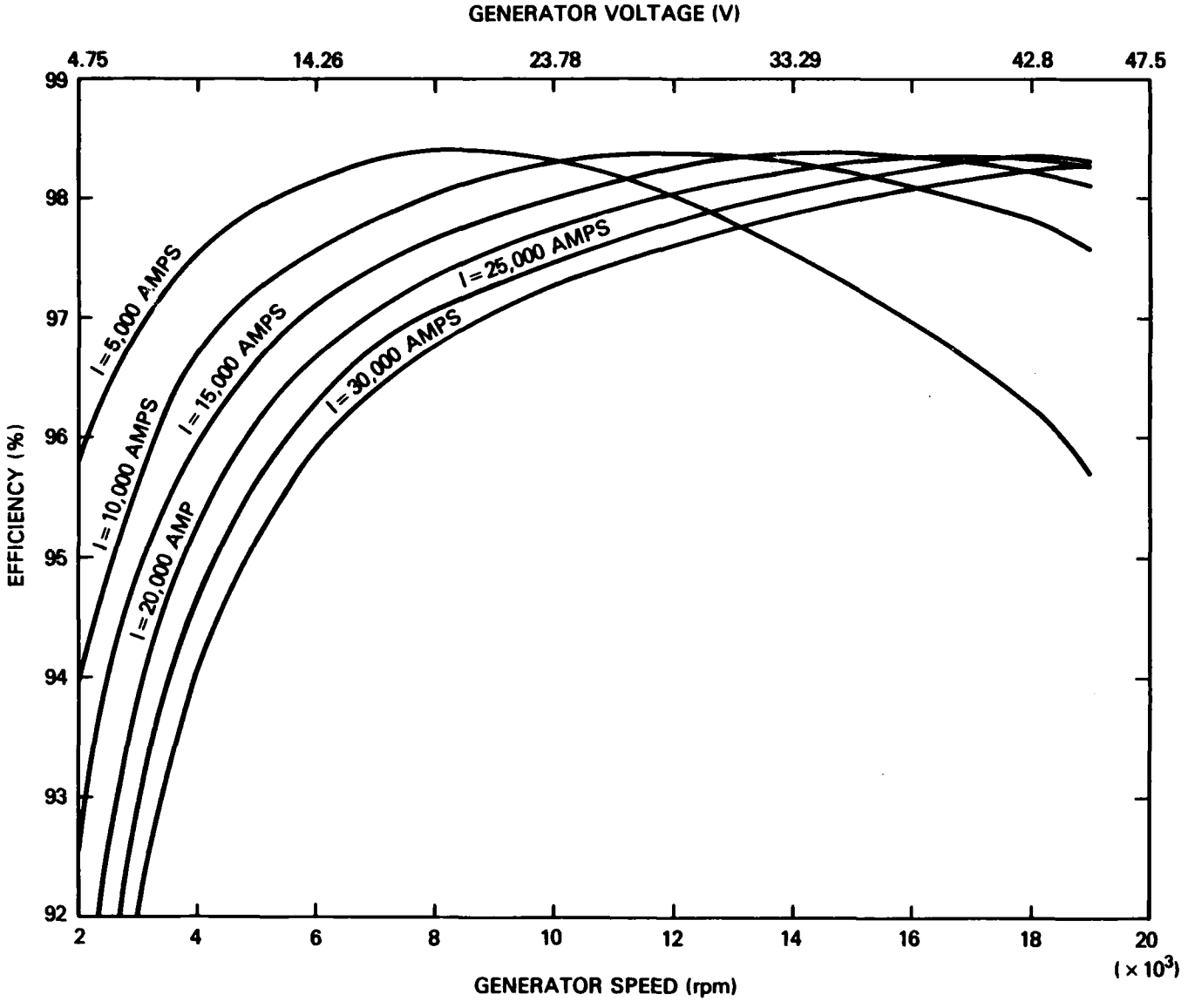

Figure 38 — Generator Efficiency Characteristics (135-Ampere Field Current)

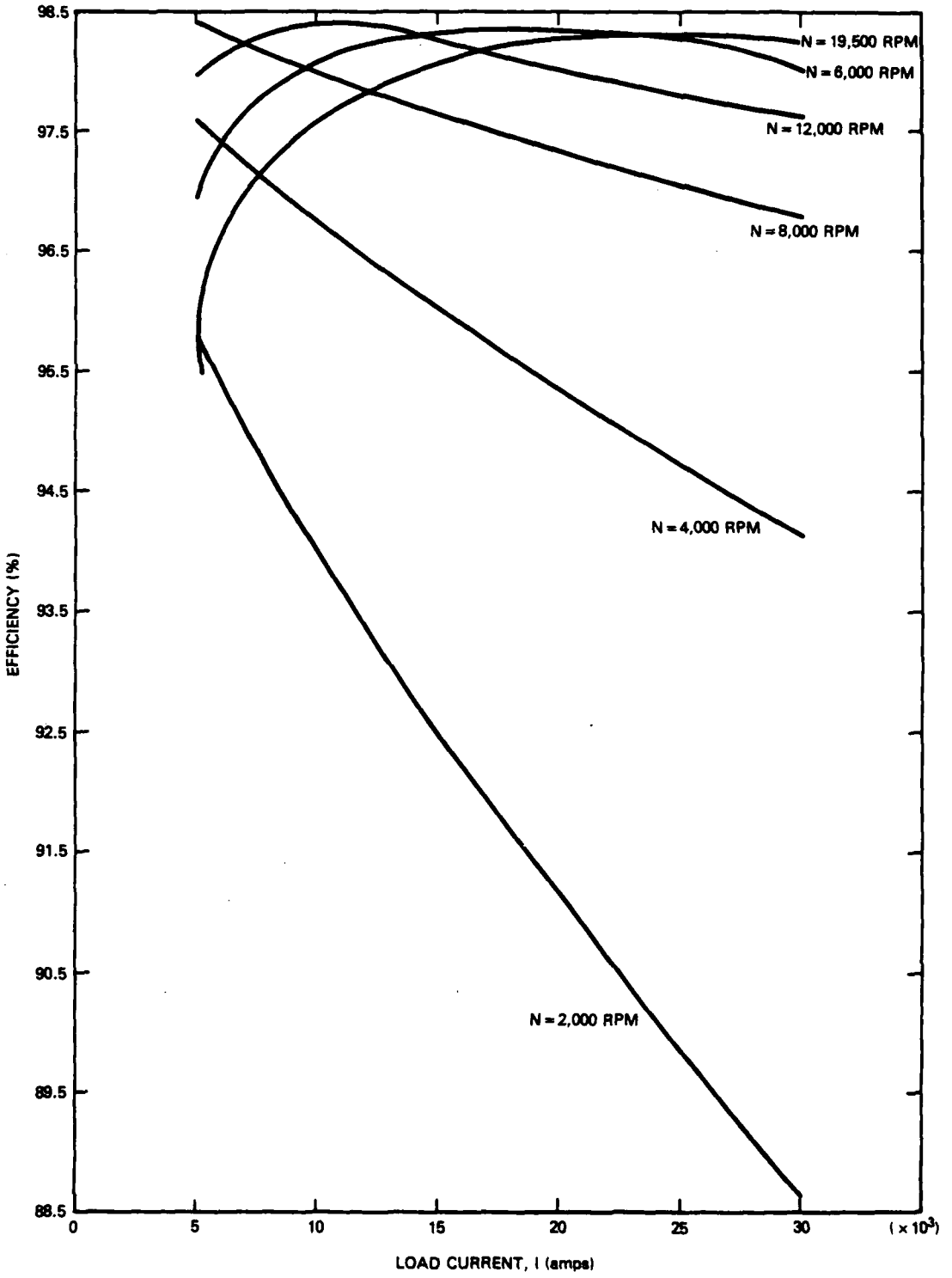

Figure 39 — Generator Efficiency Characteristics (135-Ampere Field Current)

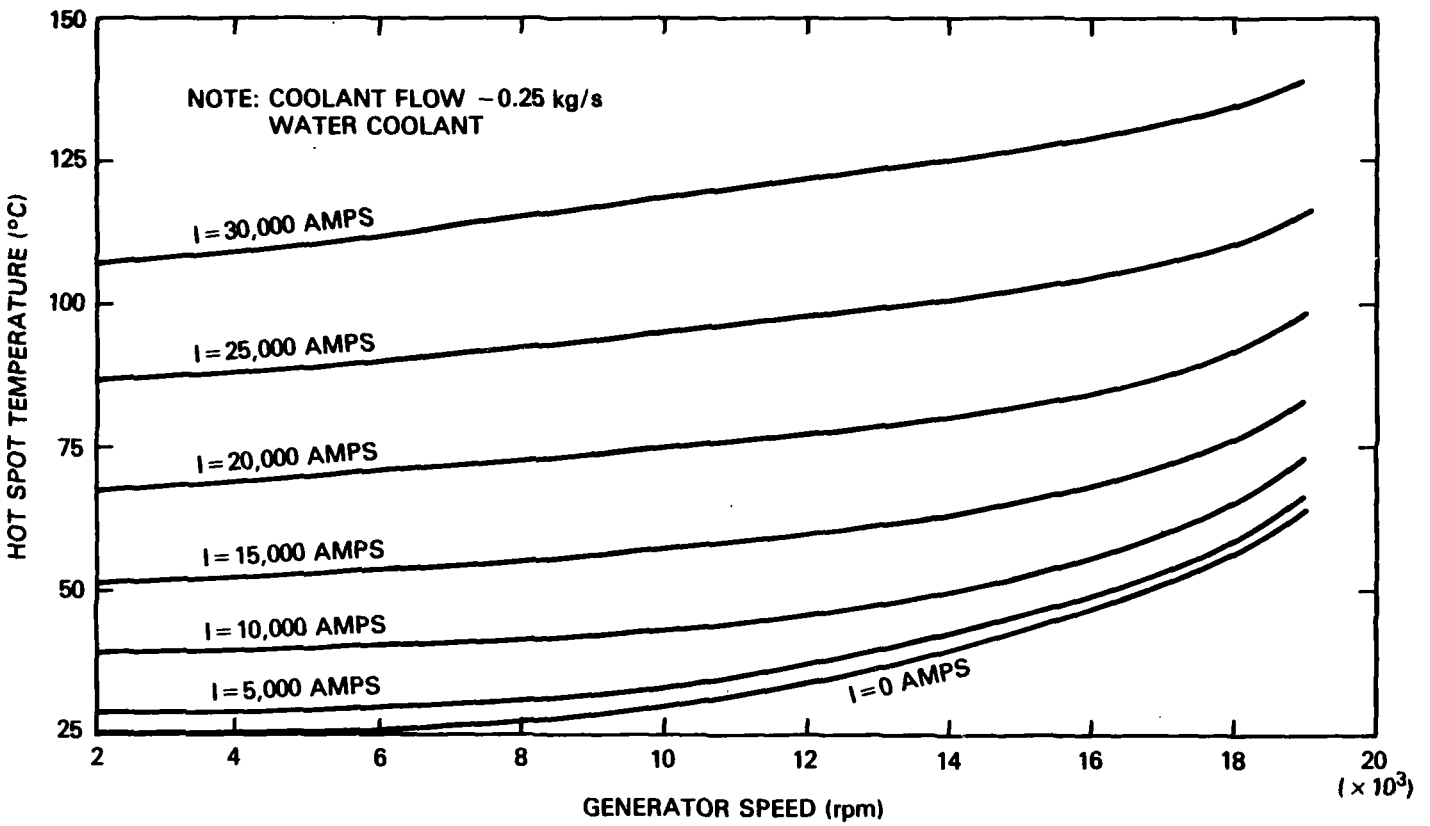

Figure 40 — Generator Thermal Characteristics (135-Ampere Field Current)

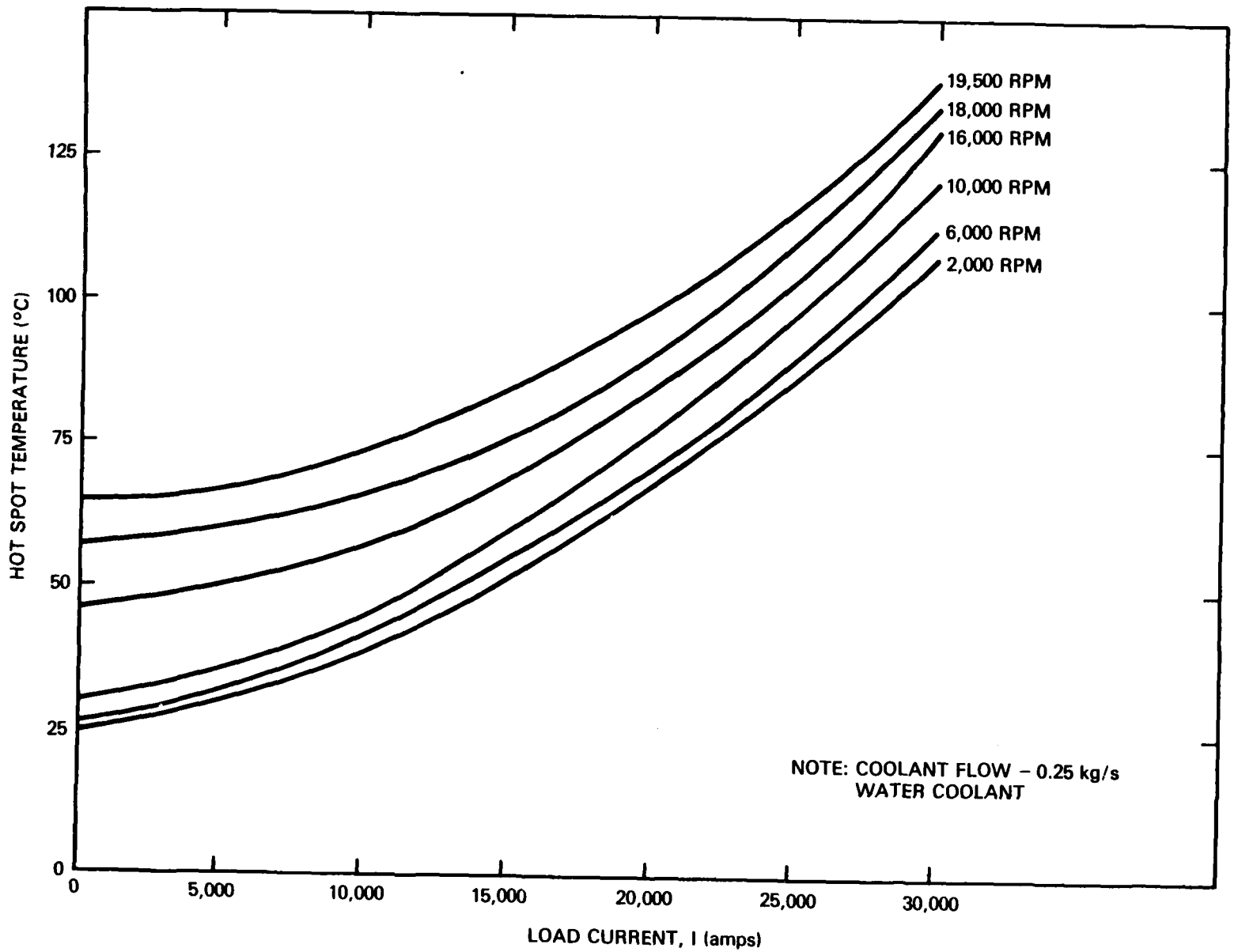

Figure 41 — Generator Thermal Characteristics (135-Ampere Field Current)

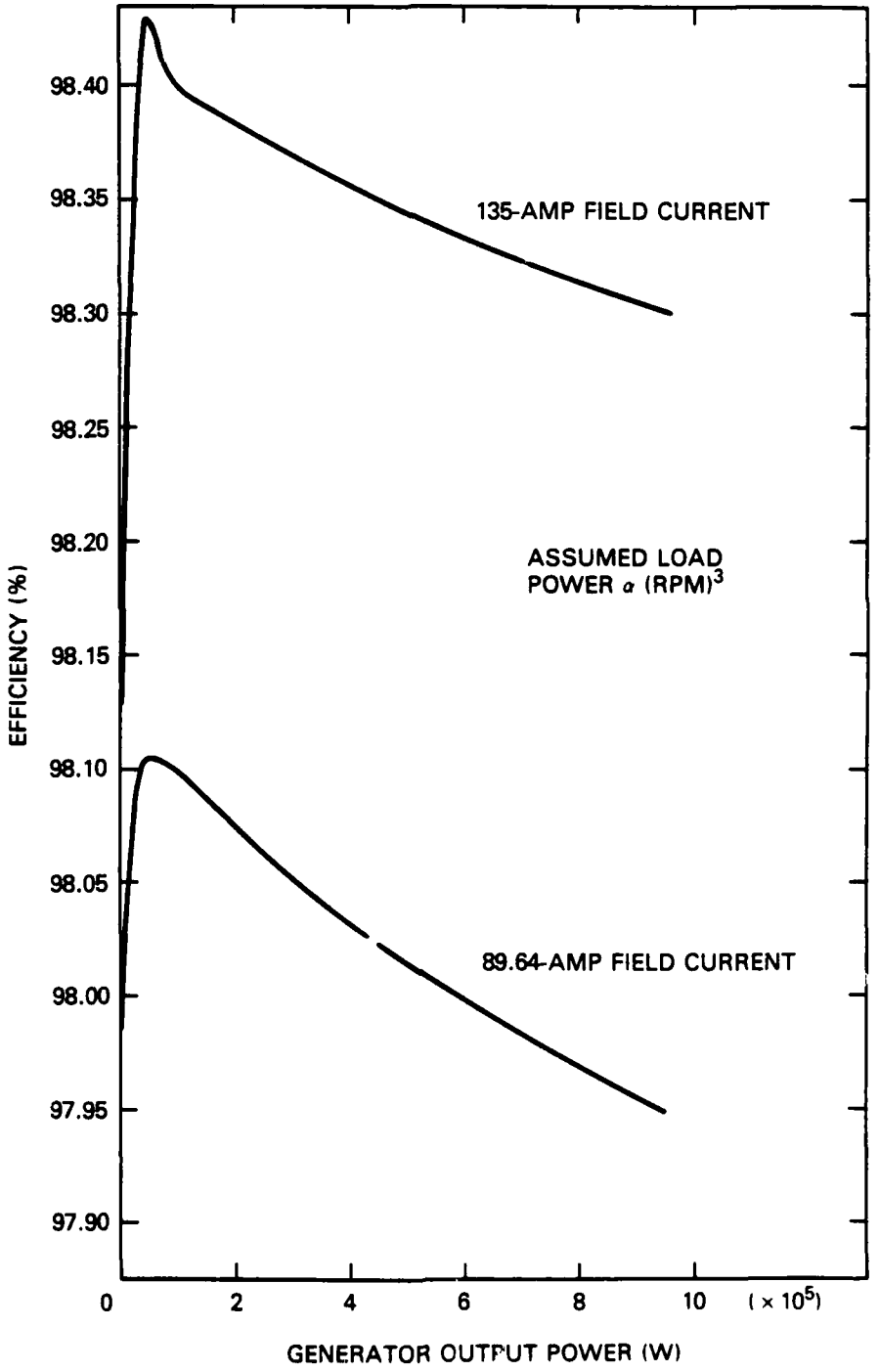

Figure 42 — Generator Efficiency Parameters

AD-A107 513 DAVID W TAYLOR NAVAL SHIP RESEARCH AND DEVELOPMENT CE--ETC F/G 10/2
ACTIVE SUPERCONDUCTIVE GENERATOR DEVELOPMENT 400-HORSEPOWER GEN--ETC(U)
OCT 81 H O STEVENS, M J CANNELL

UNCLASSIFIED DTNSRDC/PAS-81/14 NL

2 OF 2
AD
AD/A...8

END
DATE FILMED
12-81
DTIC

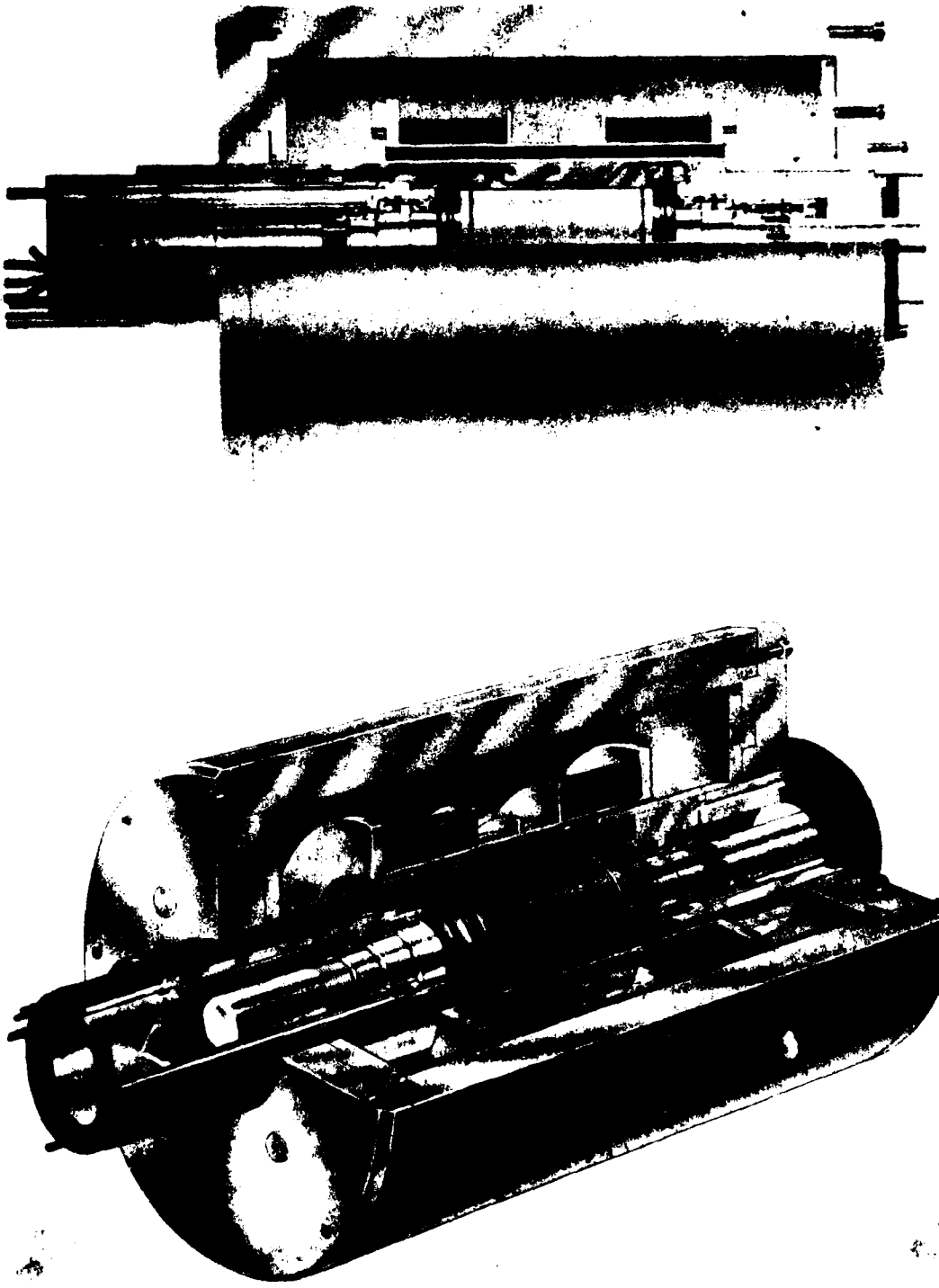

Figure 43 Superconducting Generator Details

water brake, in a test craft to demonstrate the overall feasibility and performance potential of a shipboard superconductive propulsion system.

A report will be issued at a later date describing the construction details and test results of the generator described herein.

ACKNOWLEDGMENTS

The authors wish to thank the Independent Exploratory Development staff at this Center for their initial confidence and financial assistance in beginning this work. Art Chaikin of the Naval Sea Systems Command provided the continuing encouragement and financial support to continue this program. Tim Doyle, Dr. W. J. Levedahl, and Roy Dunnington provided technical assistance in the generator design; and John Stevens reduced the design calculations to hardware specifications for construction. Mike Superczynski, with the able assistance of Frank McDonald and Bill Romoser, did an outstanding job of constructing and testing the superconducting magnet for the generator and provided assistance in the dewar and shield design.

APPENDIX A

LIQUID-METAL CURRENT COLLECTOR DESIGN

The information contained in this appendix was generated subsequent to the writing of this report and represents more recent results of the generator current collector development. The original collector design indicated in this report was tested with *NaK* in a laboratory mockup, and was found to be hydrodynamically unstable above 8000 rpm. Above this speed, the collector fluid no longer filled the annular collector gap. Several alternative collector geometries were tested including the arrangement shown in Figure A.1. This particular collector design exhibited satisfactory performance above collector speeds of 16,000 rpm, representing a tip speed of 148 m/s (485 ft/s). This design was selected for inclusion in the generator prior to the completion of fabrication. The analyses included in this report are still applicable to this new collector design, since the dimensions of the wetted areas remain the same. Detailed results of the current collector development program will be given in a future report.

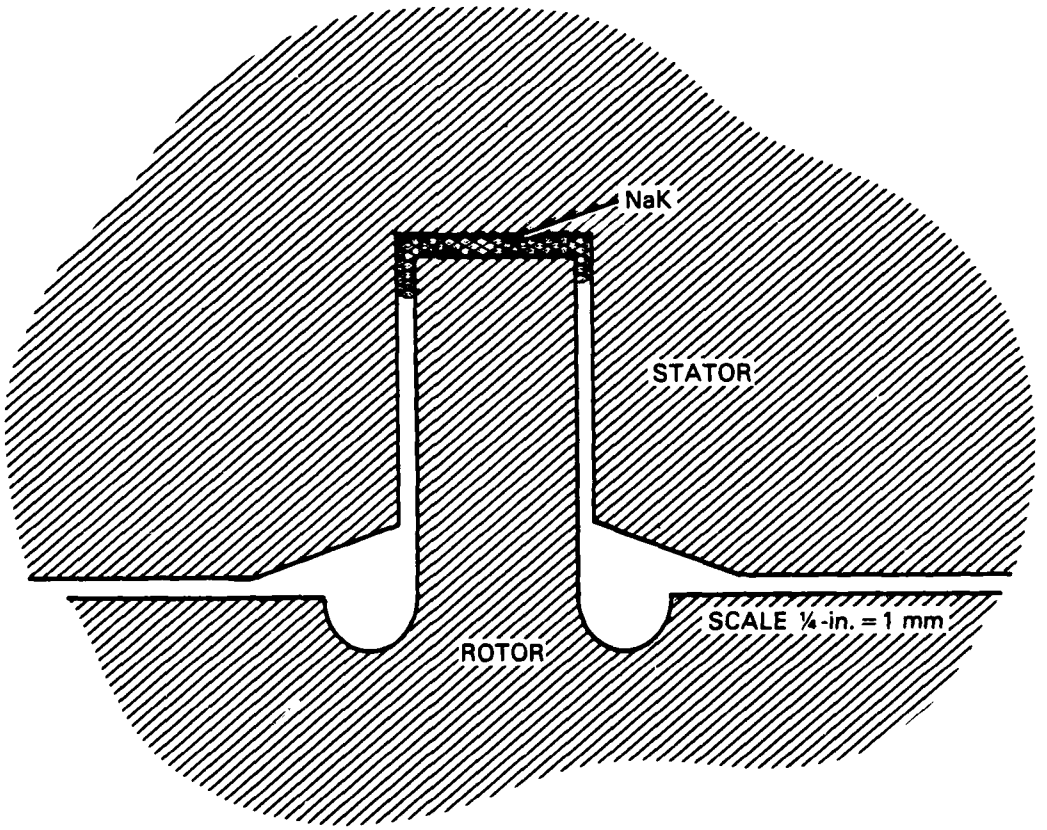

Figure A.1 — Generator Current Collector, Final Design

APPENDIX B*

LOW-FREQUENCY SUPPORT SYSTEM DESIGN ANALYSIS

1. Resonance Condition

For a mass support by a single spring,

$$f_n \approx \frac{1}{2\pi}\left(\frac{K_E}{M}\right)^{1/2} \tag{B.1}$$

where K_E is the effective spring constant, i.e., the force, dF, to displace the mass; a distance, da, is given by

$$\frac{dF}{da} = -k_E. \tag{B.2}$$

For 75-Hz resonance and 100-lb mass, k_E = 57.5 lb/mil.

2. Effect of Magnetic Forces

The magnetic forces given are 10 lb/mil axial and 20 lb/mil radial. These forces are opposed to the restoring source of the support system. To retain the same effective restoring constant, df/da, values of k_E must be increased by these amounts

$$\begin{aligned} k_E \text{ radial} &= k_{Er} = 77.5 \text{ lb/mil} \\ k_E, \text{ axial} &= k_{EZ} = 67.5 \text{ lb/mil}. \end{aligned} \tag{B.3}$$

3. Actual Spring Constant Required

A support system is desired which restrains the magnet in all directions and which, under all conditions of motion, preferably keeps each support under tension at all times. Consider a mass supported between two springs, as illustrated in Figure B.1. For a displacement of Δx downwards ($F_1 = F_2$ at initial equilibrium), $F_1' = F_1 + k\Delta a$ and $F_2' - k\Delta a$.

*Excerpted from Develco, Inc. Report 580-730423, Contract N00600-22-C-1233.

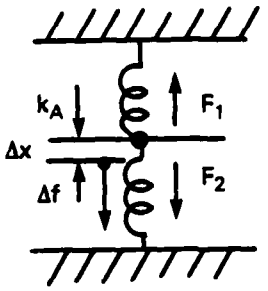

Figure B.1 — Mass Supported Between Two Springs

The force required for this is $\Delta f = F_1' - F_2'$. Therefore, $df/da = 2k_A$.

To retain the same df/da, therefore, requires an actual spring constant

$$k_A = \frac{1}{2} k_E \tag{B.4}$$

or

$$\frac{dF_r}{dr} = \frac{1}{2} k_{Er} \qquad \frac{dF_z}{dZ} = \frac{1}{2} k_{EZ}. \tag{B.5}$$

4. Support System Geometry

The support system which offers stable constraint to all deflections of the magnet with a minimum number of penetrations of the insulation is composed of four wires attached at each end of the magnet. The sketch shown in Figure B.2 shows the support at one end; the opposite end has the identical support geometry and would appear exactly the same.

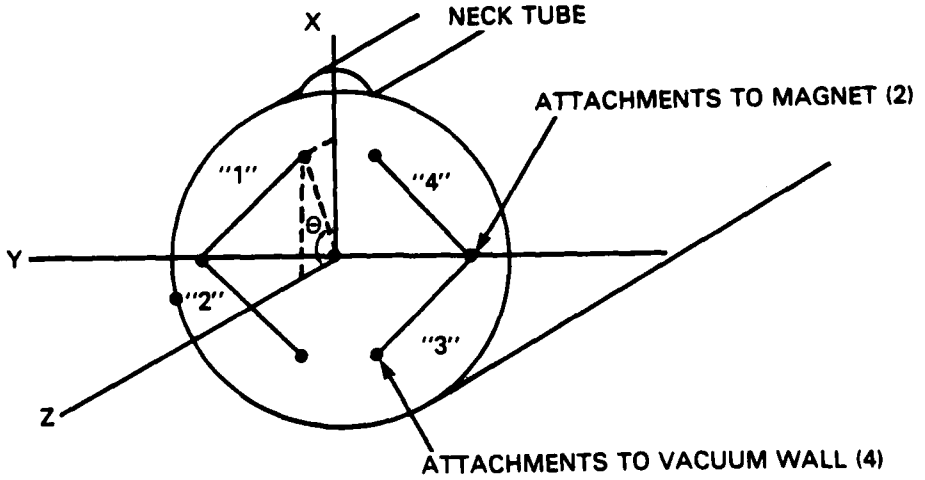

Figure B.2 — Support at One End.

Consider the geometry defined in Figure B.3, which shows defining notation for the wire labeled "1" in Figure B.2. Z is the axial direction; for clarity, the X and Y axes have been rotated 90 degrees from the previous sketch.

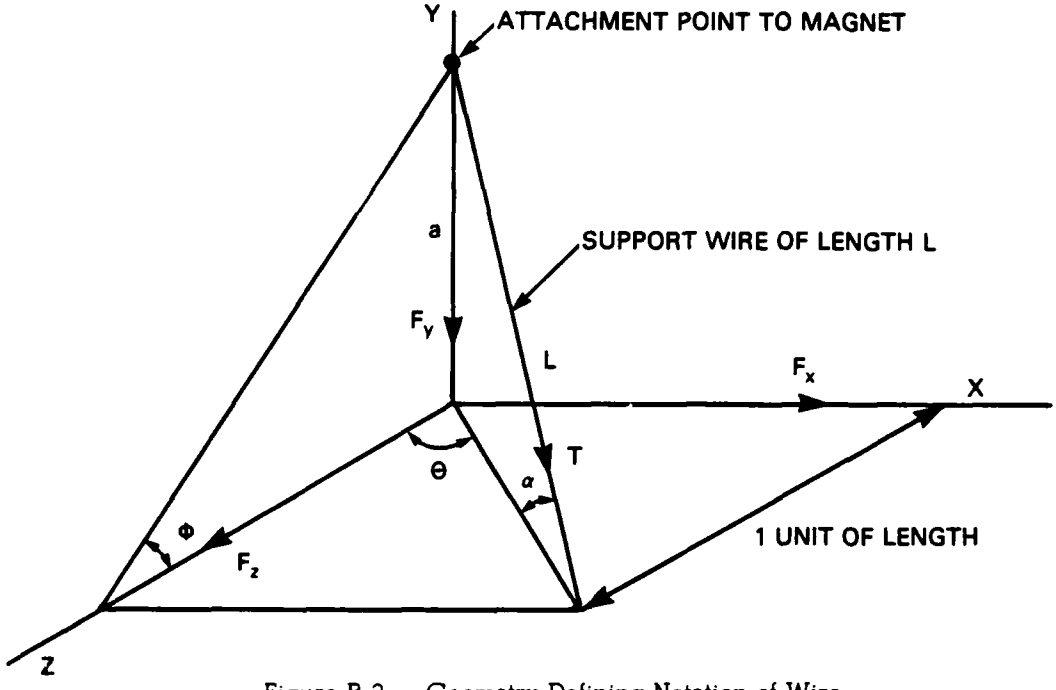

Figure B.3 — Geometry Defining Notation of Wire

As the magnet is displaced in any given direction, four wires of the support system restrain the magnet from motion in that direction. We now consider *only* these four wires (whichever set they may be) to be attached to the magnet, so that it may be treated as a mass supported by a single spring.

$$\begin{aligned} F_x &= 4T\cos\alpha\sin\theta \\ F_y &= 4T\sin\alpha \\ F_z &= 4T\cos\alpha\cos\theta. \end{aligned} \tag{B.6}$$

We have

$$\tan\alpha = \frac{a}{b} = \frac{\tan\phi}{1/\cos\theta} = \cos\theta\tan\phi = \frac{\sin\alpha}{\cos\alpha} = \frac{\sqrt{1-\cos^2\alpha}}{\cos\alpha}$$

$$\cos\alpha = \frac{1}{\sqrt{1+\tan^2\phi\cos^2\theta}} \tag{B.7}$$

$$\sin\alpha = \tan\alpha\cos\alpha = \frac{\tan\phi\cos\theta}{\sqrt{1+\tan^2\phi\cos^2\theta}}.$$

We must now calculate the change in length of the wire, dL, for given small displacements, dx, dy, and dz. Consider the triangle shown:

Assume a is constant $L = (a^2 + b^2)^{1/2}$

$$\frac{dL}{db} = \frac{1}{2}(a^2 + b^2)^{-1/2} 2b = \frac{b}{L}$$

Therefore, $\frac{dL}{db} = \cos \alpha$

$$\frac{dx}{db} = \frac{b}{x} = \frac{1}{\sin \theta}, \; dx = \frac{db}{\sin \theta} \text{ or } db = dx \sin \theta$$

Therefore, $\frac{dL}{dx} = \frac{dL}{db} \frac{db}{dx} = \cos \alpha \sin \theta \, dx.$

or
$$dL = dx \frac{\sin \theta}{\sqrt{1 + \tan^2 \phi \cos^2 \theta}}. \tag{B.8}$$

Similarly,

$$dL = dy \frac{\tan \phi \cos \theta}{\sqrt{1 + \tan^2 \phi \cos^2 \theta}} \tag{B.9}$$

$$dL - dz \frac{\cos \theta}{\sqrt{1 + \tan^2 \phi \cos^2 \theta}}. \tag{B.10}$$

From Equations (B.6) and (B.7),

$$dF_x = 4 \, dT \frac{\sin \theta}{\sqrt{1 + \tan^2 \phi \cos^2 \theta}}$$

Using Equation (B.8) and inverting

$$\frac{dT}{dL} = \frac{dF_x}{dx} \frac{1 + \tan^2 \phi \cos^2 \theta}{4 \sin^2 \theta}. \tag{B.11}$$

Similarly,

$$\frac{dT}{dL} = \frac{dF_y}{dy} \frac{1 + \tan^2 \phi \cos^2 \theta}{4 \tan^2 \phi \cos^2 \theta} \tag{B.12}$$

$$\frac{dT}{dL} = \frac{dF_z}{dz} \frac{1 + \tan^2 \phi \cos^2 \theta}{4 \cos^2 \theta}. \tag{B.13}$$

5. Calculation of Support Angle and Spring Constant

dT/dL must be the same for all deflections (being dependent only upon dimensions and material properties of the support). Furthermore, the same radial resonance behavior in both x and y directions implies that $dF_x/dx = dF_y/dy$. Using Equations (B.11) and (B.12), this implies

$$4 \sin^2 \theta = 4 \tan^2 \phi \cos^2 \theta$$
$$\tan^2 \theta = \tan^2 \phi$$
$$\theta = \phi.$$

Thus, Equations (B.11) through (B.13) may be simplified:

$$\frac{dT}{dL} = \frac{dF_x}{dx} \frac{1 + \sin^2 \theta}{4 \sin^2 \theta}$$

$$= \frac{dF_y}{dy} \frac{1 + \sin^2 \theta}{4 \sin^2 \theta} \tag{B.14}$$

$$= \frac{dF_z}{dz} \frac{1 + \sin^2 \theta}{4 \cos^2 \theta}.$$

Using Equations (B.5) and (B.3) with these we have:

$$\frac{dT}{dL} = \frac{1}{2} (77.5 \text{ lb/mil}) \frac{1 + \sin^2 \theta}{4 \sin^2 \theta} \text{ for } x \text{ and } y \text{ components}$$

$$= \frac{1}{2} (67.5 \text{ lb/mil}) \frac{1 + \sin^2 \theta}{4 \cos^2 \theta} \text{ for } z \text{ component.}$$

Therefore,

$$\frac{\sin^2\theta}{\cos^2\theta} = \tan^2\theta = \frac{77.5}{67.5} \text{ and } \theta = 47° = \phi. \tag{B.15}$$

The mechanical size of the support may now be calculated:

$$\frac{dT}{dL} = \frac{1}{2}(77.5\text{ lb/mil})\frac{1 + \sin^2\theta}{4\sin^2\theta} = 27.81\text{ lb/mil} \tag{B.16}$$

For each wire

$$k_{wire} = 27.81\text{ lb/mil} = E\frac{A}{\ell}.$$

For Ti-6Al-4V wire, $E \cong 15 \times 10^6$ lb/in.^{2} Therefore,

$$\frac{A}{\ell} = \frac{27.81 \times 10^3}{15 \times 10^6} = 1.86 \times 10^{-3}\text{ in.} \tag{B.17}$$

6. G-Loading and Pretension; Actual Wire Dimensions

The requirement on G-loading is that 15 G mechanical loads applied to the dewar should not cause permanent deformation or damage. A 15 G load will deflect the magnet a distance

$$\frac{15 \times 100\text{ lb}}{57.5\text{ lb/mil}} = 26.1\text{ mils} = \Delta x = \Delta y = \Delta z.$$

Using Equations (B.8) through (B.10) and (B.15), we have

$$\frac{\Delta L}{\Delta x} = \frac{\Delta L}{\Delta y} = 0.59 \left[\text{and } \frac{\Delta L}{\Delta z} = 0.55\right].$$

Accordingly, for radial (x or y) deflections $\Delta L_r = 0.59\ (26.1\text{ mils}) = 15.4\text{ mils}$ [and $\Delta L_a = 0.55\ (26.1) = 14.4\text{ mils}$]. This is the amount of initial stretch which is required in the lower support wires ("2" and "3" in Figure B.2 and their equivalent at the opposite end) to allow them to remain in tension for a downward loading of 15 G. The upper support wires ("1" and "4" and their equivalent in Figure B.2) must have this

amount of pretension *plus* the amount required to support the weight of the magnet; this value is $\Delta L = 0.59$ (1 x 100/57.5) = 0.001 in. The total pretension required from these wires is, therefore, the force to stretch them (15.4 + 1) mils = 16.4 mils. G-loading at a value of 15 G's will deflect them an additional 15.4 mils.

$$\Delta L_{Total} = 32 \text{ mils.}$$

The tension developed in doing this is given by $T = E \Delta L A/\ell$.

The spring constant of the wire must be 27.81 lb/mil (see test immediately preceding Equation B.17) and therefore

$$T_{max} = 27.81 \text{ lb/mil} \times 32 \text{ mils} = 890 \text{ lb.}$$

Using the value $\sigma_y = 120{,}000$ psi and $A/\ell = 1.86 \times 10^3$ in., the shortest wire which will withstand the G-loading and retain the desired resonance behavior is

$$L_{min} = \left(\frac{890 \text{ lb}}{120{,}000 \text{ lb/in}^2} \right) / (1.86 \times 10^{-3}) = 4 \text{ in.}$$

The projection of this onto the z axis is

$$z_{min} = L \frac{\cos \theta}{\sqrt{1 + \sin^2 \theta}} = 1.99 \text{ in.}$$

Additional space is necessary for required fittings, etc.

7. Anticipated Helium Consumption

Since $A/\ell = 1.86 \times 10^3$ in. and eight support wires are being used, if no vapor cooling were used on the supports, their heat load contribution would be equivalent to about 2.8 ℓ/hr of liquid helium. The use of one vapor-cooling station at approximately 70K will reduce this to approximately 0.4 ℓ/hr. Other contributions are the current leads ($\cong$0.5 ℓ/hr) and superinsulation ($\cong$0.5 ℓ/hr). Thus helium consumption should be approximately 1.5 ℓ/hr when the magnet is operating at full design current, and is effectively independent of any G-loading.

7. Revised Values for Support System Analysis

The revised wire diameter is 0.125 in., and the length is 5.110 in. Thus, we have $A/\ell = 2.4 \times 10^{-3}$. From Equation (B.17), therefore, $K_{wire} = E A/\ell$

$$K_{wire} = 36 \text{ lb/mil.}$$

Since $\theta = 47°$ as before, from Equation (B.16), we have

$$K_{er} = \frac{36 \times 2 \times 4 \sin^2 \theta}{1 \times \sin^2 \theta} = 100.36 \text{ lb/mil}$$

$$K_{ea} = \frac{36 \times 2 \times 4 \cos^2 \theta}{1 + \sin^2 \theta} = 87.27 \text{ lb/mil.}$$

Subtracting the magnetic force constants we have

$$K_r = 80.36 \text{ lb/mil}$$

$$K_a = 77.27 \text{ lb/mil.}$$

Since the suspended weight is 100.4 lb, we have

$$f_r = \frac{1}{2}\pi\sqrt{K_r \times 386/100.4} = 88.46 \, Hz$$

$$f_a = \frac{1}{2}\pi\sqrt{K_a \times 386/100.4} = 86.75 \, Hz.$$

A 15 G radial load will deflect the magnet

$$\frac{15 \times 100.4}{80.36} = 18.7 \text{ mils radially.}$$

A 15 G axial load will deflect the magnet

$$\frac{15 \times 100.4}{77.27} = 19.5 \text{ mils axially.}$$

Thus, for radial deflections, $\Delta\ell_r = 0.59\ (18.7) = 11.0$ mils and for axial deflections $\Delta\ell_a = 0.55\ (19.5) = 10.7$ mils; that is, 11 mils stretch is required in the lower support wires to allow them to remain in tension for a

downward loading of 15 G. The upper support wires must have this plus 0.001 in. Hence, $\Delta \ell_{total} = 11 + 12 = 23$ mils, and the tension developed in doing this is $T = EA^{\Delta \ell}/\ell = 828$ lb.

Consequently, considerable safety margin exists for radial (and axial) loading. In fact the G-loading which can be withstood is computed as follows

$$\Delta \ell_{max} = T_{max}/E(A/\ell) = \frac{1472}{15 \times 10^6 \times 2.4 \times 10^{-3}} = 0.041 \text{ in.}$$

Thus assuming pretension to one-half the yield point

$$g_r = \frac{34.5 \times 80.36}{100.4} = 27.6 \text{ G's}$$

$$G_a = \frac{37 \times 77.27}{100.4} = 28.5 \text{ G's.}$$

APPENDIX C

TABULAR DATA FROM THERMAL DESIGN CALCULATIONS

Coolant System and Thermal Characteristics

The following tables are the result of a computer run on the thermal properties of the generator at various operating points, coolant properties, and flow rates. The indicated variables are:

J = Magnet current (amps)
I = Load current (amps)
N = RPM
M = Mass flow rate for coolant through each circuit (kg/s)
T (out) = The coolant outlet temperature (°C)
T (stat) = Maximum stator temperature (°C)
T (NaK) = Maximum NaK temperature (°C)
T (Max) = Hot spot temperature on rotor (°C)

Note that the total flow rate for coolant should be $4 \times M$ if coolant loops are connected in parallel, or T (out) would increase if loops were connected in series. Coolant inlet temperature is assumed to be 25°C. Water or Coolanol are used as coolant fluid as indicated.

COOLANOL

J	I	H	M	T(OUT)	T(STAT)	T(MAX)	T(MAX)
35	0	2000	.25	25.006	25.0435	25.072	25.072
35	0	4000	.25	25.0493	25.3472	25.5761	25.5761
35	0	6000	.25	25.1631	26.1752	26.2445	26.2445
35	0	8000	.25	25.3967	27.7262	29.61	29.61
35	0	10000	.25	25.7553	30.4425	34.0053	34.0053
35	0	12000	.25	26.3053	34.4062	40.5635	40.5635
35	0	14000	.25	27.0732	39.9329	49.7179	49.7179
35	0	16000	.25	28.0951	47.3023	61.9024	61.9024
35	0	18000	.25	29.4076	56.7609	77.5506	77.5506
135	5000	2000	.25	25.5302	29.1212	31.9192	32.5057
135	5000	4000	.25	25.6753	29.2664	33.052	33.6385
35	5000	6000	.25	25.7664	30.5923	34.1372	34.7247
135	5000	8000	.25	25.9508	31.1309	35.1442	35.7317
135	5000	10000	.25	26.1311	33.1504	38.4857	39.0732
135	5000	12000	.25	26.6222	36.6705	44.3414	44.9290
135	5000	14000	.25	27.3479	41.9199	52.9041	53.5916
135	5000	16000	.25	28.3393	49.0554	64.2022	65.3897
135	5000	18000	.25	29.6262	57.3359	80.1577	80.7452
135	10000	2000	.25	26.5156	36.6416	44.2623	46.6123
135	10000	4000	.25	26.7651	37.7199	46.0443	48.3943
135	10000	6000	.25	26.9735	38.2211	48.5302	50.8802
135	10000	8000	.25	27.1646	40.5975	50.2076	53.1576
135	10000	10000	.25	27.2584	41.2741	51.9271	54.2771
135	10000	12000	.25	27.5729	43.5393	55.6753	58.0253
135	10000	14000	.25	28.1723	47.259	62.8226	65.1726
135	10000	16000	.25	29.068	54.3131	73.5016	75.8516
135	10000	18000	.25	30.2922	63.0629	87.979	90.329
135	15000	2000	.25	27.9724	45.4197	60.4305	65.727
135	15000	4000	.25	28.1612	47.7791	62.6904	67.9770
135	15000	6000	.25	28.4445	49.9204	66.068	71.3555
135	15000	8000	.25	28.767	52.1445	69.9135	75.2011
135	15000	10000	.25	29.0338	54.0672	73.0943	78.3823
135	15000	12000	.25	29.1572	54.9552	74.5651	79.9526
135	15000	14000	.25	29.5462	57.7591	79.2034	84.4909
135	15000	16000	.25	30.284	63.076	88.0007	93.2382
135	15000	18000	.25	31.3755	70.9413	101.015	106.302
135	20000	2000	.25	29.5979	58.1392	79.2323	86.2323
135	20000	4000	.25	29.8201	59.7328	82.469	91.269
135	20000	6000	.25	30.1624	62.1998	86.551	95.951
135	20000	8000	.25	30.5309	65.2152	91.5403	100.94
135	20000	10000	.25	31.0022	69.2511	96.5634	105.963
135	20000	12000	.25	31.3096	70.4561	100.227	109.629
135	20000	14000	.25	31.4596	71.6193	102.137	111.537
135	20000	16000	.25	31.9965	75.3441	108.209	117.609
135	20000	18000	.25	32.9062	81.9709	119.264	129.664
135	25000	2000	.25	31.4542	71.5945	102.079	116.766
135	25000	4000	.25	31.7141	73.391	105.051	119.739
135	25000	6000	.25	32.1052	76.2105	109.733	124.421
135	25000	8000	.25	32.6039	79.7926	115.66	130.347
135	25000	10000	.25	33.144	83.6948	122.1	136.788
135	25000	12000	.25	33.6345	87.2189	127.948	142.635
135	25000	14000	.25	33.9326	89.367	131.502	146.189
135	25000	16000	.25	34.1755	91.1172	134.398	149.085
135	25000	18000	.25	34.2742	96.1519	142.727	157.416

135	30000	2000	.25	33.5435	95.6067	126.934	149.084
135	30000	4000	.25	33.924	93.5743	130.203	151.759
135	30000	6000	.25	34.2612	91.7351	135.42	156.57
135	30000	8000	.25	34.2264	95.0077	142.159	163.309
135	30000	10000	.25	35.4659	100.416	149.773	170.933
135	30000	12000	.25	36.1009	104.033	157.755	178.505
135	30000	14000	.25	36.6167	108.709	163.505	184.655
135	30000	16000	.25	36.8509	110.396	166.236	187.446
135	30000	18000	.25	37.2795	113.474	171.406	192.556
135	5000	19500	.25	30.309	66.3517	94.2421	94.7354
135	10000	19500	.25	31.4127	71.2522	101.522	102.272
135	15000	19500	.25	32.4365	77.5262	113.664	117.351
135	20000	19500	.25	33.3614	82.2532	120.657	120.053
135	25000	19500	.25	35.6334	102.055	150.435	167.192
135	30000	19500	.25	37.9325	119.19	173.132	200.349

WATER

J	T	N	M	T(OUT)	T(STAT)	T(MAX)	(T(MAX))
135	0	2000	.25	25.0022	25.015	25.0435	25.0435
135	0	4000	.25	25.0173	25.1203	25.3429	25.3429
135	0	6000	.25	25.0535	25.405	26.1753	26.1753
135	0	8000	.25	25.1326	25.3024	27.7269	27.7269
135	0	10000	.25	25.2702	26.23	30.4427	30.4427
135	0	12000	.25	25.468	27.2431	34.4064	34.4064
135	0	14000	.25	25.7432	30.1502	39.9393	39.9393
135	0	16000	.25	26.1096	32.7039	47.3035	47.3035
135	0	18000	.25	26.5201	35.9707	56.7611	56.7611
135	5000	2000	.25	25.203	26.4443	29.1313	29.7622
135	5000	4000	.25	25.2421	26.671	29.9665	30.454
135	5000	6000	.25	25.2747	26.9075	30.5225	31.11
135	5000	8000	.25	25.305	27.1179	31.1311	31.7126
135	5000	10000	.25	25.4055	27.7153	33.1506	33.7371
135	5000	12000	.25	25.5715	28.8379	36.6739	37.2773
135	5000	14000	.25	25.7417	30.2442	41.2134	42.5069
135	5000	16000	.25	26.1367	33.3083	49.0561	49.6436
135	5000	17000	.25	26.6525	36.515	53.3763	53.9043
135	10000	2000	.25	25.5732	28.0913	36.6419	37.2819
135	10000	4000	.25	25.6302	28.3934	37.7193	40.0693
135	10000	6000	.25	25.7075	28.9123	39.2914	41.5714
135	10000	8000	.25	25.776	29.3977	40.5073	42.8479
135	10000	10000	.25	25.7996	29.6214	41.0745	43.4245
135	10000	12000	.25	25.9223	31.4039	43.5393	45.9893
135	10000	14000	.25	26.1372	32.796	47.0596	50.0096
135	10000	16000	.25	26.4533	35.1955	54.3139	56.6639
135	10000	17000	.25	26.7336	37.1479	59.064	65.414
135	15000	2000	.25	26.0656	32.3385	45.4193	51.7067
135	15000	4000	.25	26.1333	32.7694	47.7737	53.0679
135	15000	6000	.25	26.2342	33.5736	49.9911	55.1096
135	15000	8000	.25	26.3504	34.3764	52.1453	57.4393
135	15000	10000	.25	26.4461	35.0405	54.062	59.3555
135	15000	12000	.25	26.4907	35.3475	54.9567	60.2442
135	15000	14000	.25	26.6207	36.3153	57.76	63.0475
135	15000	16000	.25	26.7343	37.1524	63.0771	69.3646
135	15000	17000	.25	27.2756	40.2692	70.9425	76.23
135	20000	2000	.25	26.6427	36.4471	57.1401	67.5401

135	20000	4000	.25	26.729	36.3075	53.7337	69.1337
135	20000	6000	.25	26.8507	37.3407	69.3003	71.6003
135	20000	8000	.25	27.0007	38.3013	65.2163	74.6163
135	20000	10000	.25	27.1517	39.3399	67.9503	77.6503
135	20000	12000	.25	27.3619	40.705	70.4673	79.3673
135	20000	14000	.25	27.3193	41.1034	71.6006	81.0006
135	20000	16000	.25	27.5046	42.33	75.3454	84.7454
135	20000	18000	.25	27.3343	44.6791	71.3795	81.3795
135	25000	2000	.25	27.3176	41.0914	71.5353	80.9733
135	25000	4000	.25	27.4063	41.7113	73.3793	82.6633
135	25000	6000	.25	27.5477	42.6783	76.2113	85.7304
135	25000	8000	.25	27.7259	43.9956	79.7041	89.4716
135	25000	10000	.25	27.9196	45.2711	83.6364	93.3733
135	25000	12000	.25	28.0954	46.4913	87.0306	101.903
135	25000	14000	.25	28.2022	47.2339	89.3637	104.056
135	25000	16000	.25	28.2283	47.2394	91.113	105.807
135	25000	18000	.25	28.5399	49.5776	96.1539	110.741
135	30000	2000	.25	28.0649	46.2203	86.603	107.753
135	30000	4000	.25	28.1633	46.3537	88.5265	103.737
135	30000	6000	.25	28.3201	47.0519	91.7363	110.777
135	30000	8000	.25	28.5227	48.4587	95.7037	116.86
135	30000	10000	.25	28.7519	51.0503	100.413	121.563
135	30000	12000	.25	28.9796	52.631	104.994	126.144
135	30000	14000	.25	29.1645	53.9149	108.711	129.761
135	30000	16000	.25	29.2424	54.4976	110.333	131.583
135	30000	18000	.25	29.4021	55.5646	113.477	134.637
135	5000	19500	.25	27.0921	39.4566	66.9529	67.4404
135	10000	19500	.25	27.301	40.9766	71.2534	73.6034
135	15000	19500	.25	27.6659	43.5099	77.5976	83.2751
135	20000	19500	.25	28.1757	47.0566	88.2555	92.9555
135	25000	19500	.25	28.7335	51.6166	100.057	116.745
135	30000	19500	.25	29.6362	57.19	119.139	139.349

COOLANOL J	I	N	M	T(OUT)	T(STAT)	T(NAK)	T(MAX)
89.64	0	2000	.25	25.006	25.0435	25.072	25.072
89.64	0	4000	.25	25.0483	25.3483	25.5763	25.5763
89.64	0	6000	.25	25.1632	26.1759	26.9457	26.9457
89.64	0	8000	.25	25.387	27.7883	29.6135	29.6135
89.64	0	10000	.25	25.756	30.4478	34.0139	34.0139
89.64	0	12000	.25	26.3069	34.417	40.5815	40.5815
89.64	0	14000	.25	27.076	39.9591	49.7513	49.7513
89.64	0	16000	.25	28.0999	47.3373	61.9593	61.9593
89.64	0	18000	.25	29.4152	56.8154	77.6418	77.6418
89.64	5000	2000	.25	25.3338	27.4055	28.9801	29.5676
89.64	5000	4000	.25	25.4017	27.8945	29.7893	30.3768
89.64	5000	6000	.25	25.4452	28.2083	30.3084	30.8959
89.64	5000	8000	.25	25.604	29.3527	32.202	32.7895
89.64	5000	10000	.25	25.9342	31.7314	36.1378	36.7253
89.64	5000	12000	.25	26.459	35.5134	42.3955	42.983
89.64	5000	14000	.25	27.2096	40.9217	51.3442	51.9317
89.64	5000	16000	.25	28.2196	48.1996	63.3862	63.9737
89.64	5000	18000	.25	29.5241	57.5998	78.9397	79.5272
89.64	10000	2000	.25	25.9293	31.6962	36.0796	38.4296
89.64	10000	4000	.25	26.0451	32.5307	37.4603	39.8103
89.64	10000	6000	.25	26.184	33.5319	39.117	41.467
89.64	10000	8000	.25	26.2553	34.0458	39.9672	42.3172
89.64	10000	10000	.25	26.4685	35.5821	42.5092	44.8592
89.64	10000	12000	.25	26.9155	38.8026	47.8378	50.1878
89.64	10000	14000	.25	27.6103	43.8097	56.1227	58.4727
89.64	10000	16000	.25	28.5786	50.7868	67.6669	70.0169
89.64	10000	18000	.25	29.8506	59.9529	82.8332	85.1832
89.64	15000	2000	.25	26.7179	37.3792	45.4827	50.7702
89.64	15000	4000	.25	26.8671	38.4541	47.2612	52.5487
89.64	15000	6000	.25	27.0749	39.9517	49.7391	55.0266
89.64	15000	8000	.25	27.2648	41.3201	52.0033	57.2908
89.64	15000	10000	.25	27.3592	42.	53.1282	58.4157
89.64	15000	12000	.25	27.6762	44.2845	56.9081	62.1956
89.64	15000	14000	.25	28.2783	48.6231	64.0868	69.3743
89.64	15000	16000	.25	29.177	55.0987	74.8015	80.089
89.64	15000	18000	.25	30.3949	63.8749	89.3225	94.61
89.64	20000	2000	.25	27.6724	44.2568	56.8624	66.2624
89.64	20000	4000	.25	27.8487	45.5272	58.9643	68.3643
89.64	20000	6000	.25	28.1087	47.4006	62.0642	71.4642
89.64	20000	8000	.25	28.3919	49.4415	65.441	74.841
89.64	20000	10000	.25	28.5907	50.8744	67.8118	77.2118
89.64	20000	12000	.25	28.7413	51.9591	69.6066	79.0066
89.64	20000	14000	.25	29.2135	55.3618	75.2367	84.6367
89.64	20000	16000	.25	30.0147	61.1354	84.7898	94.1898
89.64	20000	18000	.25	31.1569	69.3656	98.4074	107.807
89.64	25000	2000	.25	28.7764	52.2123	70.0256	84.7131
89.64	25000	4000	.25	28.9762	53.6516	72.4071	87.0946
89.64	25000	6000	.25	29.2797	55.8387	76.0258	90.7133

89.64	25000	8000	.25	29.6357	58.404	80.2705	94.958
89.64	25000	10000	.25	29.9581	60.7271	84.1142	98.8017
89.64	25000	12000	.25	30.1106	61.8265	85.9333	100.621
89.64	25000	14000	.25	30.4158	64.0258	89.5722	104.26
89.64	25000	16000	.25	31.0918	68.8969	97.6319	112.319
89.64	25000	18000	.25	32.1366	76.425	110.088	124.776
89.64	30000	2000	.25	30.019	61.1662	84.8407	105.991
89.64	30000	4000	.25	30.2397	62.7564	87.472	108.622
89.64	30000	6000	.25	30.5813	65.2178	91.5445	112.694
89.64	30000	8000	.25	30.9986	68.2248	96.5199	117.67
89.64	30000	10000	.25	31.4182	71.2484	101.523	122.673
89.64	30000	12000	.25	31.7229	73.4445	105.156	126.306
89.64	30000	14000	.25	31.8854	74.6151	107.093	128.243
89.64	30000	16000	.25	32.4083	78.3831	113.328	134.478
89.64	30000	18000	.25	33.334	85.0533	124.364	145.514
89.64	5000	19500	.25	30.7172	66.1973	93.1652	93.7527
89.64	10000	19500	.25	31.0238	68.4064	96.8205	99.1705
89.64	15000	19500	.25	31.5347	72.0884	102.913	103.2
89.64	20000	19500	.25	32.2501	77.2431	111.442	120.842
89.64	25000	19500	.25	33.1698	83.8706	122.408	137.095
89.64	30000	19500	.25	34.2939	91.9709	135.81	156.96

WATER

J	I	N	M	T(OUT)	T(STAT)	T(NAK)	T(MAX)
89.64	0	2000	.25	25.0022	25.015	25.0435	25.0435
89.64	0	4000	.25	25.0173	25.1203	25.3483	25.3483
89.64	0	6000	.25	25.0585	25.4062	26.1759	26.1759
89.64	0	8000	.25	25.1387	25.9631	27.7884	27.7884
89.64	0	10000	.25	25.271	26.8818	30.4479	30.4479
89.64	0	12000	.25	25.4685	28.2529	34.4173	34.4173
89.64	0	14000	.25	25.7442	30.1672	39.9595	39.9595
89.64	0	16000	.25	26.1113	32.7158	47.3379	47.3379
89.64	0	18000	.25	26.5828	35.9898	56.8162	56.8162
89.64	5000	2000	.25	25.1197	25.8309	27.4055	27.993
89.64	5000	4000	.25	25.144	25.9998	27.8946	28.4821
89.64	5000	6000	.25	25.1596	26.1082	28.2084	28.7959
89.64	5000	8000	.25	25.2165	26.5035	29.3528	29.9403
89.64	5000	10000	.25	25.3349	27.3252	31.7316	32.3191
89.64	5000	12000	.25	25.523	28.6316	35.5137	36.1012
89.64	5000	14000	.25	25.7921	30.4997	40.9222	41.5097
89.64	5000	16000	.25	26.1542	33.0137	48.2003	48.7878
89.64	5000	18000	.25	26.6218	36.2607	57.6006	58.1881
89.64	10000	2000	.25	25.3331	27.313	31.6964	34.0464
89.64	10000	4000	.25	25.3746	27.6013	32.5309	34.8809
89.64	10000	6000	.25	25.4245	27.9471	33.5322	35.8822
89.64	10000	8000	.25	25.45	28.1246	34.046	36.396
89.64	10000	10000	.25	25.5265	28.6553	35.5824	37.9324
89.64	10000	12000	.25	25.6867	29.7677	38.8029	41.1529
89.64	10000	14000	.25	25.9358	31.4973	43.8102	46.1602
89.64	10000	16000	.25	26.2829	33.9074	50.7875	53.1375
89.64	10000	18000	.25	26.7389	37.0736	59.9539	62.3039

89.64	15000	2000	.25	25.6159	29.2761	37.3796	42.6671
89.64	15000	4000	.25	25.6693	29.6474	38.4544	43.7419
89.64	15000	6000	.25	25.7438	30.1647	39.9521	45.2396
89.64	15000	8000	.25	25.8119	30.6373	41.3205	46.608
89.64	15000	10000	.25	25.8457	30.8722	42.0004	47.2879
89.64	15000	12000	.25	25.9594	31.6613	44.285	49.5725
89.64	15000	14000	.25	26.1752	33.16	48.6237	53.9112
89.64	15000	16000	.25	26.4974	35.3968	55.0995	60.387
89.64	15000	18000	.25	26.934	38.4283	63.8759	69.1634
89.64	20000	2000	.25	25.958	31.6518	44.2573	53.6573
89.64	20000	4000	.25	26.0212	32.0906	45.5277	54.9277
89.64	20000	6000	.25	26.1144	32.7377	47.4012	56.8012
89.64	20000	8000	.25	26.216	33.4427	49.4422	58.8422
89.64	20000	10000	.25	26.2872	33.9376	50.8751	60.2751
89.64	20000	12000	.25	26.3412	34.3123	51.9598	61.3598
89.64	20000	14000	.25	26.5105	35.4877	55.3626	64.7626
89.64	20000	16000	.25	26.7977	37.482	61.1364	70.5364
89.64	20000	18000	.25	27.2072	40.3249	69.3668	78.7668
89.64	25000	2000	.25	26.3538	34.3998	52.213	66.9005
89.64	25000	4000	.25	26.4254	34.8969	53.6524	68.3399
89.64	25000	6000	.25	26.5342	35.6524	55.8395	70.527
89.64	25000	8000	.25	26.6618	36.5385	58.405	73.0925
89.64	25000	10000	.25	26.7774	37.341	60.7281	75.4156
89.64	25000	12000	.25	26.8321	37.7207	61.8275	76.515
89.64	25000	14000	.25	26.9415	38.4804	64.0268	78.7143
89.64	25000	16000	.25	27.1839	40.163	68.8981	83.5856
89.64	25000	18000	.25	27.5584	42.7634	76.4264	91.1139
89.64	30000	2000	.25	26.7993	37.4927	61.1672	82.3172
89.64	30000	4000	.25	26.8784	38.042	62.7575	83.9075
89.64	30000	6000	.25	27.0008	38.8922	65.2189	86.3689
89.64	30000	8000	.25	27.1504	39.9309	68.2259	89.3759
89.64	30000	10000	.25	27.3009	40.9753	71.2496	92.3996
89.64	30000	12000	.25	27.4101	41.7339	73.4458	94.5958
89.64	30000	14000	.25	27.4683	42.1382	74.6165	95.7665
89.64	30000	16000	.25	27.6558	43.4398	78.3846	99.5346
89.64	30000	18000	.25	27.9876	45.7438	85.0549	106.205
89.64	5000	19500	.25	27.0496	39.2305	66.1984	66.7859
89.64	10000	19500	.25	27.1595	39.9936	68.4076	70.7576
89.64	15000	19500	.25	27.3426	41.2654	72.0897	77.3772
89.64	20000	19500	.25	27.5991	43.046	77.2445	86.6445
89.64	25000	19500	.25	27.9288	45.3353	83.8722	98.5597
89.64	30000	19500	.25	28.3318	48.1333	91.9727	113.123

REFERENCES

1. Levedahl, W.J., *et al,* "Performance Advantages of Superconductive Ship Propulsion," presented at CND-CNR Workshop on Naval Applications of Superconductivity, Washington, DC (28-29 Nov 1973).

2. Levedahl, W.J., "Superconducting Naval Propulsion Systems," presented at 1972 Applied Superconductivity Conference (1 May 1972).

3. McCann, E.F., and C.J. Mole, "Superconducting Electric Propulsion Systems for Advanced Ship Concepts," Westinghouse Electric Corp., presented at the Advanced Marine Vehicles Meeting, Annapolis, MD (17-19 Jul 1972).

4. Levedahl, W.J., and T.J. Doyle, "Superconductive Machinery for Naval Propulsion Systems," presented at the 1972 IECEC (5 Sep 1972).

5. Appleton, A.D., "Status of Superconducting Machines at IRD," IRD Co., Ltd., London, England, presented to 1972 Applied Superconductivity Conference (1 May 1972).

6. Doyle, T.J., "Magnetically Shielded Electric Machines with Superconductive Field Windings," Patent 3,657,580 (18 Apr 1972).

7. Doyle, T.J., and M.J. Cannell, "Development of the Shaped Field Superconductive Motor," NSRDC Report 27-578 (Dec 1973).

8. Waltman, D.J., *et al,* "Design Construction and Test of a 0.6-Meter-Diameter Epoxy-Impregnated Superconductive Magnet," DTNSRDC Rept PAS-81/18 (in preparation).

9. Appleton, A.D., "Motors, Generators,and Flux Pumps," *Cryogenics* (Jun 1969).

10. Rhodenizer, R.L., "Development of Solid and/or Liquid Metal Collectors for Acyclic Machines," Final Report of 18 Jun 1968 to 31 Dec 1969, General Electric Co. NAVSEA Contract N00024-68-C5415 (27 Feb 1970).

11. Mole, C.J., "Electrical Propulsion Machinery Study," Westinghouse Electric Corp., ONR Contract N00014-72-C-0393 (Mar 1973).

12. Rhodenizer, R.L., "Development of Solid and/or Liquid-Metal Collectors for Acyclic Machines," Final Report of 1 Jan 1970 to 30 Sep 1971, General Electric Co., NAVSEA Contract N00024-68-C-5415 (30 Sep 1971).

13. Dunnington, L.T., "Liquid Metal Current Collector Development," NSRDC Report 27-580 (Oct 1974).

INITIAL DISTRIBUTION

Copies

5 NAVSEA
- 2 SEA 05R
- 1 SEA 543
- 2 SEA 996

2 CHONR
- 1 Code 473
- 1 Code 211

1 AiResearch Manufacturing Co.
2525 West 190th Street
Torrance, CA 90509
Attn: Mr. W. Rumer

1 General Electric Co.
Corporate Research and
Development
P.O. Box 43
Schenectady, NY 12301
Attn: Mr. R. A. Marshall

1 Westinghouse Electric Corp.
Research Laboratories
130 Beulah Road
Pittsburg, PA 15235
Attn: Dr. D. Greene

12 DTIC

CENTER DISTRIBUTION

Copies	Code
1	271
1	2702
10	2711
2	2712
1	2713
1	522.1
1	522.2
2	5231
1	93

DTNSRDC ISSUES THREE TYPES OF REPORTS

1. DTNSRDC REPORTS, A FORMAL SERIES, CONTAIN INFORMATION OF PERMANENT TECHNICAL VALUE. THEY CARRY A CONSECUTIVE NUMERICAL IDENTIFICATION REGARDLESS OF THEIR CLASSIFICATION OR THE ORIGINATING DEPARTMENT.

2. DEPARTMENTAL REPORTS, A SEMIFORMAL SERIES, CONTAIN INFORMATION OF A PRELIMINARY, TEMPORARY, OR PROPRIETARY NATURE OR OF LIMITED INTEREST OR SIGNIFICANCE. THEY CARRY A DEPARTMENTAL ALPHANUMERICAL IDENTIFICATION.

3. TECHNICAL MEMORANDA, AN INFORMAL SERIES, CONTAIN TECHNICAL DOCUMENTATION OF LIMITED USE AND INTEREST. THEY ARE PRIMARILY WORKING PAPERS INTENDED FOR INTERNAL USE. THEY CARRY AN IDENTIFYING NUMBER WHICH INDICATES THEIR TYPE AND THE NUMERICAL CODE OF THE ORIGINATING DEPARTMENT. ANY DISTRIBUTION OUTSIDE DTNSRDC MUST BE APPROVED BY THE HEAD OF THE ORIGINATING DEPARTMENT ON A CASE-BY-CASE BASIS.